calculated from the overall drying rates was somewhere between 80 and 90°C.

In the case of LPSSD it can be seen that the overall drying rates of continuous LPSSD were slightly lower than those of intermittent drying. In the case of intermittent drying, steam was not injected into the drying chamber during the off period; therefore, the drying medium in the tempering (off) period was less humid. Thus, the mass transfer driving force between the sample surface and the drying medium in the case of intermittent drying was larger than in the case of continuous drying.

However, it was found that the effect of intermittent (time-varying) temperature LPSSD on the drying kinetics was not significant when the on-period setting temperatures were 70 and 80°C. During the tempering period, the energy in the case of intermittent drying at 90°C was accumulated within the sample more significantly than in the case of intermittent drying at lower temperatures. Therefore, when energy was supplied again in the effective drying period, the moisture removal was greater. Hence, the effect of intermittent drying on the drying behavior at 90°C was clearer than that at 70 and 80°C.

The average total and net drying times for banana chips under various conditions are listed in Table 2. It is seen from this table that the total drying time of intermittent LPSSD was similar to that for continuous LPSSD. Although the sample and chamber temperatures (shown here only for the case with the setting temperature of 70°C for the sake of brevity; see Fig. 4; the trends at other setting temperature were similar) in the case of intermittent drying were lower than those in the case of continuous drying, the drying system in the tempering period acted like vacuum drying, whose drying rates were greater than those of LPSSD, as mentioned earlier. This led to the steady decrease of moisture content in the case of intermittent drying. However, the effective or net drying time of intermittent drying was significantly shorter than that of continuous drying. These savings could be directly translated into the energy savings as discussed later.

In the case of vacuum drying it is observed from Fig. 3 that the effect of intermittency on the vacuum drying kinetics is again not significant when setting the on-period temperature at 70°C. However, the drying rates of intermittent drying were lower than those of continuous drying, especially at longer tempering (off) time, at the setting temperatures of 80 and 90°C. In the case of intermittent drying, an off period (heater turned off) led to reduced sample and chamber temperatures (Fig. 5; only results at the setting temperature of 70°C are shown). Thus, vapor pressure gradients, which are the driving force of the drying process, were reduced. At higher drying temperatures, the sample temperature, which was reduced during the tempering period, affected the vapor pressure even more significantly than at lower temperatures. Hence, the effect of intermittency was more obvious at the setting temperature of 90°C. This behavior is shown in Fig. 6, which is the representative plots of the evolution of vapor pressure of continuous and intermittent drying at an on:off period of 10:20 min at various setting temperatures; only selected plots are again shown here for the sake of brevity as the

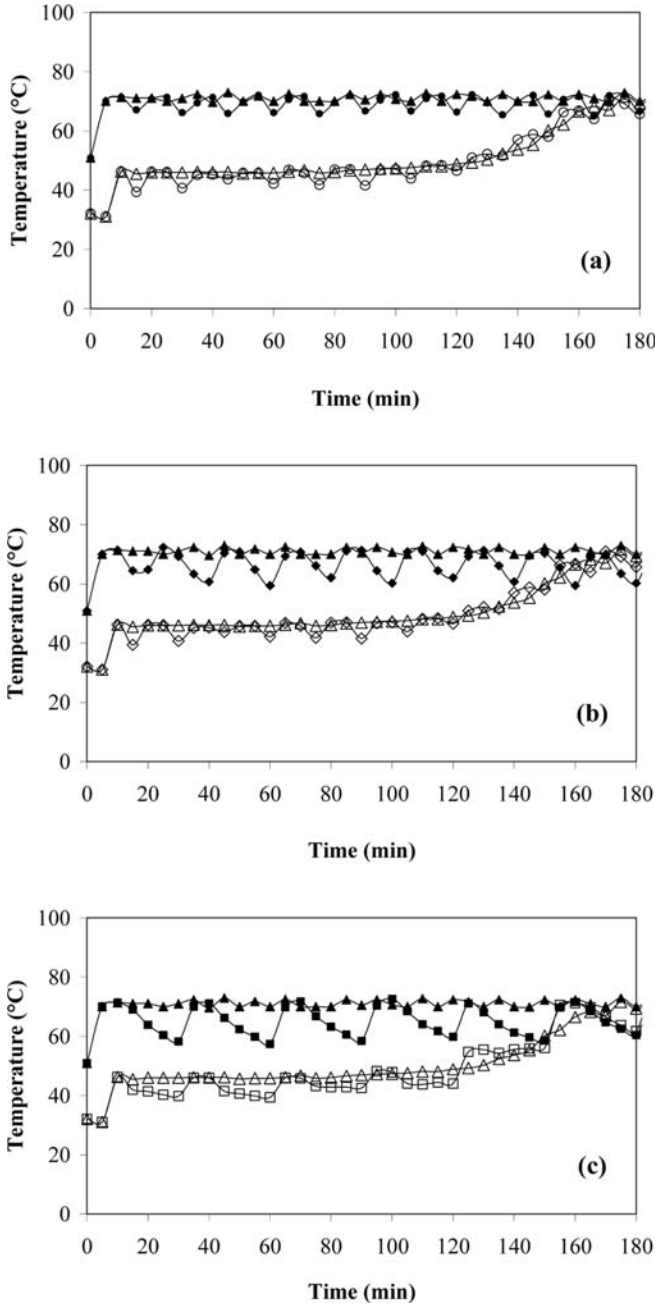

FIG. 4. Chamber (opaque sign) and sample (transparent sign) temperatures during continuous and intermittent temperature LPSSD at 70°C. Continuous drying (Δ) vs. intermittent drying at on:off period of (a) 10:5 (◯), (b) 10:10 (◇), and (c) 10:20 (€).

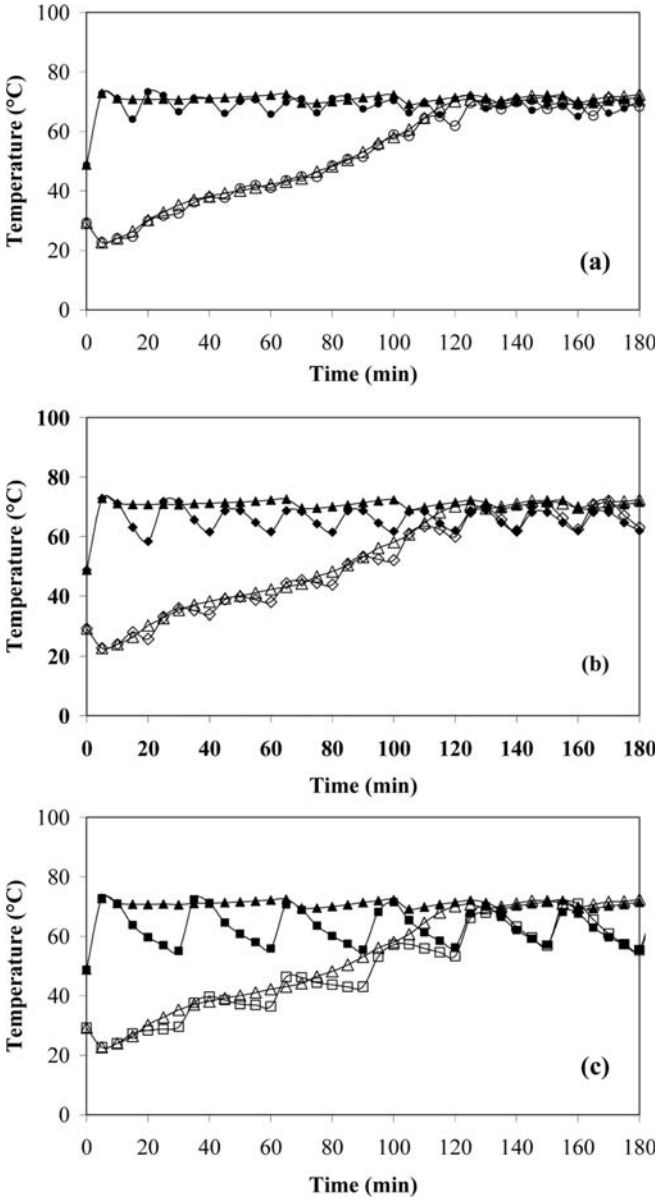

FIG. 5. Chamber (opaque sign) and sample (transparent sign) temperatures during continuous and intermittent temperature vacuum drying at 70°C. Continuous drying (Δ) vs. intermittent drying at on:off period of (a) 10:5 (◯), (b) 10:10 (◇), and (c) 10:20 (€).

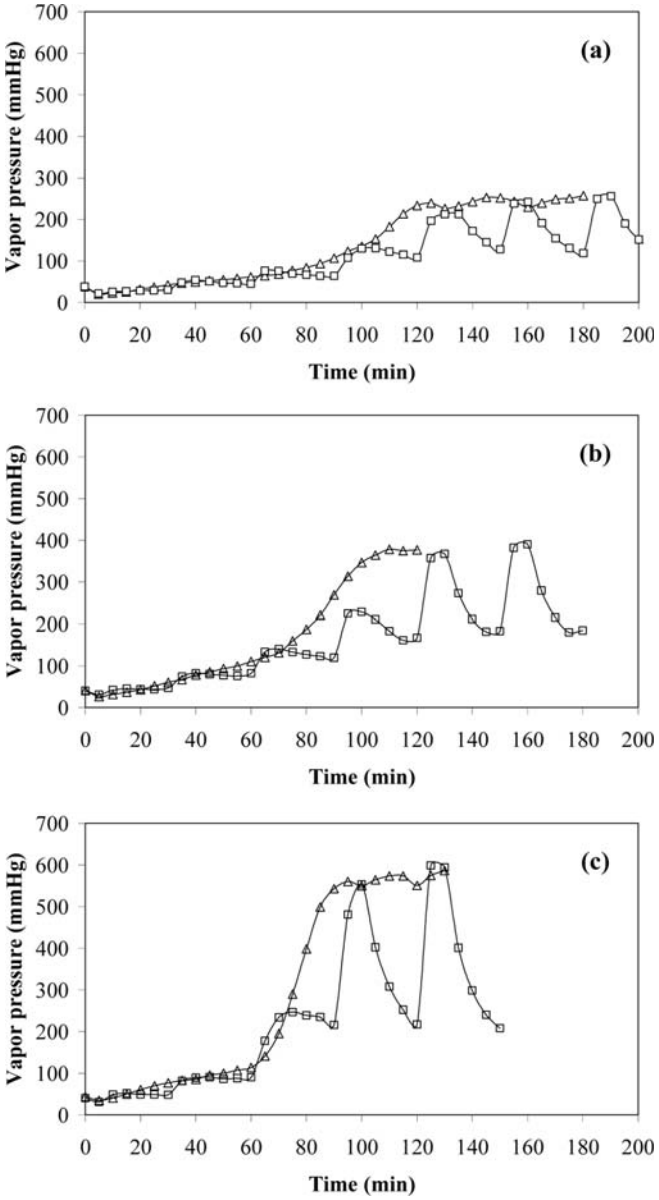

FIG. 6. Vapor pressure of continuous and intermittent vacuum drying at an on:off period of 10:20 min (€) at temperatures of (a) 70°C, (b) 80°C, and (c) 90°C.

trends of vapor pressure changes were the same at all tested conditions. Table 2 also shows that the total drying time of intermittent drying was significantly longer than that of continuous drying. However, the effective or net drying time was again significantly shorter than that of continuous drying.

Intermittent Pressure Drying

The drying curves of banana chips undergoing intermittent pressure LPSSD and vacuum drying are displayed in Figs. 7 and 8, respectively. The drying time of LPSSD at the setting temperature of 80°C was longer than that of vacuum drying. However, the drying time of LPSSD and vacuum drying at 90°C was similar. This may be due to the effect of an inversion phenomenon, as mentioned earlier.

It is seen that the drying rates of intermittent drying at all conditions were obviously higher than those of continuous drying. This is due to the higher sample surface temperatures in the case of intermittent drying. This behavior is shown in Figs. 9 and 10, which are the representative

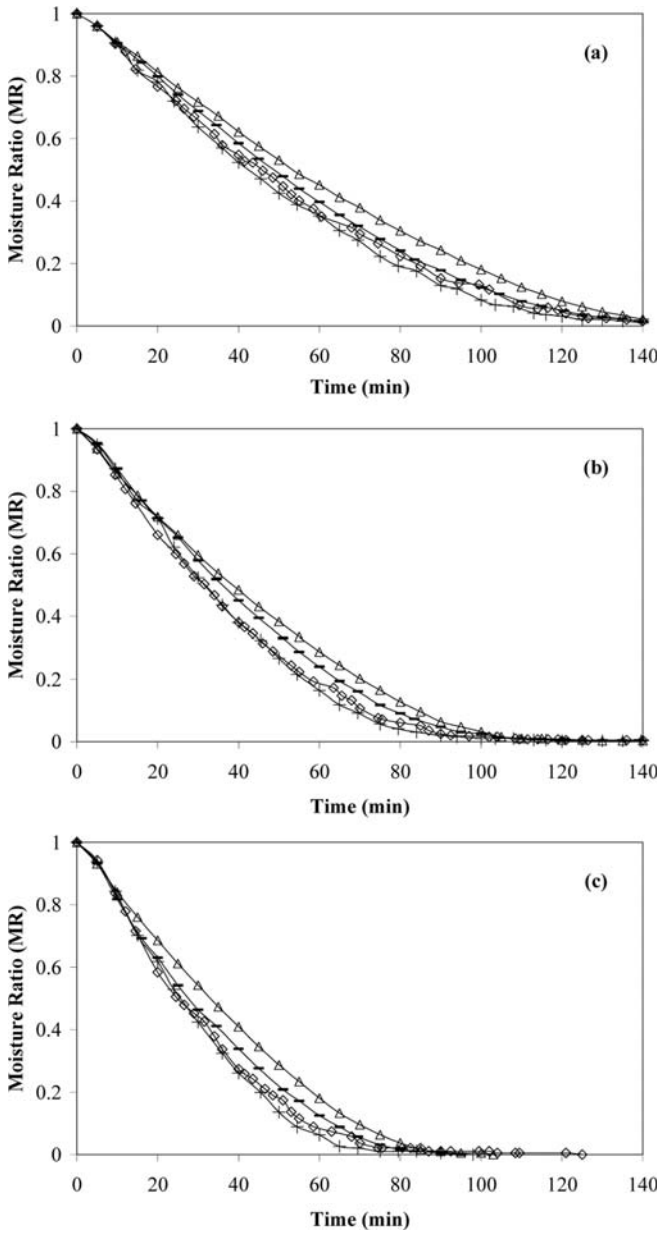

FIG. 7. Drying curves of banana chips undergoing intermittent pressure LPSSD at on:off period of 5:0 (−), 5:5 (+), 5:10 (◇), and continuous drying (Δ) at temperatures of (a) 70°C, (b) 80°C, and (c) 90°C.

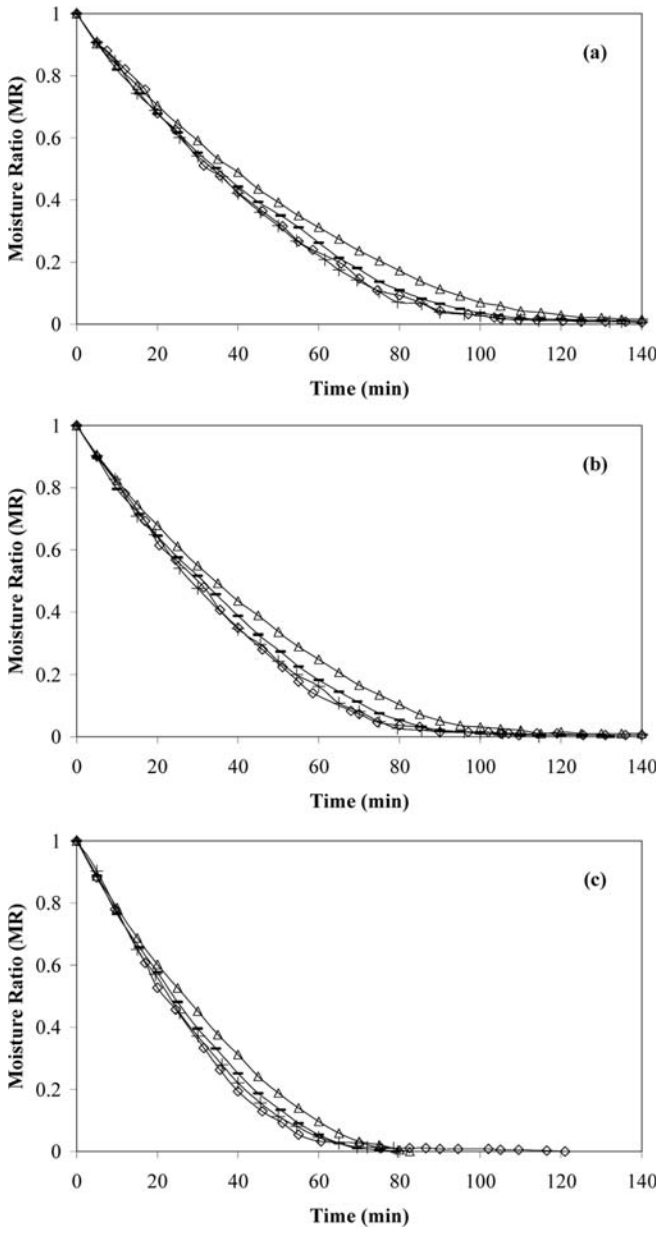

FIG. 8. Drying curves of banana chips undergoing intermittent pressure vacuum drying at on:off period of 5:0 (−), 5:5 (+), 5:10 (◇), and continuous drying (Δ) at temperatures of (a) 70°C, (b) 80°C, and (c) 90°C.

plots of the evolution of the chamber and sample temperatures; only selected plots are shown here for the sake of brevity, as the trends of temperature changes were the same at all tested conditions. In the case of intermittent pressure drying, the chamber absolute pressure was pulsed from 7 kPa during an on period to 100 kPa during an off or tempering period. This led to a higher boiling temperature of the water. In the case of LPSSD, the sample surface temperature corresponds to the saturation temperature of water at the dryer operating pressure in the constant drying rate period. Hence, the sample temperature increased during an off period and then decreased back to the boiling temperature corresponding to the operating pressure of 7 kPa during an on period. On the other hand, the sample temperature in the case of continuous drying rose suddenly from its initial value and reached and remained rather constant at the boiling temperature of water corresponding to the operating pressure of 7 kPa until the constant drying

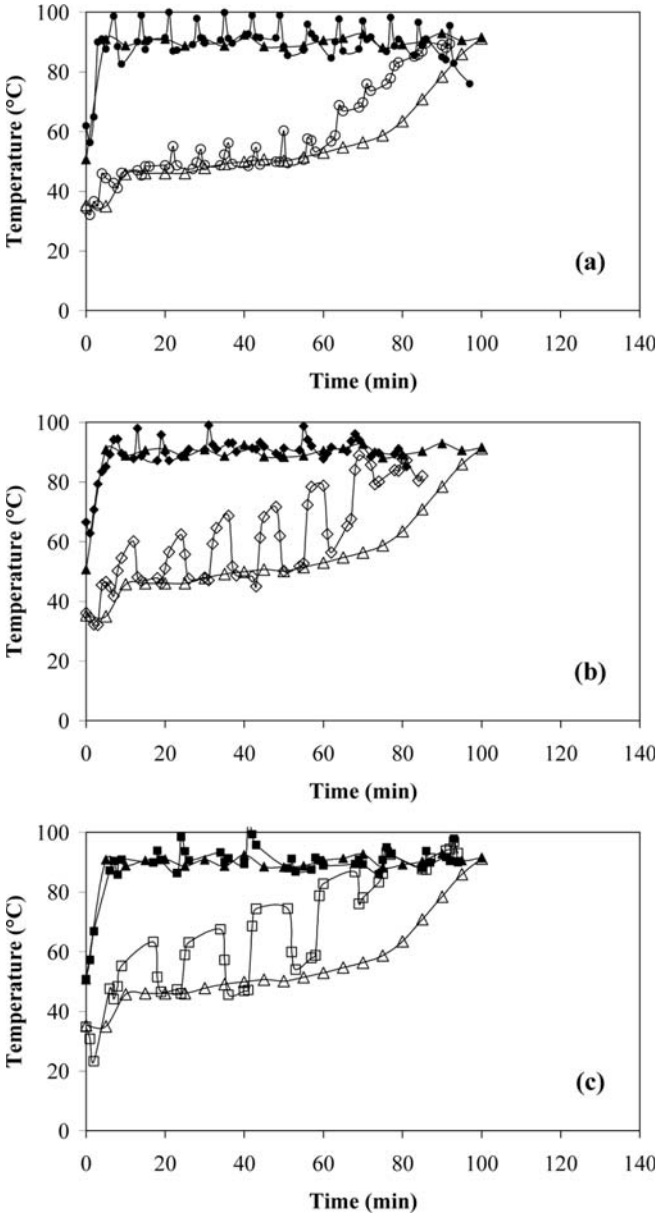

FIG. 9. Chamber (opaque sign) and sample (transparent sign) temperatures during continuous and intermittent pressure LPSSD at 90°C. Continuous drying (Δ) vs. intermittent drying at on:off period of (a) 5:0 (○), (b) 5:5 (◇), and (c) 5:10 (€).

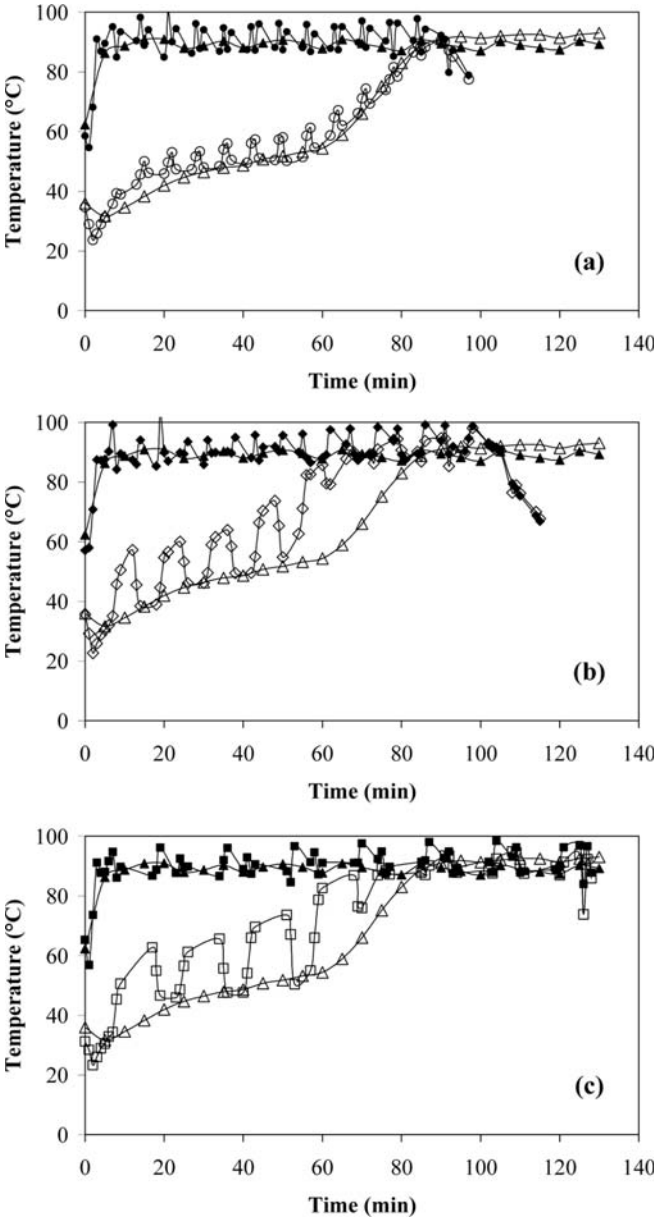

FIG. 10. Chamber (opaque sign) and sample (transparent sign) temperatures during continuous and intermittent pressure vacuum drying at 90°C. Continuous drying (Δ) vs. intermittent drying at on:off period of (a) 5:0 (◯), (b) 5:5 (◇), and (c) 5:10 (€).

rate period ended. Then the sample temperature rose again to approach the drying medium temperature.

In the case of vacuum drying, the sample temperature in the case of continuous drying rose steadily from its initial value to the drying medium temperature. A similar behavior was also noted by Devahastin et al.[3] The temperature of samples undergoing intermittent vacuum drying was also higher than that of continuous drying due to the effect of pressure variation. It was noted also that the sample temperature at longer tempering or off period was higher for longer duration. This phenomenon led to higher drying rates. Moreover, the decompression of pressure induced porous structure of the sample. This is the tunneling effect mentioned by Chua et al.;[18] after the drying process, the blind pores were observed to transform to interconnected pores. With the network of interconnected pores, the moisture diffusivity could be expected to improve significantly. The internal moisture was thus able to migrate

easily to the product surface.[13] This result promoted moisture transport within the sample and therefore improved the drying rates.

It is seen in Table 2 that the total drying time at on:off periods of 5:0 and 5:5 min at all conditions was similar to that of continuous drying while at an on:off period of 5:10 min the total drying time of intermittent drying was longer. However, it is seen in Table 2 that the net (or effective) drying time in the case of intermittent drying was shorter than the drying time of continuous drying.

Table 3 shows the energy savings of intermittent LPSSD and vacuum drying in comparison with continuous drying at various conditions. The savings in drying time were first calculated by subtracting the drying time of continuous drying with the net or effective drying time, which was the time that the drying process was actually on, and then

TABLE 3
Energy savings of intermittent LPSSD and vacuum drying at various conditions

Condition				Energy saving over continuous drying (%)		
Drying scheme	Drying method	Temp. (°C)	Intermittency (on:off, min)	Vacuum pump	Electric heater	Steam
Intermittent temperature scheme	LPSSD	70	10:5	—	N/A	N/A
			10:10	—	N/A	N/A
			10:20	—	N/A	N/A
		80	10:5	—	36	36
			10:10	—	53	53
			10:20	—	66	66
		90	10:5	—	30	30
			10:10	—	46	46
			10:20	—	65	65
	Vacuum drying	70	10:5	—	N/A	—
			10:10	—	N/A	—
			10:20	—	N/A	—
		80	10:5	—	24	—
			10:10	—	33	—
			10:20	—	52	—
		90	10:5	—	20	—
			10:10	—	32	—
			10:20	—	49	—
Intermittent pressure scheme	LPSSD	70	5:0	N/A	—	N/A
			5:5	N/A	—	N/A
			5:10	N/A	—	N/A
		80	5:0	11	—	26
			5:5	53	—	60
			5:10	61	—	67
		90	5:0	22	—	34
			5:5	55	—	62
			5:10	51	—	58
	Vacuum drying	70	5:0	N/A	—	—
			5:5	N/A	—	—
			5:10	N/A	—	—
		80	5:0	9	—	—
			5:5	50	—	—
			5:10	52	—	—
		90	5:0	22	—	—
			5:5	55	—	—
			5:10	53	—	—

N/A implies that, at this condition, the final banana moisture content of 0.025 kg/kg (d.b.) was not achievable.

dividing the result with the drying time of continuous drying. In the case of intermittent temperature drying, the vacuum pump was continuously used to maintain the pressure at 7 kPa. In the case of intermittent pressure drying, the heater was turned on continuously to maintain the temperature at the setting values. This information was used along with the time savings calculated above to determine the energy savings at each condition. Energy savings of steam in the case of intermittent vacuum drying was not calculated since steam was not injected into the chamber during vacuum drying.

It was found that intermittent temperature LPSSD at all temperatures could save the energy consumption of the electric heater more (up to about 65% at an on:off period of 10:20 min) than in the case of intermittent vacuum drying. Moreover, the power of the heater (in kWh) used in the case of LPSSD was lower than in the case of vacuum drying due to the fact that the electric heater was used more often during vacuum drying. Steam could also be saved up to about 65% in the case of intermittent LPSSD, both at 80 and 90°C, at an on:off period of 10:20 min.

In the case of intermittent pressure drying, it was observed that the energy savings of the vacuum pump in the case of LPSSD at fixed values of temperature and intermittency were similar to that of vacuum drying, which was around 50–60%. The energy savings of intermittent pressure LPSSD at 80°C and at an on:off period of 5:10 min was especially large due to a very long drying time of continuous drying at this condition. It is important to mention that, in the case of intermittent pressure LPSSD, steam was injected into the chamber during each vacuum cycle when the pressure was reduced to 7 kPa, which occurred after the vacuum pump was started for about 1.5 min. Therefore, the energy savings in terms of steam was larger than in terms of vacuum pump since the pump needed to be on longer than the on period of steam injection.

Considering the behavior of both drying processes at all conditions it was found that the drying rates in both intermittent pressure LPSSD and vacuum drying cases were higher than those in the cases of continuous drying and intermittent temperature drying. However, it was noted that the drying rates in the case of intermittent pressure

TABLE 4
Color changes of banana chips dried by intermittent temperature drying

Condition			Color changes		
Drying method	Temp. (°C)	Intermittency (on:off, min)	$\Delta L/L_0$	$\Delta a/a_0$	$\Delta b/b_0$
LPSSD	70	Continuous drying	N/A	N/A	N/A
		10:5	N/A	N/A	N/A
		10:10	N/A	N/A	N/A
		10:20	N/A	N/A	N/A
	80	Continuous drying	-0.01 ± 0.002^{c}	-0.41 ± 0.10^{c}	0.07 ± 0.009^{ab}
		10:5	-0.01 ± 0.006^{c}	-0.39 ± 0.02^{c}	0.05 ± 0.006^{ab}
		10:10	-0.01 ± 0.003^{c}	-0.33 ± 0.54^{c}	0.09 ± 0.009^{ab}
		10:20	-0.01 ± 0.007^{c}	-0.32 ± 0.01^{c}	0.10 ± 0.008^{ab}
	90	Continuous drying	-0.06 ± 0.003^{ab}	-0.54 ± 0.01^{bc}	0.08 ± 0.010^{ab}
		10:5	-0.05 ± 0.002^{bc}	-0.57 ± 0.02^{bc}	0.10 ± 0.001^{b}
		10:10	-0.03 ± 0.008^{bc}	-0.44 ± 0.04^{bc}	0.10 ± 0.003^{b}
		10:20	-0.02 ± 0.005^{c}	-0.66 ± 0.19^{bc}	0.07 ± 0.005^{ab}
Vacuum drying	70	Continuous drying	N/A	N/A	N/A
		10:5	N/A	N/A	N/A
		10:10	N/A	N/A	N/A
		10:20	N/A	N/A	N/A
	80	Continuous drying	-0.01 ± 0.003^{c}	-0.66 ± 0.01^{abc}	0.07 ± 0.005^{ab}
		10:5	-0.02 ± 0.005^{c}	-0.66 ± 0.02^{abc}	0.11 ± 0.011^{b}
		10:10	-0.02 ± 0.003^{c}	-0.64 ± 0.01^{bc}	0.10 ± 0.008^{b}
		10:20	-0.01 ± 0.005^{c}	-0.57 ± 0.02^{bc}	0.16 ± 0.001^{c}
	90	Continuous drying	-0.07 ± 0.008^{ab}	-0.89 ± 0.08^{ab}	0.07 ± 0.004^{ab}
		10:5	-0.08 ± 0.008^{a}	-0.91 ± 0.08^{ab}	0.09 ± 0.014^{ab}
		10:10	-0.06 ± 0.006^{ab}	-0.92 ± 0.05^{ab}	0.10 ± 0.014^{ab}
		10:20	-0.05 ± 0.007^{bc}	-0.66 ± 0.02^{abc}	0.17 ± 0.009^{c}

N/A implies that, at this condition, the final banana moisture content of 0.025 kg/kg (d.b.) was not achievable.
Different letters in the same column indicate that values are significantly different ($\alpha < 0.05$).

LPSSD at fixed temperature and on:off period were similar to those in the case of intermittent pressure vacuum drying. However, the energy consumption of vacuum drying was lower than that of LPSSD due to the absence of steam injection.

Quality of Dried Banana Chips

The quality of banana chips was investigated after drying with different schemes as mentioned earlier; the final moisture content of the product was set at 0.025 kg/kg (d.b.). However, the equilibrium moisture content of banana chips dried either by LPSSD or vacuum drying at 70°C (approximately 0.04 kg/kg dry basis) was more than the desired final moisture content. Thus, the quality of banana chips dried at 70°C was not determined in this study.

Colors

Hunter color parameters (L, a, and b) were determined in order to investigate the color changes of banana chips. The normalized changes of lightness ($\Delta L/L_0$), redness ($\Delta a/a_0$), and yellowness ($\Delta b/b_0$) of banana underwent intermittent temperature drying and intermittent pressure drying are shown in Tables 4 and 5, respectively.

It was observed that the drying methods (LPSSD and vacuum drying at the same temperature) did not significantly affect the color changes of banana chips when continuous drying was performed. However, the trend was that the color changes (especially lightness and redness) of banana chips dried by LPSSD were less than those dried by vacuum drying. This may be due to enzymatic browning reactions, which mainly depend on the level of oxygen and temperature of the product. Since LPSSD is an airless drying process and contains no oxygen in the system, the samples suffered less changes of color. Furthermore, it is seen in Figs. 4 and 5 that the temperature of samples undergoing LPSSD was lower than those undergoing vacuum drying.

The effect of drying temperature on the color changes was also observed. It is seen in Table 4 that at a high temperature of 90°C, colors changed more obviously than at lower temperatures of 70 and 80°C. This is because higher temperature leads to a higher rate of browning reaction.

TABLE 5
Color changes of banana chips dried by intermittent pressure drying

Condition			Color changes		
Drying method	Temp. (°C)	Intermittency (on:off, min)	$\Delta L/L_0$	$\Delta a/a_0$	$\Delta b/b_0$
LPSSD	70	Continuous drying	N/A	N/A	N/A
		5:0	N/A	N/A	N/A
		5:5	N/A	N/A	N/A
		5:10	N/A	N/A	N/A
	80	Continuous drying	-0.01 ± 0.002^{d}	-0.41 ± 0.10^{c}	0.07 ± 0.009^{d}
		5:0	-0.09 ± 0.01^{c}	-1.40 ± 0.53^{abc}	-0.01 ± 0.005^{d}
		5:5	-0.24 ± 0.02^{a}	-2.18 ± 0.91^{ab}	-0.14 ± 0.004^{b}
		5:10	-0.27 ± 0.01^{a}	-2.00 ± 0.77^{ab}	-0.15 ± 0.015^{b}
	90	Continuous drying	-0.06 ± 0.003^{c}	-0.54 ± 0.01^{bc}	0.08 ± 0.001^{d}
		5:0	-0.16 ± 0.01^{b}	-1.38 ± 0.80^{abc}	0.03 ± 0.011^{cd}
		5:5	-0.24 ± 0.01^{a}	-1.75 ± 0.55^{abc}	-0.18 ± 0.007^{ab}
		5:10	-0.24 ± 0.01^{a}	-2.49 ± 0.96^{a}	-0.17 ± 0.009^{ab}
Vacuum drying	70	Continuous drying	N/A	N/A	N/A
		5:0	N/A	N/A	N/A
		5:5	N/A	N/A	N/A
		5:10	N/A	N/A	N/A
	80	Continuous drying	-0.01 ± 0.003^{d}	-0.66 ± 0.01^{c}	0.07 ± 0.001^{d}
		5:0	-0.17 ± 0.01^{b}	-0.91 ± 0.20^{bc}	-0.05 ± 0.011^{c}
		5:5	-0.24 ± 0.01^{a}	-1.22 ± 0.17^{abc}	-0.12 ± 0.003^{b}
		5:10	-0.26 ± 0.01^{a}	-1.16 ± 0.19^{abc}	-0.16 ± 0.006^{ab}
	90	Continuous drying	-0.07 ± 0.008^{c}	-0.89 ± 0.08^{c}	0.07 ± 0.005^{d}
		5:0	-0.19 ± 0.01^{b}	-0.94 ± 0.01^{bc}	-0.03 ± 0.003^{c}
		5:5	-0.27 ± 0.01^{a}	-1.80 ± 0.03^{abc}	-0.16 ± 0.002^{b}
		5:10	-0.29 ± 0.01^{a}	-2.01 ± 0.02^{abc}	-0.16 ± 0.001^{ab}

N/A implies that, at this condition, the final banana moisture content of 0.025 kg/kg (d.b.) was not achievable.
Different letters in the same column indicate that values are significantly different ($\alpha < 0.05$).

Nevertheless, temperature only significantly affected the lightness of the samples; this trend was also observed only in the case of vacuum drying as well.

In addition, the effect of the intermittency of time-varying temperature drying on color change was determined. It was found that, compared to continuous drying, intermittent drying significantly reduced the change of lightness only when LPSSD was performed at 90°C and at an on:off period of 10:20 min. At this condition, the time that the sample was subjected to a high-temperature environment during an effective (on) drying period was the shortest. In the case of redness it was observed that the redness of banana chips that underwent intermittent drying was insignificantly different from that obtained by continuous drying. In the case of intermittent LPSSD, steam was not injected into the drying chamber during the off period; therefore, the drying medium in the tempering (off) period was similar to that of vacuum drying. Thus, the level of oxygen was greater than in the case of continuous drying. However, the temperature of the product was lower and therefore redness changes were not significantly different from those of continuous drying. In the case of yellowness, the changes of this color parameter in the case of intermittent drying were higher than those of continuous drying only when an on:off period of 10:20 min was used in the case of vacuum drying.

Overall, it was observed that, in almost all cases, the effect of intermittency or tempering period on the color changes was not significant when the same drying technique was used at the same setting temperature.

For the case of intermittent pressure drying the measured color changes are listed in Table 5. It was observed that the color changes of LPSSD samples were similar to those of vacuum drying. In the case of intermittent drying, the pressure increased from a vacuum condition to an atmospheric condition during the tempering period. The air with a high amount of oxygen was fed into the chamber to raise the chamber pressure, so the rates of browning reaction increased with the tempering time; this induced changes of colors of the samples. Therefore, at the same

TABLE 6
Texture of banana chips dried by intermittent temperature drying

Condition			Texture	
Drying method	Temp. (°C)	Intermittency (on:off, min)	Hardness (N)	Crispness (No. of peak)
LPSSD	70	Continuous drying	N/A	N/A
		10:5	N/A	N/A
		10:10	N/A	N/A
		10:20	N/A	N/A
	80	Continuous drying	21.52 ± 2.23^{ab}	27 ± 3^{abc}
		10:5	18.50 ± 2.97^{a}	27 ± 1^{ab}
		10:10	19.41 ± 1.12^{a}	31 ± 3^{abc}
		10:20	20.12 ± 2.90^{a}	32 ± 4^{abc}
	90	Continuous drying	24.09 ± 1.26^{ab}	28 ± 6^{abc}
		10:5	26.05 ± 2.47^{b}	33 ± 3^{abc}
		10:10	21.52 ± 5.43^{ab}	35 ± 2^{bc}
		10:20	20.49 ± 3.65^{ab}	36 ± 3^{c}
Vacuum drying	70	Continuous drying	N/A	N/A
		10:5	N/A	N/A
		10:10	N/A	N/A
		10:20	N/A	N/A
	80	Continuous drying	25.64 ± 7.21^{ab}	27 ± 1^{ab}
		10:5	22.79 ± 1.31^{ab}	23 ± 2^{a}
		10:10	20.46 ± 3.37^{ab}	30 ± 2^{abc}
		10:20	18.46 ± 2.12^{a}	31 ± 1^{abc}
	90	Continuous drying	26.44 ± 5.60^{b}	28 ± 7^{abc}
		10:5	20.99 ± 1.36^{ab}	28 ± 2^{abc}
		10:10	21.37 ± 4.49^{ab}	20 ± 4^{abc}
		10:20	16.81 ± 2.90^{a}	33 ± 6^{abc}

N/A implies that, at this condition, the final banana moisture content of 0.025 kg/kg (d.b.) was not achievable.
Different letters in the same column indicate that values are significantly different ($\alpha < 0.05$).

intermittency, the color changes of both drying methods were similar. However, it is seen in this table that the change of lightness of samples underwent LPSSD at 80°C with an on:off value of 5:0 min was significantly lower than for those that underwent vacuum drying. The same trends were observed for the change of yellowness. At an on:off period of 5:0 min, the time that the oxygen entered into the system was rather short. Hence, the effect of high oxygen content during the tempering period was small. It is seen that LPSSD yields lighter dried products due to the absence of oxygen during an on period.

Considering the effect of temperature (for the same drying method), it was found that the effect of temperature was only seen in change of lightness in the case of LPSSD at an on:off period of 5:0 min. The darker color at higher temperatures was due to the higher rates of browning reaction.

Regarding the effect of intermittency in each drying method and at each temperature, the lightness of samples that underwent intermittent drying significantly differed from those that underwent continuous drying. The products were darker at longer tempering periods due to the higher amount of oxygen in the system. It was observed that on:off periods of 5:0 and 5:5 min, both in the case of LPSSD and vacuum drying, significantly affected the change of lightness of the samples. However, when an on:off period changed to 5:10 min, the results were not significantly different. The changes of redness of intermittently dried products were also larger than those in the case of continuous drying. The results, however, were more significant for longer tempering periods in the case of LPSSD since the difference in the amount of oxygen between an on period where the drying medium was steam and tempering period where the drying medium was moist air was larger.

It was observed that the yellowness changes in the case of intermittent vacuum drying were significantly higher than those in the case of continuous vacuum drying. It was found that, at both temperatures, when the tempering period was longer, the yellowness of the products was lower.

TABLE 7
Texture of banana chips dried by intermittent pressure drying

Condition			Texture	
Drying method	Temp. (°C)	Intermittency (on:off, min)	Hardness (N)	Crispness (No. of peak)
LPSSD	70	Continuous drying	N/A	N/A
		5:0	N/A	N/A
		5:5	N/A	N/A
		5:10	N/A	N/A
	80	Continuous drying	21.52 ± 2.23^{ab}	27 ± 3^{a}
		5:0	20.12 ± 2.90^{ab}	32 ± 1^{a}
		5:5	27.26 ± 2.12^{abc}	27 ± 1^{a}
		5:10	27.34 ± 6.48^{abcd}	30 ± 5^{a}
	90	Continuous drying	24.09 ± 1.26^{abc}	28 ± 6^{a}
		5:0	19.41 ± 1.12^{ab}	35 ± 4^{a}
		5:5	33.71 ± 2.52^{cd}	33 ± 8^{a}
		5:10	35.07 ± 1.04^{d}	32 ± 6^{a}
Vacuum drying	70	Continuous drying	N/A	N/A
		5:0	N/A	N/A
		5:5	N/A	N/A
		5:10	N/A	N/A
	80	Continuous drying	25.64 ± 7.21^{abcd}	27 ± 1^{a}
		5:0	18.50 ± 2.97^{a}	33 ± 5^{a}
		5:5	23.87 ± 4.91^{abc}	30 ± 5^{a}
		5:10	27.38 ± 4.49^{abcd}	31 ± 3^{a}
	90	Continuous drying	26.44 ± 5.60^{abcd}	28 ± 7^{a}
		5:0	17.71 ± 1.12^{a}	37 ± 6^{a}
		5:5	25.05 ± 2.47^{abcd}	33 ± 2^{a}
		5:10	30.91 ± 5.54^{bcd}	32 ± 5^{a}

N/A implies that, at this condition, the final banana moisture content of 0.025 kg/kg (d.b.) was not achievable.
Different letters in the same column indicate that values are significantly different ($\alpha < 0.05$).

Texture

The texture (Tables 6 and 7) of dried banana chips is reported in terms of the hardness, which is the maximum breaking force, and crispness, which is the number of peaks in a force-deformation curve. A part of the samples with puffing (not core part) was cut to avoid the effect of dense structure at the core on the textural quality of the samples. This is because the samples were not puffed uniformly; less puffing was especially observed at the core. The blade-type probe was selected to cut the samples to represent the biting action of human front teeth.

Within the same drying method, the hardness and crispness of the products dried at a higher temperature (90°C) were higher than those obtained at a lower temperature (80°C). At higher temperature, water evaporated more intensely inside the sample and pushed open the cell structure, leading to high-porosity products. Hence, the products dried at higher temperature were crispier. However, more case hardening occurred at higher temperatures, leading to higher values of hardness. Nevertheless, the effect of temperature on these textural parameters was not significantly different. The effects of drying methods were not also significantly observed.

The effect of intermittency on the texture of the products was also determined. It was observed that generally the products that underwent intermittent temperature drying (Table 6) were less hard but crispier than those obtained with a continuous drying method. During a tempering period, in the case of intermittent temperature drying, heat was not supplied to the products. Therefore, moisture within the samples redistributed and moved to the surface. Hence, the samples were less stiff due to lower level of moisture gradient-induced stresses. Case hardening might occur to a lesser extent in the case of intermittent drying. However, the results were not significantly different among different conditions used.

In the case of intermittent pressure drying (Table 7), it is seen that the hardness at an on:off period of 5:0 min was not affected, whereas at on:off periods of 5:5 and 5:10 min the hardness was higher than in the case of continuous drying. During the tempering period in intermittent pressure drying, the sample temperature increased and approached the boiling point of water at higher pressure, as mentioned earlier. Rapid drying occurred in this period leading to case hardening. However, the period of high temperature when an on:off period of 5:0 min was used was rather short, so the effect on the hardness at this condition was negligible.

The results of hardness and crispness were also compared with those of commercially available freeze-dried banana chips. Hardness and crispness (number of peaks) of the commercially available vacuum–freeze-dried banana chips (Fruit King^{TM}) were 55.72 ± 5.48 N and 16 ± 3, respectively. Thus, all samples in this study had lower values of hardness and were crispier than the commercially available banana chips.

Shrinkage

Since it was noticed that, although banana pieces puffed and hence their volume increased, the cross-sectional area of dried banana chips seemed to be smaller than that of fresh banana, shrinkage was determined in terms of the change of the cross-sectional area compared with the original area of the sample.

It is seen in Table 8 that shrinkage of banana chips in the case of LPSSD at 80°C was higher than at 90°C. This might be because case hardening occurred least at this condition; case hardening prevented shrinkage of the

TABLE 8
Shrinkage of banana chips dried by intermittent temperature drying

Condition			
Drying method	Temp. (°C)	Intermittency (on:off, min)	Shrinkage (%) $(\Delta A/A_0) \times 100$
LPSSD	70	Continuous drying	N/A
		10:5	N/A
		10:10	N/A
		10:20	N/A
	80	Continuous drying	20.18 ± 1.70^{bc}
		10:5	22.23 ± 1.13^{c}
		10:10	21.23 ± 1.31^{c}
		10:20	22.19 ± 1.73^{c}
	90	Continuous drying	13.23 ± 0.61^{a}
		10:5	14.84 ± 0.57^{ab}
		10:10	14.90 ± 1.11^{ab}
		10:20	14.70 ± 1.85^{ab}
Vacuum drying	70	Continuous drying	N/A
		10:5	N/A
		10:10	N/A
		10:20	N/A
	80	Continuous drying	19.20 ± 0.81^{bc}
		10:5	19.14 ± 1.60^{bc}
		10:10	16.34 ± 0.29^{ab}
		10:20	16.72 ± 0.79^{abc}
	90	Continuous drying	16.05 ± 0.03^{ab}
		10:5	18.11 ± 1.41^{abc}
		10:10	16.34 ± 0.42^{ab}
		10:20	18.16 ± 1.64^{abc}

N/A implies that, at this condition, the final banana moisture content of 0.025 kg/kg (d.b.) was not achievable.

Different letters in the same column indicate that values are significantly different ($\alpha < 0.05$).

sample. The same trend was found for vacuum drying, for which shrinkage was less when a higher temperature was used. However, it was noted that the drying method did not significantly affect the shrinkage at the same drying temperature.

Shrinkage in the case of intermittent pressure drying was also observed (Table 9). It was found that shrinkage of the samples that underwent intermittent pressure drying was more obvious than in the case of continuous drying at all conditions. This may be due to the effect of pressure compression. In the case of intermittent drying, pressure was raised from 7 to 100 kPa during an off period. Therefore, the samples were pressed by the external pressure (force) and then collapsed. This collapse in turn led to more shrinkage of the samples.

Ascorbic Acid Retention

The percentages of ascorbic acid retention in banana chips that underwent intermittent temperature and intermittent pressure drying are shown in Tables 10 and 11, respectively. It was observed that LPSSD prevents degradation of ascorbic acid better than vacuum drying. This is because the amount of oxygen, which causes aerobic degradation of ascorbic acid, in LPSSD was lower than in the case of vacuum drying.

Temperature was also found to affect the degradation of ascorbic acid. As expected, the ascorbic acid retention at a high temperature was less than at a low temperature in both LPSSD and vacuum drying. A similar result was found when drying gooseberry flake in LPSSD and vacuum drying.[4]

TABLE 9
Shrinkage of banana chips dried by intermittent pressure drying

Condition			
Drying method	Temp. (°C)	Intermittency (on:off, min)	Shrinkage (%) $(\Delta A/A_0) \times 100$
LPSSD	70	Continuous drying	N/A
		5:0	N/A
		5:5	N/A
		5:10	N/A
	80	Continuous drying	20.18 ± 1.70^{cd}
		5:0	26.48 ± 0.63^{e}
		5:5	28.52 ± 0.20^{e}
		5:10	27.79 ± 0.05^{e}
	90	Continuous drying	13.23 ± 0.61^{a}
		5:0	18.86 ± 0.75^{bc}
		5:5	21.48 ± 1.01^{d}
		5:10	21.82 ± 0.28^{d}
Vacuum drying	70	Continuous drying	N/A
		5:0	N/A
		5:5	N/A
		5:10	N/A
	80	Continuous drying	19.20 ± 0.81^{cd}
		5:0	19.88 ± 1.65^{bcd}
		5:5	20.76 ± 0.77^{cd}
		5:10	20.83 ± 0.81^{d}
	90	Continuous drying	16.05 ± 0.03^{ab}
		5:0	16.48 ± 1.50^{ab}
		5:5	21.37 ± 0.83^{d}
		5:10	21.36 ± 0.96^{d}

N/A implies that, at this condition, the final banana moisture content of 0.025 kg/kg (d.b.) was not achievable.

Different letters in the same column indicate that values are significantly different ($\alpha < 0.05$).

TABLE 10
Ascorbic acid retention of banana chips dried by intermittent temperature drying

Condition			
Drying method	Temp. (°C)	Intermittency (on:off, min)	Ascorbic acid retention (%)
LPSSD	70	Continuous drying	N/A
		10:5	N/A
		10:10	N/A
		10:20	N/A
	80	Continuous drying	53.14 ± 2.79^{bc}
		10:5	62.09 ± 1.94^{cd}
		10:10	65.09 ± 2.07^{d}
		10:20	63.99 ± 0.52^{d}
	90	Continuous drying	41.33 ± 2.76^{a}
		10:5	52.78 ± 2.40^{bc}
		10:10	64.46 ± 4.39^{d}
		10:20	55.78 ± 2.55^{d}
Vacuum drying	70	Continuous drying	N/A
		10:5	N/A
		10:10	N/A
		10:20	N/A
	80	Continuous drying	40.75 ± 2.73^{a}
		10:5	44.63 ± 3.73^{ab}
		10:10	44.94 ± 2.47^{ab}
		10:20	55.37 ± 2.73^{cd}
	90	Continuous drying	37.76 ± 2.63^{a}
		10:5	44.10 ± 0.80^{a}
		10:10	54.04 ± 1.53^{bcd}
		10:20	58.35 ± 3.01^{d}

N/A implies that, at this condition, the final banana moisture content of 0.025 kg/kg (d.b.) was not achievable.

Different letters in the same column indicate that values are significantly different ($\alpha < 0.05$).

TABLE 11
Ascorbic acid retention of banana chips dried by intermittent pressure drying

Condition			
Drying method	Temp. (°C)	Intermittency (on:off, min)	Ascorbic acid retention (%)
LPSSD	70	Continuous drying	N/A
		5:0	N/A
		5:5	N/A
		5:10	N/A
	80	Continuous drying	53.14 ± 2.79^{g}
		5:0	47.74 ± 2.21^{fg}
		5:5	41.60 ± 2.62^{ef}
		5:10	30.05 ± 2.42^{bc}
	90	Continuous drying	41.33 ± 2.76^{ef}
		5:0	37.04 ± 1.70^{de}
		5:5	31.20 ± 3.17^{bcd}
		5:10	25.76 ± 1.89^{ab}
Vacuum drying	70	Continuous drying	N/A
		5:0	N/A
		5:5	N/A
		5:10	N/A
	80	Continuous drying	40.75 ± 2.73^{ef}
		5:0	37.78 ± 0.41^{de}
		5:5	31.67 ± 0.89^{bcd}
		5:10	29.14 ± 2.53^{bc}
	90	Continuous drying	37.76 ± 2.63^{de}
		5:0	33.20 ± 1.42^{cde}
		5:5	30.47 ± 2.14^{bcd}
		5:10	21.82 ± 1.82^{a}

N/A implies that, at this condition, the final banana moisture content of 0.025 kg/kg (d.b.) was not achievable.

Different letters in the same column indicate that values are significantly different ($\alpha < 0.05$).

Intermittent temperature drying conditions led to a higher level of ascorbic acid retention, especially at longer tempering (off) period, because the samples were subjected less to high-temperature environment during drying. For long tempering period (10:20 min), the effect of the drying method was not observed, however; this may be because intermittent LPSSD system effectively became vacuum drying under this condition.

Regarding the effect of intermittent pressure drying on ascorbic acid retention, it was found that intermittent pressure drying led to more degradation of ascorbic acid. In the case of intermittent pressure drying, oxygen was fed into the chamber with air to raise the chamber pressure to atmosphere in tempering period. This caused more aerobic loss of ascorbic acid. Moreover, the temperatures of the samples during intermittent drying were higher than in the case of continuous drying, leading to higher levels of ascorbic acid degradation.

CONCLUSIONS

The effects of intermittency and on-period setting drying temperature on the drying kinetics and quality of banana chips undergoing intermittent LPSSD and vacuum drying were investigated and compared with the results of continuous drying. In the case of intermittent temperature LPSSD, the overall drying rates of intermittent and continuous LPSSD were not significantly different. However, the effective or net drying time of intermittent drying was significantly shorter than that of continuous drying, especially at longer tempering periods, leading to high energy savings. Intermittent temperature LPSSD at 90°C and an on:off period of 10:20 min can reduce energy consumption by up to 65% compared with continuous drying. It was noted that the drying rates of intermittent pressure LPSSD and vacuum drying at all conditions were obviously higher than those of continuous drying. This implied energy savings of the vacuum pump of up to 51 and 53% in the cases of intermittent pressure LPSSD and vacuum drying, respectively; steam savings in the case of intermittent pressure LPSSD of up to 58% could be achieved.

The quality measurements showed that the effect of intermittency in intermittent temperature drying in almost all cases, when compared with continuous drying, was not significant except for changes in lightness, which was reduced only when LPSSD was performed at 90°C and at an on:off period of 10:20 min. Besides, it was observed that the colors of the products in the case of intermittent pressure drying was worse than that in the case of continuous drying. It was found that the product texture in almost all cases was not significantly different. Moreover, it was observed that intermittent temperature drying did not affect the shrinkage of the product, whereas the shrinkage of the samples that underwent intermittent pressure drying was more obvious than in the case of continuous drying at all conditions. Finally, intermittent temperature drying led to higher level of ascorbic acid retention, especially at longer tempering (off) periods. On the other hand, intermittent pressure drying led to greater degradation of ascorbic acid.

ACKNOWLEDGEMENTS

The authors express their sincere appreciation to the Commission on Higher Education, the Thailand Research Fund (TRF), and the International Foundation for Science (IFS), Sweden, for supporting this study financially.

REFERENCES

1. Elustondo, D.; Elustondo, M.P.; Urbicain, M.J. Mathematical modeling of moisture evaporation from foodstuffs exposed to subatmospheric pressure superheated steam. Journal of Food Engineering **2001**, *49*, 15–24.

2. Mujumdar, A.S. Superheated steam drying-technology of the future. In *Mujumdar's Practical Guide to Industrial Drying*, Devahastin, S., Ed.; Exergex: Brossard, Canada, 2000; 115–138.
3. Devahastin, S.; Suvarnakuta, P.; Soponronnarit, S.; Mujumdar, A.S. A comparative study of low-pressure superheated steam and vacuum drying of a heat-sensitive material. Drying Technology **2004**, *22*, 1845–1867.
4. Methakhup, S.; Chiewchan, N.; Devahastin, S. Effects of drying methods and conditions on drying kinetics and quality of Indian gooseberry flake. Lebensmittel-Wissenschaft und-Technologie **2005**, *38*, 579–587.
5. Suvarnakuta, P.; Devahastin, S.; Mujumdar, A.S. Drying kinetics and β-carotene degradation in carrot undergoing different drying processes. Journal of Food Science **2005**, *70*, S520–S526.
6. Leeratanarak, N.; Devahastin, S.; Chiewchan, N. Drying kinetics and quality of potato chips undergoing different drying techniques. Journal of Food Engineering **2006**, *77*, 635–643.
7. Ratti, C.; Mujumdar, A.S. Fixed-bed batch drying of shrinking particles with time varying drying air conditions. Drying Technology **1993**, *11*, 1311–1355.
8. Jumah, R.Y.; Mujumdar, A.S.; Raghavan, G.S.V. A mathematical model for constant and intermittent batch drying of grains in a novel rotating jet spouted bed. Canadian Journal of Chemical Engineering **1996**, *74*, 479–486.
9. Devahastin, S.; Mujumdar, A.S. Batch drying of grains in a well-mixed dryer—Effect of continuous and stepwise change in drying air temperature. Transactions of the ASAE **1999**, *42*, 421–425.
10. Jumah, R.Y.; Mujumdar, A.S. Modeling intermittent drying using an adaptive neuro-fuzzy inference system. Drying Technology **2005**, *23*, 1075–1092.
11. Chua, K.J.; Mujumdar, A.S.; Hawlader, M.N.A.; Chou, S.K.; Ho, J.C. Batch drying of banana pieces—Effect of stepwise change in drying air temperature on drying kinetics and product colour. Food Research International **2001**, *34*, 721–731.
12. Islam, M.R.; Ho, J.C.; Mujumdar, A.S. Convective drying with time-varying heat input: Simulation results. Drying Technology **2003**, *21*, 1333–1356.
13. Rakotozafy, H.; Louka, N.; Therisod, M.; Therisod, H.; Allaf, K. Drying of baker's yeast by a new method: Dehydration by successive pressure drops: Effect on cell survival and enzymatic activities. Drying Technology **2000**, *18*, 2253–2271.
14. Gunasekaran, S. Pulsed microwave-vacuum drying of food materials. Drying Technology **1999**, *17*, 395–412.
15. Xing, H.; Takhar, P.S.; Helms, G.; He, B. NMR imaging of continuous and intermittent drying of pasta. Journal of Food Engineering **2007**, *78*, 61–68.
16. Association of Official Analytical Chemists. *Official Methods of Analysis*, 15th Ed.; AOAC: Washington, D.C., 1995.
17. Suvarnakuta, P.; Devahastin, S.; Soponronnarit, S.; Mujumdar, A.S. Drying kinetics and inversion temperature in a low-pressure superheated steam drying system. Industrial & Engineering Chemistry Research **2005**, *44*, 1934–1941.
18. Chua, K.J.; Chou, S.K. On the experimental study of a pressure regulatory system for bioproducts dehydration. Journal of Food Engineering **2004**, *62*, 151–158.

Drying Technology, 24: 1509–1513, 2006

ISSN: 0737-3937 print/1532-2300 online
DOI: 10.1080/07373930600961306

Taylor & Francis
Taylor & Francis Group

Effects of Drying Methods and Tea Preparation Temperature on the Amount of Vitamin C in Indian Gooseberry Tea

Pao Kongsoontornkijkul, Prakaithip Ekwongsupasarn, Naphaporn Chiewchan, and Sakamon Devahastin

Department of Food Engineering, Faculty of Engineering, King Mongkut's University of Technology Thonburi, Bangkok, Thailand

Indian gooseberry is a rich source of vitamin C. The fruit can be consumed either fresh or after processing into different products including Indian gooseberry tea. Both drying and tea preparation steps affect quality of the gooseberry tea drink made using dried gooseberry. This study investigated the effects of different drying methods, i.e., hot air drying, vacuum drying, and low-pressure superheated steam drying, on the retention and degradation of vitamin C (in terms of the total ascorbic acid content, TAA) in dried gooseberry flakes. In addition, the effect of temperature of water used to prepare the tea on the release of TAA and on its later degradation was also investigated.

Keywords Ascorbic acid; Hot air drying; Leachability; Low-pressure superheated steam drying; Porosity; Release kinetics; Vacuum drying

INTRODUCTION

Indian gooseberry (*Phyllanthus emblica* Linn.), or "Ma-khaam Pom" in Thai and "Amla" in Hindi and several Indian languages, is a fruit native to the tropical Southeast Asian region.[1] The fruit is known as a good source of natural vitamin C or ascorbic acid and its flesh is used as an ingredient in herbal medicine; it can also be processed into various forms such as pickles, marmalades, and beverage products, including herbal or fruit tea.

Indian gooseberry tea is an alternative drink to typical or fruit teas. The tea production simply starts from grinding Indian gooseberry flesh into small pieces, subjecting the ground product to a drying process, and then packing the dried product in a tea bag. Drying is one of the most important steps during the tea production as it affects directly the quality of the dried product, in terms of its physical and/or nutraceutical property, which is naturally related to the quality of the tea. Application of a suitable drying technology and selection of appropriate drying conditions are therefore of great importance in the production of a good quality tea product.

Methakhup et al.[2] studied the effects of drying methods, i.e., vacuum drying and low-pressure superheated steam drying, and conditions on the drying kinetics and quality of Indian gooseberry flakes. Their results showed that the product subjected to vacuum drying at 75°C and at an absolute pressure of 7 kPa contained similar level of ascorbic acid retention compared to those dried by low-pressure superheated steam drying at 65 and 75°C at absolute pressures of 7–13 kPa.

In addition to the loss during drying, vitamin C contained in the dried flake also degrades during the tea preparation step due to the use of high-temperature water to prepare tea. Moreover, the leachability of vitamin C from the solid structure of the flake is also of importance; this ability is again related directly to the choices of the drying process and conditions, which in turn affect the microstructure of the dried product.[3–8]

This work aimed at a study of the effects of various drying methods, viz. hot air drying, vacuum drying, and low-pressure superheated steam drying, and the water temperature during Indian gooseberry tea preparation on the amount of ascorbic acid available in the final tea drink. Consideration was given on both the release of vitamin C (in terms of TAA) from the dried flakes and on the degradation of vitamin C during tea preparation.

MATERIALS AND METHODS

Materials

Fresh Indian gooseberry was obtained from a local market and stored in a refrigerator at 5°C until the time of experiment. After rinsing with tap water, the seeds of the fruit were removed. The flesh was then cut into small pieces and blended for one minute in an electric blender (Moulinex, AS184, France). Forty grams of the prepared sample

Correspondence: Naphaporn Chiewchan, Department of Food Engineering, Faculty of Engineering, King Mongkut's University of Technology Thonburi, 126 Pracha u-tid Road, Bangkok 10140, Thailand; E-mail: naphaporn.rat@kmutt.ac.th

was then spread on an aluminum foil sample holder ($9.5 \times 9.5\,cm^2$) and introduced to a drying process.

Experimental Setup

A schematic diagram of a low-pressure superheated steam dryer and its accessories is shown in Fig. 1.[9] The dryer consists of a stainless steel drying chamber with inner dimensions of $45 \times 45 \times 45\,cm^3$; a steam reservoir, which received the steam from a boiler and maintained its pressure at around 200 kPa (gage); and a liquid ring vacuum pump (Nash, ET32030, Trumbull, Connecticut), which was used to maintain the vacuum in the drying chamber. A steam trap was installed to reduce the excess steam condensation in the reservoir. An electric heater, rated at 1.5 kW, which was controlled by a proportional-integral-derivative controller (Omron, E5CN, Tokyo, Japan), was installed in the drying chamber to control the steam temperature and to minimize the condensation of steam in the drying chamber during the startup period. A variable-speed electric fan was used to disperse steam throughout the drying chamber. The sample holder was made of stainless steel with dimensions of $12 \times 12\,cm^2$. The change of the mass of the sample was detected continuously (at 30-s intervals) using a load cell (Minibea, Ucg-3 kg, Nagano, Japan), which was installed in a smaller chamber connected to the drying chamber and also to an indicator and recorder (A & D Co., AD 4329, Tokyo, Japan). The temperatures of the steam and of the drying sample were measured continuously using type K thermocouples, which were connected to an expansion board (Omega Engineering, EXP-32, Stamford, Connecticut). Thermocouple signals were multiplexed to a data acquisition card (Omega Engineering, CIO-DAS16Jr.) installed on a PC. LABTECH NOTEBOOK software (version 12.1, Laboratory Technologies Corp., Massachusetts) was used to read and record the temperature data.

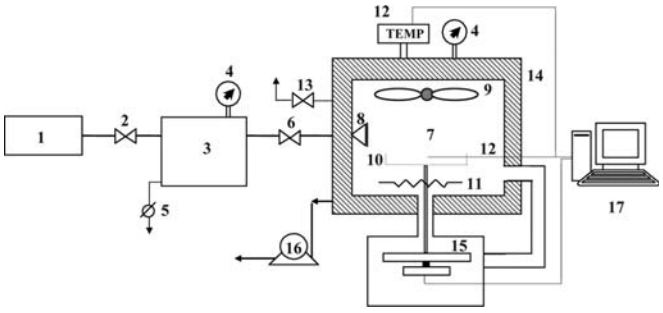

FIG. 1. schematic diagram of low-pressure superheated steam dryer and associated units. 1, boiler; 2, steam valve; 3, steam reservoir; 4, pressure gauge; 5, steam trap; 6, steam regulator; 7, drying chamber; 8, steam inlet and distributor; 9, electric fan; 10, sample holder; 11, electric heater; 12, on-line temperature sensor and logger; 13, vacuum break-up valve; 14, insulator; 15, on-line mass indicator and logger; 16, vacuum pump; 17, PC with installed data acquisition card.

For the vacuum drying experiments the same experimental set-up was used but without application of steam to the drying chamber. A hot air oven (Memmert, ULM 600 II, Germany) was used for hot air drying experiments.

Production of Indian Gooseberry Flakes

Based on the previous study and our preliminary investigation, the sample was subjected to drying in a hot air oven at 75°C for 180 min while it was dried in a vacuum dryer at 75°C, 7 kPa for 145 min and a low-pressure superheated steam dryer, also at 75°C, 7 kPa, for 280 min.[2] These conditions gave the final moisture content of Indian gooseberry flake of 0.07 kg/kg (d.b.), which is the standard moisture content recommended for tea.[10] Two grams of dried flake were packed into a tea bag ($4 \times 5\,cm^2$). The tea bag was vacuum packed in a laminated aluminum packet to protect vitamin C from oxidative reaction prior to subsequent tea preparation.

Tea Preparation

Two hundred fifty milliliters of distilled water was heated and controlled at 70 ± 1°C, 80 ± 1°C, and 90 ± 1°C, which are typical temperatures used to prepare tea, by a water bath. A tea bag containing dried gooseberry flake from each of the three drying processes was then soaked into 250 mL of hot water. The prepared tea was sampled at 0, 1, 2, 5, 8, 11, 14, 17, and 20 min for TAA analysis. All experiments were performed in duplicate.

Total Ascorbic Acid (TAA) Determination

In this study, vitamin C was determined in terms of TAA by Roe and Kuther's method.[11] The assay estimates the intensity of osazone formed by the coupling of 2,4-dinitrophenylhydrazine (DNPH) with the oxidative forms of ascorbic acid, which are dehydroascorbic acid (DHAA) and diketogulonic acid (DKGA), using a spectrophotometer at 520 nm (Shimadzu, UV-2101 PC, Tokyo, Japan).

TAA in fresh fruits, dried flake, and tea samples at different sampling periods and gooseberry residues after tea preparation was determined and used for the determination of release and degradation of vitamin C during drying and tea preparation. The cumulative release of vitamin C during tea preparation is expressed by:

$$\text{TAA Cumulative Release (\%)} = \frac{(\text{Instantaneous amount of TAA in tea} \times 100)}{\text{Initial TAA in dried flake} - \text{TAA in gooseberry residue after } 20\,\text{min}} \quad (1)$$

The cumulative TAA release is the amount of TAA that was released and degraded during tea preparation

TABLE 1
Degradation of TAA of Indian gooseberry flake underwent different drying processes

Drying method	TAA (g/100 g d.b.)		Drying time (min)	Degradation (%)
	Fresh	Dried		
Hot air drying at 75°C	5.8275 ± 0.0867	4.4845 ± 0.0452	180	23
Vacuum drying at 75°C, 7 kPa	5.1683 ± 0.1678	4.1558 ± 0.1357	145	20
LPSSD at 75°C, 7 kPa	4.8485 ± 0.0193	4.1696 ± 0.0313	280	14

compared with an ideal amount of TAA that would present in tea drink if there was no degradation.

Moreover, after tea preparation, the total degradation of TAA during tea preparation was calculated by Eq. (2), which represents the fraction of TAA which degraded to the initial TAA in dried flake.

$$\text{Total Degradation (\%)} = \frac{\text{Initial TAA in dried flake} - (\text{TAA in tea} + \text{TAA in residue})}{\text{Initial TAA in dried flake}} \quad (2)$$

Statistical Analysis

The experiments were designed complete randomly. The data were analyzed and presented as mean values with standard deviations. Differences between mean values were established using Duncan's multiple range tests. Values were considered at 95% confidence level ($p < 0.05$) and all experiments were performed in duplicate.

RESULTS AND DISCUSSION

Indian gooseberry flake was dried using different drying techniques and conditions as listed in Table 1; the selected conditions were based on the earlier study of Methakhup et al.[2] Upon drying the amount of TAA in Indian gooseberry flakes expectedly decreased, as also shown in Table 1.

Based on the results summarized in Table 1 it can be seen that although hot air drying was the fastest drying process, it led to most TAA degradation. LPSSD, on the other hand, required the longest time to dry the product from an initial average moisture content of 4.60 kg/kg (d.b.) to 0.07 kg/kg (d.b.). However, LPSSD could best maintain the level of TAA compared with the other two drying methods. This is due to the oxygen-free environment of LPSSD, which prohibited aerobic degradation of ascorbic acid. This trend of results is similar to that reported by Methakhup et al.[2]

Release of TAA from Dried Indian Gooseberry Flake

The release of TAA from the dried flake during tea preparation was determined by soaking the dried gooseberry flake in hot water at 70, 80, and 90°C for 20 min. During tea preparation some TAA was released from the flake while some was still captured inside the flake and was destroyed by the high-temperature water used to prepare tea.[12] Therefore, the experimental data are presented in terms of TAA cumulative release (%), which is shown in Table 2. Table 3, on the other hand, shows the TAA degradation during tea preparation. The use of flake obtained from LPSSD and water temperature at 90°C gave the highest total TAA degradation, while the lowest degradation was observed when using flake dried by hot air at 70°C and tea preparation temperature of 70°C.

Figures 2–4 show the percentage of cumulative release of TAA from flake at various tea preparation times and at different tea preparation temperatures. TAA in tea drink

TABLE 2
Average cumulative TAA release during tea preparation

Method used to prepare flake	Water temperature (°C)	Cumulative TAA release (%)
Hot air drying at 75°C	70	79.9 ± 1.0^{c}
	80	83.6 ± 1.0^{b}
	90	82.8 ± 1.0^{b}
Vacuum drying at 75°C, 7 kPa	70	86.9 ± 0.6^{a}
	80	78.0 ± 0.6^{c}
	90	72.8 ± 0.6^{d}
LPSSD at 75°C, 7 kPa	70	74.1 ± 0.6^{d}
	80	66.6 ± 0.6^{e}
	90	51.8 ± 0.6^{f}

Different letters in the same column indicate that values are significantly different ($p < 0.05$).

TABLE 3
TAA degradation of Indian gooseberry flake during tea preparation at various temperatures

Method used to prepare flake	Degradation (%)		
	70°C	80°C	90°C
Hot air drying at 75°C	5.0	3.0	2.0
Vacuum drying at 75°C, 7 kPa	6.0	11.0	15.0
LPSSD at 75°C, 7 kPa	12.0	16.0	38.0

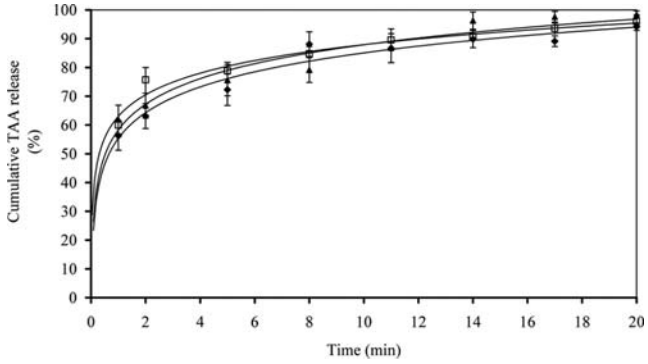

FIG. 2. TAA release of hot air dried (75°C) flake at water temperature of 70°C (◆), 80°C (□), and 90°C (▲).

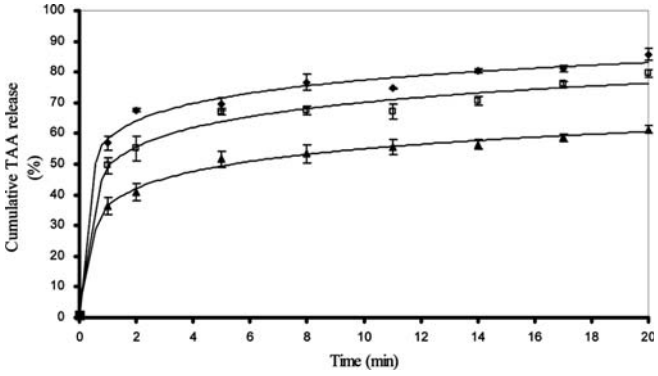

FIG. 4. TAA release of LPSSD (75°C) flake at water temperature of 70°C (◆), 80°C (□), and 90°C (▲).

rapidly increased during the first minutes of soaking and then increased steadily along with the soaking time. The effect of tea preparation temperature on the release rates of TAA from hot air dried flake was not as obvious as those from vacuum dried and LPSSD flakes. In general, degradation of TAA occurred both in tea drink and in flake and higher water temperatures naturally caused more destruction of ascorbic acid.[13–15]

Considering the results at the same hot water temperature, the rates of TAA released from the flake to water were much higher than the rates of ascorbic acid degradation during the first minutes of tea preparation. After this initial period, the release of TAA occurred at slower rates as less TAA remained in the flake hence lower gradients for the release. However, the thermal degradation of TAA in tea drink still continued at constant rates. Therefore, the amount of TAA dissolved in the tea drink increased only slowly and finally approached constant values.

The structure of the flake also played an important role on the rate of release of TAA. High-porosity flake, which was obtained when subjecting the flake to LPSSD,[2,9] facilitated hot water to transport into the flake. Thermal degradation of ascorbic acid in the flake thus occurred at higher rates than that in the flakes obtained by hot air drying and vacuum drying.[7,16] Therefore, the rates of release of TAA into tea drink were lowered in the case of LPSSD flake. It is important to note again, however, that the initial values of TAA in LPSSD flake were higher than those in hot air– and vacuum-dried flakes (see Table 1).

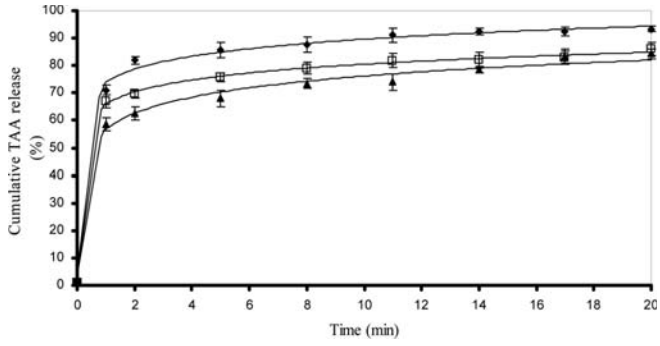

FIG. 3. TAA release of vacuum dried (75°C) flake at water temperature of 70°C (◆), 80°C (□), and 90°C (▲).

Combined Effects of Drying Techniques and Tea Preparation Methods on TAA Content

When considering the drying process it was found that the dried flake obtained from LPSSD had the highest TAA retention while the flake obtained from hot air drying had the lowest TAA retention. However, when these flakes were subjected to high-temperature water during the tea preparation process the situation was quite different. To aid understanding of the degradation of TAA during both drying and tea preparation processes a complete sketch of the processes is illustrated in Fig. 5. The total TAA degradation ranged between 24 and 47% as presented in Table 4.

Based on the results presented in Table 4, it is seen that at lower tea preparation temperature (70°C) the TAA degradation was similar, regardless of the type of dryer used to dry flake. However, at higher tea preparation temperatures, especially at 90°C, TAA degradation in tea prepared from LPSSD flake was the highest. This is probably due to the more porous structure of LPSSD flake, which facilitated movement of hot water into its structure; this hot water then had higher chance to be in contact with TAA and hence led to higher levels of degradation. In addition, since the initial level of TAA in LPSSD flake was high, more TAA was released and destroyed in the high-temperature environment; the level of degradation thus appeared higher than in the case of hot air or vacuum dried flake. Nevertheless, upon inspecting the data presented in Table 4, it could still be concluded that drying the flake by LPSSD led to the least TAA degradation, if a water temperature of 70°C was used to prepare tea.

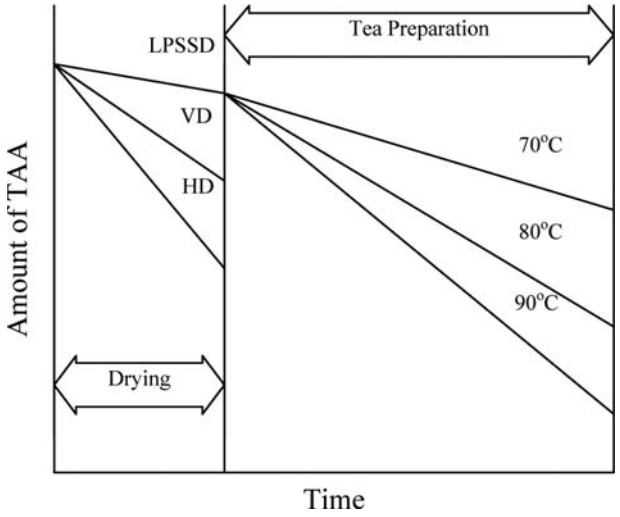

FIG. 5. Sketch of TAA evolution of Indian gooseberry during drying and tea preparation processes.

TABLE 4
Total TAA degradation

Method used to prepare flake	Total TAA degradation (%)		
	70°C	80°C	90°C
Hot air drying at 75°C	26.9	25.3	24.5
Vacuum drying at 75°C, 7 kPa	24.8	28.8	32.0
LPSSD at 75°C, 7 kPa	24.3	27.7	46.4

CONCLUSION

The present study demonstrated that the degradation of ascorbic acid, an antioxidant agent found in Indian gooseberry, could occur during drying and tea drink preparation. Furthermore, the release of ascorbic acid was dependent on both drying technique and hot water temperature for tea preparation. LPSSD helped retaining TAA in dried flake better than hot air and vacuum drying. Lower the hot water temperature during tea preparation was recommended to retard the ascorbic acid degradation. As Indian gooseberry contained various bioactive agents monitoring of such substances during processing and at the point of consumption should be conducted to optimize the suitable process conditions.

ACKNOWLEDGEMENTS

The authors express their sincere appreciation to the Commission on Higher Education, the Thailand Research Fund (TRF), the National Research Council of Thailand and the International Foundation for Science (IFS, Sweden) for supporting the study financially.

REFERENCES

1. Chatchavalchokchai, N. Effect of some ruminants on seed quality of *Phyllanthus emblica* Linn., *Elaeocarpus madopetalous* Pierre, *Spondias pinnata* Kurz and *Terminalia chebula* Retz. M.Sc. Thesis, Botany Program, Kasetsart University, Thailand, 1987.
2. Methakhup, S.; Chiewchan, N.; Devahastin, S. Effects of drying methods and conditions on drying kinetics and quality of Indian gooseberry flake. Lebensmittel-Wissenschaft und-Technologie **2005**, *38*, 579–587.
3. Iyota, H.; Nishimura, N.; Onuma, T.; Nomura, T. Drying of sliced raw potatoes in superheated steam and hot air. Drying Technology **2001**, *19*, 1411–1424.
4. Mujumdar, A.S.; Devahastin, S. Fundamental principles of drying. In *Mujumdar's Practical Guide to Industrial Drying*; Devahastin, S., Ed.; Exergex: Brossard, Canada, 2000; 1–22.
5. Namsanguan, Y.; Tia, W.; Devahastin, S.; Soponronnarit, S. Drying kinetics and quality of shrimp undergoing different two-stage drying processes. Drying Technology, New Hamphire, **2004**, *22*, 759–778.
6. Devahastin, S.; Suvarnakuta, P. Superheated steam drying of food products. In *Dehydration of Products of Biological Origin*; Mujumdar, A.S., Ed.; Science Publishers: Enfield, New Hamphire, 2004; 493–512.
7. Siepmann, J.; Faisant, N.; Akiki, J.; Richard, J.; Benoit, J.P. Effect of the size of biodegradable microparticles on drug release: Experiment and theory. Journal of Controlled Release **2004**, *96*, 123–134.
8. Rahman, C.; Berkland, C.; Kim, K.; Pack, D.W. Modeling small-molecule release from PLG microspheres: Effects of polymer degradation and nonuniform drug distribution. Journal of Controlled Release **2004**, *103*, 149–158.
9. Devahastin, S.; Suvarnakuta, P.; Soponronnarit, S.; Mujumdar, A.S. A comparative study of low-pressure superheated steam and vacuum drying of a heat-sensitive material. Drying Technology **2004**, *22*, 1845–1867.
10. Thai Industrial Standard Institute (TISI). *Black Tea*, Ministry of Industry: Thailand, 1983.
11. Damrongnukool, J. *Determination of Vitamin C Contents in Commercial Fruit Juice*; M.Sc. Thesis, Home Economics Program, Kasetsart University, Thailand, 2000.
12. İpek, U.; Arslan, E.I.; Öbek, E.; Karataş, F.; Erulaş, F.A. Determination of vitamin losses and degradation kinetics during composting. Process Biochemistry **2005**, *40*, 621–624.
13. Margarida, C.V.; Teixeira, A.A.; Silva, C.L.M.. Mathematical modeling of the thermal degradation kinetics of vitamin C in cupuaçu (*Theobroma grandiflorum*) nectar. Journal of Food Engineering **2000**, *43*, 1–7.
14. Polydera, A.C.; Stoforos, N.G.; Taoukis P.S. Comparative shelf life study and vitamin C loss kinetics in pasteurised and high pressure processed reconstituted orange juice. Journal of Food Engineering **2003**, *60*, 21–29.
15. Ayranci, E.; Tunc, S. The effect of edible coatings on water and vitamin C loss of apricots (*Armeniaca vulgaris* Lam.) and green peppers (*Capsicum annuum* L.). Food Chemistry **2004**, *87*, 339–342.
16. Lee, T.H.; Wang, J.; Wang, C.H. Double-walled microspheres for the sustained release of a highly water soluble drug: Characterization and irradiation studies. Journal of Controlled Release **2002**, *83*, 437–452.

Drying Technology
An International Journal
Publication details, including instructions for authors and subscription information:
http://www.informaworld.com/smpp/title~content=t713597247

Comparative Evaluation of Physical Properties of Edible Chitosan Films Prepared by Different Drying Methods

Pornpimon Mayachiew [a]; Sakamon Devahastin [a]
[a] Department of Food Engineering, King Mongkut's University of Technology Thonburi, Bangkok, Thailand

Online Publication Date: 01 February 2008
To cite this Article: Mayachiew, Pornpimon and Devahastin, Sakamon (2008) 'Comparative Evaluation of Physical Properties of Edible Chitosan Films Prepared by Different Drying Methods', Drying Technology, 26:2, 176 - 185
To link to this article: DOI: 10.1080/07373930701831309
URL: http://dx.doi.org/10.1080/07373930701831309

Drying Technology, 26: 176–185, 2008

ISSN: 0737-3937 print/1532-2300 online
DOI: 10.1080/07373930701831309

Taylor & Francis
Taylor & Francis Group

Comparative Evaluation of Physical Properties of Edible Chitosan Films Prepared by Different Drying Methods

Pornpimon Mayachiew and Sakamon Devahastin
Department of Food Engineering, King Mongkut's University of Technology Thonburi, Bangkok, Thailand

Edible films are alternative packaging, which have recently received much attention due mainly to environmental reasons. Edible films may be formed from edible biomaterials such as polysaccharides, proteins, or lipids. Among these biopolymers, chitosan is of interest because it has a good film-forming property and is biodegradable, biocompatible, and nontoxic. Several techniques have been used to prepare edible chitosan films with various degrees of success. However, it is always interesting to find an alternative technique to produce films of superior quality at shorter processing (drying) time. In this study, the influences of different drying methods and conditions on the drying kinetics and various properties of chitosan films were investigated. Drying at control conditions (ambient air drying and hot air drying at 40°C) as well as vacuum drying and low-pressure superheated steam drying (LPSSD) at an absolute pressure of 10 kPa were carried out at different drying temperatures (70, 80, and 90°C). The properties of chitosan films, in terms of color, tensile strength, percent elongation, water vapor permeability (WVP), glass transition temperature (T_g), and crystallinity, were also determined. Based on the results of both the drying behavior and film properties, LPSSD at 70°C was proposed as the most favorable conditions for drying chitosan films.

Keywords Biopolymers; Color; Crystallinity; Differential scanning calorimetry; Mechanical properties; Water vapor permeability; X-ray diffraction

INTRODUCTION

Food packaging provides barriers to conditions that could reduce the quality and shelf life of foods. Plastic is so far the most popular packaging but it causes environmental pollution since it does not degrade naturally. Biodegradable material, defined as a material that can be degraded completely by microorganisms into natural compounds, has been viewed as an alternative to plastic packaging.[1] To further alleviate the problem, edible film, which is defined as a thin layer of edible, biodegradable material formed on a food as a coating or placed on or between food components, may be an even better alternative for food applications because it does not have to be eliminated as solid wastes.[1] Among various biodegradable materials, chitosan is of interest because it is an edible, biodegradable, biocompatible with living tissues, odorless, and nontoxic substance and has been widely used in the food industry.[2]

Among the steps involved in the production of edible films, film formation is considered one of the most important. Chitosan can be easily formed into films by a casting/solvent evaporation technique. Drying is indeed an important step that affects the quality of chitosan and, in fact, any other polymeric films.[3–6]

Numerous researchers prepared chitosan films by drying them at ambient temperature for 24–48 h.[7–9] Some other researchers prepared chitosan films by oven drying[10,11] or infrared drying.[11] Srinivasa et al.[11] prepared chitosan films by two methods of drying (oven drying and infrared drying) at 80, 90, and 100°C and compared film properties with those of films prepared by ambient temperature drying (~27°C). It was noted that tensile strength of infrared-dried films (49.58–52.34 MPa) was less than that of ambient-dried films (56.78–59.38 MPa). Water vapor and oxygen transmission rate values were slightly reduced for oven-dried and infrared-dried films compared with those of ambient-dried films.

During the past decade, the idea of using superheated steam to dry foods and other materials to preserve or even enhance the various properties of the products has been on the rise.[12–14] Poirier,[15] for example, reported that superheated steam drying (SSD) resulted in improved (20–30% better) strength of hand sheets compared with air-dried sheets. In addition, McCall and Douglas[16] reported that filled papers containing 0–10% clay had around 23% higher tensile index when dried in superheated steam.

For heat-sensitive biomaterials, lowering the dryer operating pressure is a feasible option that not only preserves the quality of the dried product but may also enhance the drying rate as well. Recently, low-pressure superheated steam drying (LPSSD) has been tested and proved very

Correspondence: Sakamon Davahastin, Department of Food Engineering, King Mongkut's University of Technology Thonburi, 126 Pracha u-tid Road, Bangkok 10140, Thailand; E-mail: sakamon.dev@kmutt.ac.th

effective in drying a number of heat-sensitive materials, in terms of both the product physical and chemical properties.[17,18] Devahastin et al.,[17] for example, studied the drying kinetics and various quality parameters of carrot cubes undergoing both LPSSD and vacuum drying. Although LPSSD required longer drying time to achieve the same final moisture content, some of the quality attributes such as color, microstructure, shrinkage, and rehydration capability of the products were superior to those of products dried by vacuum drying. However, no report is so far available on the drying kinetics and properties of chitosan films prepared either by vacuum drying or LPSSD, which has potential for producing films of higher quality at shortened processing (drying) time.

The aim of this study was to determine and compare the drying kinetics of chitosan films undergoing different drying techniques, namely, ambient drying, hot air drying, vacuum drying, and LPSSD, at different conditions. In addition, the effects of drying methods and conditions on selected physical properties (color, water vapor permeability [WVP], tensile strength, and percent elongation), thermal properties (glass transition temperature), and crystallinity of chitosan films were also investigated. Finally, the effect of storage condition (%RH) on WVP, tensile strength, and percent elongation of the films was also determined.

MATERIALS AND METHODS

Materials

Chitosan (molecular weight of 900,000 Da and degree of deacetylation of 90.20%) was obtained from S.K. Profishery Co., Ltd. (Bangkok, Thailand). Glycerol was purchased from Carlo Erba (Val de Reuil, Italy), and acetic acid was obtained from Merck (Darmstadt, Germany).

Film Preparation

Chitosan solution (1.5% (w/v)) was prepared by dissolving chitosan in 1% (v/v) acetic acid under constant stirring at 300 rpm using a magnetic stirrer (Framo®-Gerätechnik, model M21/1, Eisenbach, Germany) at room temperature for 24 h. Twenty-five percent glycerol (w/w chitosan) was then added into the chitosan solution; stirring was then continued at room temperature for 1 h. After mixing, the solution was centrifuged for 15 min at 12,400 rpm by a refrigerated centrifuge (Hitachi, model Himac CR21, Ibaragi, Japan) to remove undissolved impurities and bubbles in the solution. The solution (21 g) was then poured on an acrylic plate with dimensions of $13 \times 10\,cm^2$ to cast a chitosan film with a constant thickness of 20 μm for a drying experiment.

Film Drying

Ambient Temperature and Hot Air Drying

The cast films were dried at ambient temperature and at 40°C in a hot air dryer (Fig. 1); the air velocity across the drying chamber was fixed at 0.25 m/s. These films were used as control samples.

Low-Pressure Superheated Steam Drying

A schematic diagram of the low-pressure superheated steam dryer and its accessories is shown in Fig. 2. The dryer consists of a stainless steel drying chamber, insulated with rock wool, with inner dimensions of $45 \times 45 \times 45\,cm^3$; a steam reservoir, which received steam from a boiler and maintained its pressure at around 200 kPa (gage); and a liquid ring vacuum pump (Nash, model ET32030, Trumball, CT), which was used to maintain the vacuum in the drying chamber (fixed at 10 kPa in this study). A steam trap was installed to reduce the excess steam condensation in the reservoir. An electric heater, rated at 1.5 kW, which was controlled by a PID controller (Omron, model E5CN, Tokyo, Japan), was installed in the drying chamber to control the steam temperature and to minimize the condensation of steam in the drying chamber during the startup period. Two variable-speed electric fans were used to disperse steam throughout the drying chamber. The steam inlet was made into a cone shape and was covered with a screen to help distributing the steam in the chamber. The sample holder was made of a stainless steel screen with dimensions of $16.5 \times 16.5\,cm^2$. The change of the mass of the sample was detected continuously (at 60-s intervals) using a load cell with an accuracy of ± 0.2 g (Minebea,

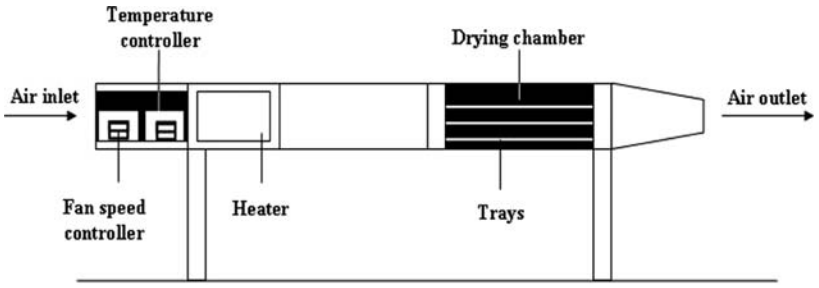

FIG. 1. A schematic diagram of hot air dryer and associated units.

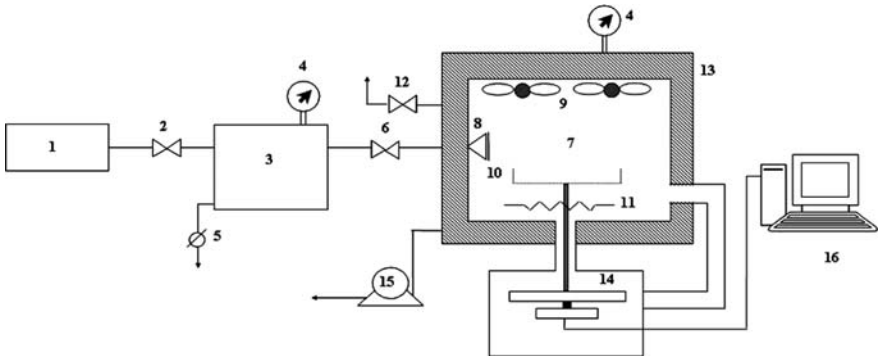

FIG. 2. A schematic diagram of the low-pressure superheated steam dryer and associated units. 1, boiler; 2, steam valve; 3, steam reservoir; 4, pressure gauge; 5, steam trap; 6, steam regulator; 7, drying chamber; 8, steam inlet and distributor; 9, electric fans; 10, sample holder; 11, electric heater; 12, vacuum break-up valve; 13, insulator; 14, on-line weight indicator and logger; 15, vacuum pump; 16, PC with installed data acquisition card.

model Ucg-3 kg, Nagano, Japan), which was installed in a smaller chamber connected to the drying chamber by a flexible hose (in order to maintain the same vacuum pressure as that in the drying chamber) and to an indicator and recorder (AND A&D Co., model AD 4329, Tokyo, Japan). The data were sent to a PC with installed data acquisition card.

Films were dried at 70, 80, and 90°C at 10 kPa in the LPSSD. The operating pressure was reduced in steps from an atmospheric pressure to 10 kPa to avoid the problem of solvent trapping in films following the pattern illustrated in Fig. 3.

Vacuum Drying

For vacuum drying experiments the same experimental setup as that used for the LPSSD experiments was used but without the application of steam to the drying chamber. Films were also dried at 70, 80, and 90°C at 10 kPa in the vacuum dryer. Again, the operating pressure was reduced in steps from an atmospheric pressure to 10 kPa following the pattern illustrated in Fig. 3.

Film Properties Determination

Chitosan films were dried at various conditions until their moisture content reached approximately 14% (d.b.).[8,19]

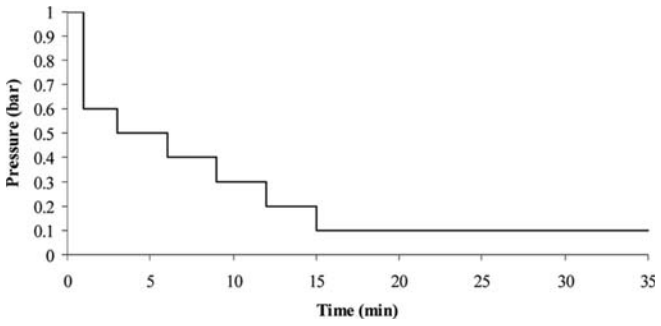

FIG. 3. Reduction of operating pressure from an atmospheric pressure to 10 kPa.

The films were then conditioned for at least 48 h either in a desiccator containing saturated salt solution of magnesium nitrate (Ajax Finechem, Seven Hills, NSW, Australia), which produced the relative humidity (RH) of 53%[11,20] or in a desiccator containing saturated salt solution of sodium chloride (Ajax Finechem, Seven Hills, NSW, Australia), which produced an RH of 75%, before further analysis. The latter RH was selected because it is an average relative humidity of the environment in Thailand.

Film Thickness Measurement

The film thickness was measured using a micrometer (Mitutoyo, Model 102-309, Tokyo, Japan) with an accuracy of $\pm 2\,\mu m$. Each film sample was measured at its center and four other positions along the edge in the case of WVP measurement and three other positions along the strips in the case of mechanical properties measurement. WVP and mechanical properties were calculated using the average thickness of each film sample.

Moisture Content Determination

The moisture content of films was determined using the standard vacuum oven method.[21] Briefly, the film was dried in a vacuum oven (Sanyo, Model Gallenkamp/OM-09980, Loughborough, UK) at 70°C at the pressure of -900 mbar for 24 h. The mass of the dried sample (bone-dry mass) was then used to determine the film moisture content by:

$$\%\ \text{Moisture content (d.b.)} = \frac{M_i - M_d}{M_d} \qquad (1)$$

where M_i is the mass of the sample at any instant (g) and M_d is the bone-dry mass (g).

Mechanical Properties Determination

The measurement of mechanical properties of chitosan films was carried out using a texture analyzer (Stable Micro

System, TA.XT.Plus, Surrey, UK). After conditioning, chitosan films were cut into $10 \times 2.54\,cm^2$ strips and tested for tensile strength and percent elongation according to the ASTM Standard Method D882.[22] Initial grip separation and crosshead speed were set at 50 mm and 50 mm/min, respectively. Tensile strength was calculated by dividing the maximum load for breaking the film by its cross-sectional area. Percent elongation was determined by dividing the film elongation at rupture by the initial grip separation. All tests were performed in triplicate and the average values were reported.

Water Vapor Permeability Determination

The water vapor permeability (WVP) of chitosan films was measured using a gravimetric method according to the ASTM E 96/E 96M–05 standard.[23] The test cup was filled with 15 mL of distilled water to produce 100% RH below the film. Chitosan film was mounted to the top of the cup. The cup was placed in a desiccator containing magnesium nitrate solution at 25°C. Fans were operated in the chamber, thus circulating the air at 152 m/min over the surface of the film to remove the permeating water vapor. The mass of the cup was recorded 6 times at 2 h interval after steady state was reached. Mass loss was plotted versus time and a straight line was obtained in duplicate. Linear regression was then used to first estimate the slope of the line to calculate the water vapor transmission rate (WVTR) as follows:

$$\mathrm{WVTR} = \frac{\mathrm{Slope}}{A} \tag{2}$$

where WVTR is the water vapor transmission rate (g/m^2 day), Slope is the slope of the mass loss versus time curve (g/day), and A is the test cup mouth area (m^2).

WVP was then determined using the WVP correction method.[24] This method is necessary when dealing with films with low water vapor resistance since it accounts for the water vapor partial pressure gradient within the stagnant air layer of the test cup. Corrected water vapor permeability can be calculated using Eq. (3); the coefficient 1.157×10^{-5} in Eq. (3) satisfies unit conversion.

$$\mathrm{WVP} = 1.157 \times 10^{-5} \frac{\mathrm{WVTR}\ L}{p_1 - p_2} \tag{3}$$

where WVP is the water vapor permeability (g/s m Pa), L is the average film thickness (m), p_1 is the partial pressure of water vapor in air at surface of distilled water in the cup (Pa), and p_2 is the partial pressure of water vapor at the film surface outside the cup (Pa).

Color Measurement

The color of films was determined with a colorimeter (Juki, JP 7100, Tokyo, Japan). The color of the films after conditioning at 53% RH for 2 days was investigated. The film specimen was covered with a standard white plate ($L = 97.75$, $a = -0.08$, and $b = -0.3$) and the values of L, a, b were evaluated by a reflectance measurement. For each sample at least three measurements were performed at different positions. The color changes (L, a, and b values) were calculated by:

$$\Delta L = L - L^*, \quad \Delta a = a - a^* \quad \text{and} \quad \Delta b = b - b^* \tag{4}$$

The total color difference (ΔE) was calculated as follows:

$$\Delta E = \sqrt{(L^* - L)^2 + (a^* - a)^2 + (b^* - b)^2} \tag{5}$$

where L^*, a^*, and b^* are the standard color values (lightness, redness/greenness, and yellowness/blueness, respectively) of the white plate and L, a, and $b$are the color values of the measured sample.[25]

Differential Scanning Calorimetry (DSC)

The thermal characteristics of chitosan films were determined using a differential scanning calorimeter (DSC; Netzsch DSC 204 F1Phoenix®, Selb, Germany). A small sample piece (10–12 mg) was cut from a film sample after conditioning at 53% RH and placed into an aluminum pan, which was then sealed. A small hole was made at the top of the pan in order to allow the release of moisture. An empty pan was used as the reference. The first scan was made from −30 to 190°C; this was followed by 1-min holding at 190°C and a rapid cooling to −30°C and another holding at −30°C for 5 min. The second scan was then implemented by raising the temperature to 250°C. The scanning rate used was 10°C/min.[26]

X-Ray Diffraction Analysis

X-ray diffraction (XRD) patterns of chitosan films after conditioning at 53% RH were obtained using a Bruker AXS D8 DISCOVER XRD (Bruker AXS GmbH, Karlsruhe, Germany) under the following conditions: 40 kV and 40 mA with CuKα radiation at a wavelength of 0.1546 nm with a scanning rate of $2^\circ\ 2\theta$/min.[11] The relative intensity of the diffraction peak was recorded in the scattering range (2θ) of 4–40° and the crystallinity (X_c) of the film was calculated by:

$$X_c = [F_c/(F_c + F_a)] \times 100\% \tag{6}$$

where F_c and F_a are the areas of crystalline and noncrystalline regions, respectively.

Statistical Analysis

All data were subjected to the analysis of variance (ANOVA) using SPSS® software and are presented as mean values with standard deviations. Differences between

mean values were established using Duncan multiple range test at a confidence level of 95%. All experiments were performed in duplicate except when stated otherwise.

RESULTS AND DISCUSSION

Drying Kinetics of Chitosan Films

Chitosan films with initial moisture contents in the range of 51.51–58.79 kg/kg (d.b.) were first dried until their equilibrium moisture contents were reached in order to construct the drying curves at different conditions. The drying curves of chitosan films undergoing different drying methods and conditions are shown in Figs. 4 and 5. It was found that the film samples dried at control conditions required longer drying time, while vacuum drying required least drying time, even less than that required by LPSSD. This is due to the larger differences between the medium and sample surface temperature in the case of vacuum drying over the range of drying temperature used. Moreover, the electric heater was used more often during vacuum drying since it was the only source of energy for drying. This might increase the amount of radiation absorbed by the chitosan film surfaces, thus explaining the higher drying rates during vacuum drying.[17]

The average drying time to reach the desired final moisture content of 14% (d.b.) is listed in Table 1. As expected, the usual trend of shorter drying time was found when the drying temperature increased. The moisture decreased faster at higher temperatures than at lower temperatures for both LPSSD and vacuum drying because the temperature differences between the medium and the samples at higher drying temperatures were greater than that at lower temperatures. Moisture diffusivity is also higher at a higher drying temperature.

The differences between the two sets of drying time (between vacuum drying and LPSSD), however, were smaller at higher drying temperatures (Table 1). Raising the drying temperature further would eventually lead to equal rates of drying at an inversion temperature (due to increased temperature difference between the steam and the sample).[27]

The equilibrium moisture contents (EMC) of chitosan films undergoing different drying methods and conditions are listed in Table 2. It was found that EMC values of vacuum-dried chitosan films were lower than those of LPSSD films because the driving force for moisture transfer within the LPSSD system is generally lower than that in the vacuum drying system. Moreover, drying temperature has an influential effect on the moisture content at equilibrium; an increase in the drying temperature resulted in lower equilibrium moisture content for all drying methods.

Physical Properties of Chitosan Films

To determine the physical properties of chitosan films, the films were first dried to the final moisture content of approximately 14% (d.b.). This value is similar to that set by Wiles et al.[8] and Nadarajah et al.,[19] which is around 10–19% (d.b.); this is to allow the films to be peeled off easily from the casting surface. All chitosan films prepared by different drying methods and conditions showed smooth and uniform surface morphology without any cracks and pinholes as observed from the scanning electron micrographs (not shown).

Color

The changes of different color parameters of chitosan films dried by different drying methods and conditions

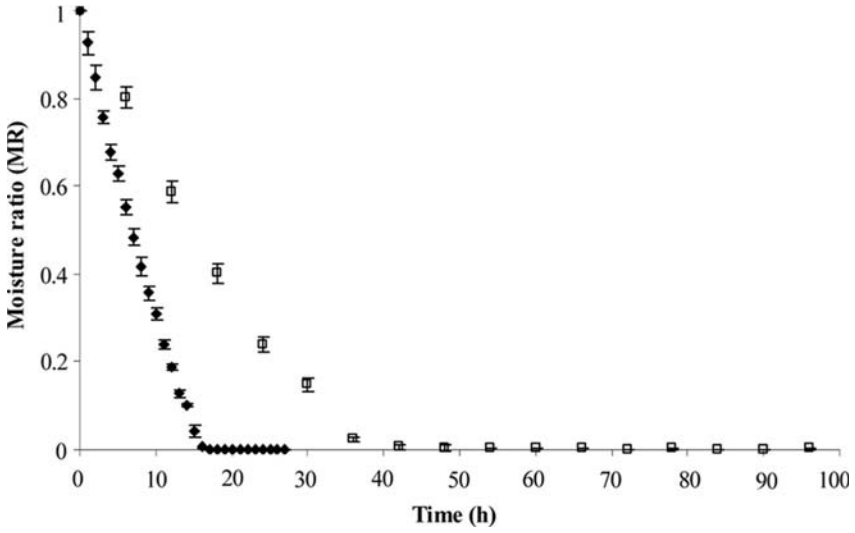

FIG. 4. Drying kinetics of chitosan films undergoing ambient drying (□) and hot air drying at 40°C (◆).

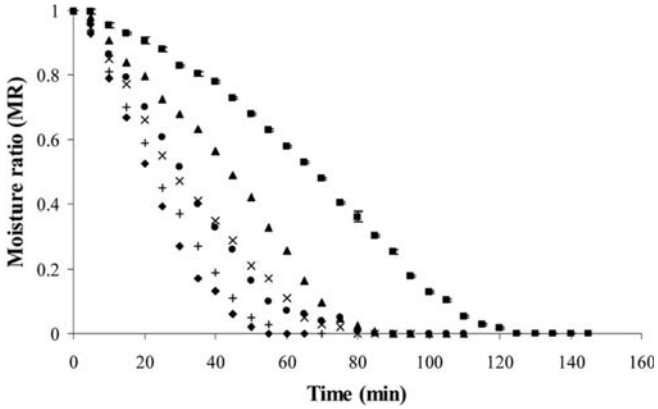

FIG. 5. Drying kinetics of chitosan films undergoing LPSSD of 70°C (■), 80°C (▲), 90°C (●); vacuum drying 70°C (×), 80°C (+), 90°C (◆) at 10 kPa.

are listed in Table 3. Regarding the effect of drying temperature on the lightness of the films, it is seen that higher drying temperatures led to slightly darker films, both in the cases of vacuum drying and LPSSD. This is because higher temperatures led to higher levels of Maillard browning reactions. It was also found that drying methods were significantly influencing the changes of lightness. Chitosan films dried by LPSSD were slightly lighter than the films dried by vacuum drying. This may be due to the fact that the film temperature increased more rapidly and stayed at higher levels in the case of vacuum drying compared with the case of LPSSD.

In terms of the redness (*a* value), it can be seen from Table 3 that the redness was also significantly affected by both the drying temperature and drying methods. Drying at higher temperatures yielded redder dried films than at lower temperatures. This is again because Maillard reactions are accelerated by temperature. The redness of films was obviously higher in the case of vacuum drying compared with the case of ambient drying and LPSSD for the reasons mentioned earlier.

In the case of yellowness (*b* value) it was found that drying temperature had a significant effect on the change of yellowness, especially in the case of vacuum drying. This is again because of Maillard reactions that occurred at larger extents at higher drying temperatures. The yellowness was also significantly affected by the drying methods. The yellowness obviously increased during vacuum drying compared with the cases of ambient drying and LPSSD.

The overall changes of color of the films could be observed from the ΔE was also significantly affected by both the drying temperature and drying methods. Regarding the effect of the drying temperature it could be seen that higher drying temperatures led to larger changes of ΔE values, as expected. In addition, the ΔE value was also significantly affected by the drying methods. It was found that vacuum-dried films had significantly higher ΔE values than ambient-dried and LPSSD films for the reasons mentioned previously.

TABLE 1
Drying time to reach final moisture content of 14% (d.b.)

Drying condition (°C)	Drying time
Control	
~30	54 h
40	18 h
Vacuum drying	
70	85 min
80	65 min
90	60 min
LPSSD	
70	130 min
80	95 min
90	90 min

TABLE 2
Equilibrium moisture content of chitosan films undergoing various drying methods and conditions

Drying condition (°C)	Equilibrium moisture content (% d.b.)
Control	
~30	17.9
40	12.0
Vacuum drying	
70	5.9
80	3.5
90	3.4
LPSSD	
70	13.7
80	10.1
90	9.9

Mechanical Properties

Regarding the mechanical properties of chitosan films it was noted that different drying methods and conditions had significant effects on the tensile strength and percent elongation of the films (Table 4); the maximum value for tensile strength was observed in the case of LPSSD at 70°C and storage condition of 53% RH. This might be due to the effects of higher degree of crystallinity and thermal cross-linkage that occurred more at this condition.

From the result of the X-ray diffraction analysis (Fig. 6), chitosan films with higher degrees of crystallinity (LPSSD and ambient-dried films) exhibited higher tensile strength when only crystallinity of the films was considered. Rajendran and Marikani[28] also stated that the mechanical

TABLE 3
Color of chitosan films

Drying condition	Temperature (°C)	ΔL	Δa	Δb	ΔE
Control					
	~30	-5.8 ± 0.1^{d}	-0.9 ± 0.1^{d}	2.0 ± 0.1^{a}	6.2 ± 0.1^{a}
	40	-5.8 ± 0.1^{d}	-1.0 ± 0.1^{cd}	2.2 ± 0.1^{ab}	6.3 ± 0.1^{a}
Vacuum drying					
	70	-6.0 ± 0.1^{b}	-1.4 ± 0.1^{b}	3.1 ± 0.1^{d}	6.9 ± 0.1^{c}
	80	-6.2 ± 0.1^{a}	-1.5 ± 0.1^{b}	3.4 ± 0.1^{e}	7.2 ± 0.1^{d}
	90	-6.2 ± 0.2^{a}	-1.7 ± 0.1^{a}	4.1 ± 0.2^{f}	7.6 ± 0.2^{e}
LPSSD					
	70	-5.9 ± 0.1^{c}	-1.0 ± 0.1^{cd}	2.1 ± 0.1^{ab}	6.4 ± 0.1^{b}
	80	-6.0 ± 0.1^{b}	-1.0 ± 0.1^{cd}	2.2 ± 0.1^{b}	6.5 ± 0.1^{b}
	90	-6.0 ± 0.1^{b}	-1.1 ± 0.2^{c}	2.5 ± 0.2^{c}	6.6 ± 0.2^{b}

Different superscripts within the same column mean that the values are significantly different ($p < 0.05$).

strength of polymer films normally increases with the degree of crystallinity. This observation agrees with that stated by Ogawa[29] that chitosan films, which exhibited higher degree of crystallinity, had higher tensile strength.

The mechanical strength of polymer films also depends upon the method of preparation. The tensile strength of LPSSD films was higher than that of vacuum-dried films due probably to the fact that LPSSD required longer drying time than did vacuum drying. Ngui and Mallapragada[30] stated that the degree of crystallinity of semicrystalline polymer films was found to increase as a function of the drying time. Slower drying allows for the polymer chains to rearrange and form more crystals. However, the tensile strength of LPSSD films was higher than that of ambient dried films because the drying temperature of LPSSD was higher, thus inducing more thermal cross-linkage within the LPSSD films. The influence of the relative humidity during storage on the tensile strength was not significant but it was still observed that the strength was slightly lower at higher relative humidity in all cases.

TABLE 4
Mechanical properties of chitosan films

Drying condition (°C)	Relative humidity (%)	Tensile strength (MPa)	Percent elongation
Control			
~30	53	40.2 ± 3.2^{cd}	23.5 ± 1.6^{de}
	75	38.7 ± 2.4^{cd}	24.6 ± 3.8^{de}
40	53	36.5 ± 2.5^{bcd}	23.1 ± 2.3^{de}
	75	34.9 ± 3.4^{bcd}	23.7 ± 2.8^{de}
Vacuum drying			
70	53	32.8 ± 2.6^{ab}	$19.2 \pm 2.\ 9^{abc}$
	75	30.9 ± 3.8^{ab}	20.2 ± 4.4^{bcde}
80	53	29.5 ± 3.0^{ab}	18.8 ± 2.4^{ab}
	75	27.0 ± 2.4^{ab}	19.8 ± 2.5^{abcd}
90	53	28.9 ± 3.5^{ab}	18.0 ± 2.5^{ab}
	75	27.2 ± 4.0^{ab}	19.7 ± 3.1^{abcd}
LPSSD			
70	53	69.1 ± 3.9^{f}	24.7 ± 4.6^{e}
	75	69.0 ± 2.8^{f}	24.9 ± 2.5^{e}
80	53	68.4 ± 5.7^{f}	24.8 ± 4.0^{e}
	75	65.8 ± 3.4^{f}	25.1 ± 4.4^{e}
90	53	52.2 ± 5.6^{e}	24.2 ± 3.0^{e}
	75	50.2 ± 4.7^{e}	24.8 ± 3.5^{e}

Different superscripts within the same column mean that the values are significantly different ($p < 0.05$).

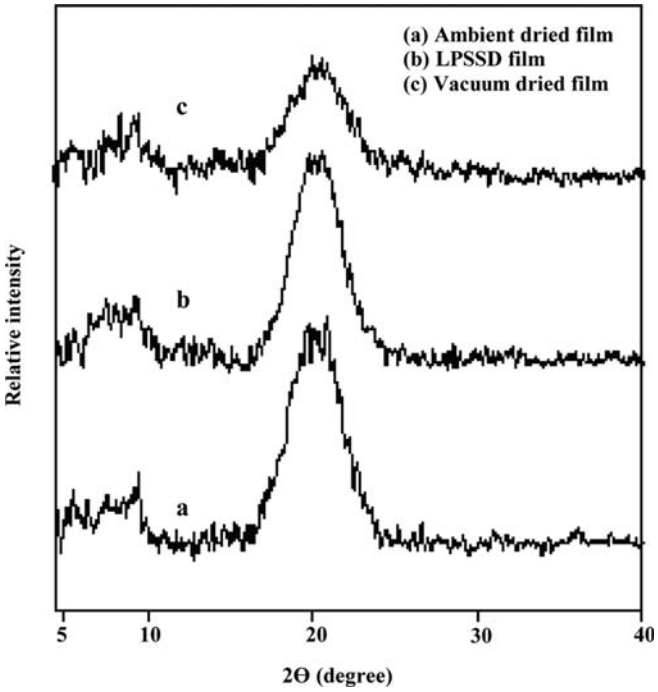

FIG. 6. X-ray diffraction patterns of chitosan films dried by ambient drying at ~30°C, LPSSD at 70°C, and vacuum drying at 70°C.

In terms of the percent elongation, which is an indicator of the film extensibility, different drying methods and conditions led to films with significantly different values of percent elongation. The percent elongation of LPSSD films was higher than that of vacuum-dried films due probably to the higher degrees of crystallinity and thermal cross-linkage that occurred more in LPSSD films. The effect of the relative humidity during storage on the percent elongation of the films was again not significant. Drying temperature also did not significantly affect the percent elongation.

According to Krochta and Johnston,[1] edible films with tensile strength of 10–100 MPa and percent elongation of 10–50% are considered to have moderate mechanical properties. Therefore, chitosan films obtained in this study, whose tensile strength was in the range of 27.04–69.12 MPa and percent elongation was in the range of 17.96–25.13, had moderate mechanical property values.

Water Vapor Permeability

WVP is an important property of films because most natural biopolymers are very likely to become plasticized when coming into contact with water. In this study, drying methods and drying temperature did not seem to have any significant effect on the WVP (Table 5). Phan The et al.[31] also observed that the WVP of arabinoxylan and hydroxylpropylmethyl cellulose films containing 15% glycerol was not affected by the drying temperature. For the effect of RH during storage it was found that RH did not significantly affect WVP of the films as well.

TABLE 5
Water vapor permeability of chitosan films

Drying condition (°C)	Relative humidity (%)	Water vapor permeability ($\times 10^{-10}$ g/m s Pa)
Control		
~30	53	2.1 ± 0.1^a
	75	2.1 ± 0.1^a
40	53	1.9 ± 0.2^a
	75	2.0 ± 0.2^a
Vacuum drying		
70	53	2.0 ± 0.3^a
	75	2.3 ± 0.2^a
80	53	2.2 ± 0.1^a
	75	2.3 ± 0.2^a
90	53	2.0 ± 0.2^a
	75	2.1 ± 0.2^a
LPSSD		
70	53	1.9 ± 0.1^a
	75	1.9 ± 0.1^a
80	53	1.9 ± 0.1^a
	75	1.9 ± 0.1^a
90	53	1.9 ± 0.2^a
	75	2.0 ± 0.2^a

Different superscripts within the same column indicate that the values are significantly different ($p < 0.05$).

WVP of chitosan films was in the range of 1.88×10^{-10} to 2.33×10^{-10} g/m s Pa. A high WVP value indicates poor barrier properties of chitosan films and WVP of most edible films is generally higher than that of common plastics. According to Krochta and Johnston,[1] WVP values in the range of 1.15×10^{-12} to 1.15×10^{-10} g/m s Pa are considered moderate. Therefore, chitosan films in this study are moderate moisture barrier when comparing with other edible and biodegradable films. WVP of films obtained in this work are nearly comparable with that of the films of Caner et al.,[7] who reported that WVP values of chitosan films with polyethylene glycol 400 as plasticizer were in the range of 1.03×10^{-10} to 1.09×10^{-10} g/m s Pa.

Glass Transition Temperature

Measurement of the glass transition temperature (T_g) of chitosan films was performed to understand the physical state of the samples. Only chitosan films dried by ambient temperature as well as by vacuum drying and LPSSD at 70°C and stored at 53% relative humidity were investigated because these conditions gave the best film properties for each drying method. To eliminate the effect of moisture on T_g measurement, the second heating run was performed.

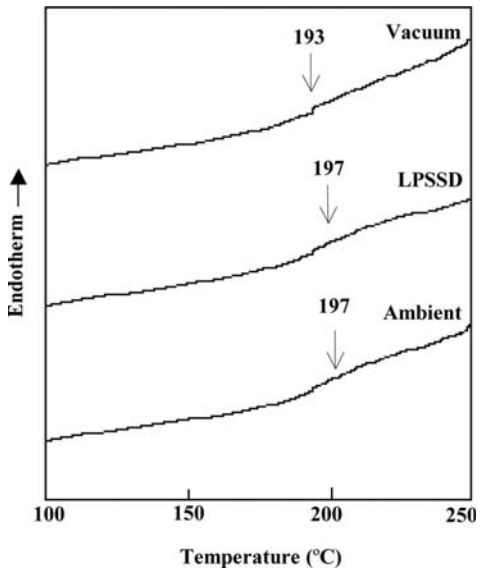

FIG. 7. DSC thermograms of chitosan films dried by ambient drying at ~30°C, LPSSD at 70°C, and vacuum drying at 70°C.

The DSC thermograms of chitosan films (Fig. 7) from the second heating run showed that the T_g of ambient-dried and LPSSD chitosan films was around 197°C while vacuum drying led to films with slightly lower T_g of around 193°C. However, the change of the inclination of the baseline was small because chitosan is only a partially crystalline polymer and has small specific volume of rigid chain.[32] Suyatma et al.[20] also reported the values of T_g of chitosan films in the range of 194 to 196°C. A wider range of T_g of chitosan films, from 161 to 203°C, was also reported by other researchers.[33]

Glass transition could be used to explain the discontinuous behavior of film properties in response to changes in temperature. Below glass transition temperature, films retain good mechanical and barrier properties. Ambient-dried and LPSSD films exhibited higher T_g than did vacuum-dried films, indicating that the former group had higher intensities of intermolecular forces.[34] This phenomenon is probably related to the mechanical properties of chitosan films in which ambient-dried and LPSSD films had higher tensile strength and percent elongation than vacuum-dried films.

X-Ray Diffraction Patterns

Figure 6 shows the XRD patterns of chitosan films. Except for the relative intensity of diffractive peaks, it was observed that the diffraction patterns of all the films were almost the same. Chitosan films showed characteristic crystalline peaks at $2\theta = 20°$, which represented the hydrated form of crystalline part of chitosan films.[29] Urbanczyk and Lipp-Symonowicz[35] indeed reported that the peak at about 20° is a typical peak for an X-ray diffraction pattern of chitosan. The crystallinities of chitosan films dried by ambient, LPSSD, and vacuum drying were 15.3, 14.5, and 7.5%, respectively; the films prepared by vacuum drying had the lowest crystallinity. Overall, however, the intensities of all the crystal peaks at about 20° were not high, indicating that all the films had low crystallinity or were in amorphous state.

In addition to the reasons mentioned earlier, LPSSD led to films of higher crystallinity and hence better mechanical properties than did vacuum drying due probably to the different amounts and forms of crystal structure. Rittidej et al.[36] observed that after moist heat treatment at 60°C and 75% RH, amide formation altered the lattice structure of chitosan salt films. This is possibly due to the intramolecular and intermolecular condensation of carboxylic acid in chitosan salt films. LPSSD, which provided relatively more humid drying environment compared with vacuum drying, might also lead to a similar effect. The altered lattice structure in turn led to the different properties and functionality of the film samples.[29]

CONCLUSIONS

The effects of drying methods and drying temperature on the drying kinetics and selected properties of chitosan films were investigated in this study. In terms of the drying kinetics the drying method was found to have a significant effect on the rates of moisture reduction of the samples. Vacuum drying and LPSSD required much shorter drying time than did ambient and hot air drying at 40°C. However, LPSSD took a longer time to dry the product to the final desired moisture content than did vacuum drying.

In terms of properties, it was found that LPSSD produced chitosan films of less yellow color than did vacuum drying. LPSSD at 70°C led to films with higher tensile strength and percent elongation than at other drying conditions. Drying technique and drying temperature did not seem to have any significant effect on the water vapor permeability, however. T_g of ambient-dried and LPSSD films was 197°C, whereas vacuum-dried films exhibited lower T_g of 193°C. Ambient-dried and LPSSD films had more crystallinity than the films dried by vacuum drying.

LPSSD at 70°C was proposed as the best conditions for producing chitosan films in this study for it could enhance some physical properties of chitosan films, making them superior to films dried by other techniques or at other conditions. A future work will study the effects of different drying methods and conditions on physical and functional properties as well as controlled release characteristics of chitosan films incorporated with plant-based antimicrobial and antioxidant extracts.

ACKNOWLEDGEMENTS

The authors express their sincere appreciation to the Commission on Higher Education, the Thailand Research Fund (TRF), and the International Foundation for Science (IFS) in Sweden for supporting the study financially.

REFERENCES

1. Krochta, J.M.; Johnston, C.M. Edible and biodegradable polymer films: Challenges and opportunities. Food Technology **1997**, *51*, 61–74.
2. Shahidi, F.; Arachchi, J.K.V.; Jeon, Y. Food applications of chitin and chitosans. Trends in Food Science and Technology **1999**, *10*, 37–51.
3. Sano, Y. Drying of polymer solution. Drying Technology **1992**, *10*, 591–622.
4. Vinjamur, M.; Cairncross, R.A. A high airflow drying experimental set-up to study drying behavior of polymer solvent coatings. Drying Technology **2001**, *19*, 1591–1612.
5. Etemad, S.G.; Etesami, N.; Bagheri, R.; Thibault, J. Drying of latex films of poly(vinyl acetate). Drying Technology **2002**, *20*, 1843–1854.
6. Wong, S.; Altinkaya, S.A.; Mallapragada, S.K. Multi-zone drying schemes for lowering the residual solvent content during multi-component drying of semicrystalline polymers. Drying Technology **2007**, *25*, 995–1002.
7. Caner, C.; Vergano, P.J.; Wiles, J.L. Chitosan film mechanical and permeation properties as affected by acid, plasticizer, and storage. Journal of Food Science **1998**, *63*, 1049–1053.
8. Wiles, J.L.; Vergano, P.J.; Barron, F.H.; Bunn, J.M.; Testin, R.F. Water vapor transmission rates and sorption behavior of chitosan films. Journal of Food Science **2000**, *65*, 1175–1179.
9. Hwang, K.T.; Kim, J.T.; Jung, S.T.; Cho, G.S.; Park, H.J. Properties of chitosan-based biopolymer films with various degrees of deacetylation and molecular weights. Journal of Applied Polymer Science **2003**, *89*, 3476–3484.
10. Butler, B.L.; Vergano, P.J.; Testin, J.M.; Bunn, J.M.; Wiles, J.L. Mechanical and barrier properties of edible chitosan films as affected by composition and storage. Journal of Food Science **1996**, *61*, 953–955, 961.
11. Srinivasa, P.C.; Ramesh, M.N.; Kumar, K.R.; Tharanathan, R.N. Properties of chitosan films prepared under different drying conditions. Journal of Food Engineering **2004**, *63*, 79–85.
12. Mujumdar, A.S. CEA Report, 817 U 671: Montreal, Canada, 1990.
13. Mujumdar, A.S. Superheated steam drying. In *Handbook of Industrial Drying*, 3rd ed.; Mujumdar, A.S., Ed. CRC Press: Boca Raton, 2007; 439–452.
14. Devahastin, S.; Suvarnakuta, P. Superheated-steam-drying of food products. In *Dehydration of Products of Biological Origin*; Mujumdar, A.S., Ed.; Science Publishers: Enfield, MA, 2004; 493–512.
15. Poirier, N.A. The effect of superheated steam drying on the properties of paper. Drying Technology **1994**, *12*, 2103–2105.
16. McCall, J.M.; Douglas, W.J.M. Enhancement of properties of diverse grades of paper by superheated steam drying. Drying Technology **2005**, *23*, 397–406.
17. Devahastin, S.; Suvarnakuta, P.; Soponronnarit, S.; Mujumdar, A.S. A comparative study of low-pressure superheated steam and vacuum drying of a heat-sensitive material. Drying Technology **2004**, *22*, 1845–1867.
18. Suvarnakuta, P.; Devahastin, S.; Mujumdar, A.S. Drying kinetics and β-carotene degradation in carrot undergoing different drying processes. Journal of Food Science **2005**, *70*, S520–S526.
19. Nadarajah, K.; Prinyawiwatkul, W.; Kyoon No, H.; Sathivel, S.; Xu, Z. Sorption behavior of crawfish chitosan films as affected by chitosan extraction processes and solvent types. Journal of Food Science **2006**, *71*, E33–E39.
20. Suyatma, N.E.; Tighzert, L.; Copinet, A; Coma, V. Effects of hydrophilic plasticizers on mechanical, thermal, and surface properties of chitosan films. Journal of Agricultural and Food Chemistry **2005**, *53*, 3950–3957.
21. Association of Official Analytical Chemists. *Official Methods of Analysis*, 14th ed.; AOAC: Washington, DC, 1995.
22. American Society for Testing and Materials. Standard test methods for tensile properties of thin plastic sheeting. In *Annual Book of ASTM Standards*; ASTM: Philadelphia, 1995, 182–190.
23. American Society for Testing and Materials. Standard test methods for water vapor transmission of materials. In *Annual Book of ASTM Standards*; ASTM: Philadelphia, 1995, 697–704.
24. Gennadios, A.; Weller, C.L.; Gooding, C.H. Measurement errors in water vapor permeability of highly permeable, hydrophilic edible films. Journal of Food Engineering **1994**, *21*, 395–409.
25. Pranoto, Y.; Rakshit, S.K.; Salokhe, V.M. Enhancing antimicrobial activity of chitosan films by incorporating garlic oil, potassium sorbate and nisin. LWT – Food Science and Technology **2005**, *38*, 859–865.
26. Suyatma, N.E.; Copinet, A.; Tighzert, L.; Coma, V. Mechanical and barrier properties of biodegradable films made from chitosan and poly(lactic acid) blends. Journal of Polymers and the Environment **2004**, *12*, 1–6.
27. Suvarnakuta, P.; Devahastin, S.; Soponronnarit, S.; Mujumdar, A.S. Drying kinetics and inversion temperature in a low-pressure superheated steam-drying system. Industrial & Engineering Chemistry Research **2005**, *44*, 1934–1941.
28. Rajendran, V.; Marikani, A. *Materials Science*; Tata McGraw-Hill: New Delhi, 2004.
29. Ogawa, K. Effect of heating an aqueous suspension of chitosan on the crystallinity and polymorphs. Agricultural Biological Chemistry **1991**, *55*, 2375–2379.
30. Ngui, M.O.; Mallapragada, S.K. Mechanistic investigation of drying regimes during solvent removal from poly(vinyl alcohol) films. Journal of Applied Polymer Science **1999**, *72*, 1913–1920.
31. Phan The, D.; Debeaufort, F.; Péroval, C.; Despré, D.; Courthaudon, J.L.; Voilley, A. Arabinoxylan-lipid-based edible films and coatings. 3. Influence of drying temperature on film structure and functional properties. Journal of Agricultural and Food Chemistry **2002**, *50*, 2423–2428.
32. Dong, Y.; Ruan, Y.; Wang, H.; Zhao, Y.; Bi, D. Studies on glass transition temperature of chitosan with four techniques. Journal of Applied Polymer Science **2004**, *93*, 1553–1558.
33. Sakurai, K.; Maegawa, T.; Takahashi, T. Glass transition temperature of chitosan and miscibility of chitosan/poly(*N*-vinyl pyrrolidone) blends. Polymer **2000**, *41*, 7051–7056.
34. Rudin, A. *The Elements of Polymer Science and Engineering: An Introductory Text and Reference for Engineers and Chemists*, 2nd ed.; Academic Press: London, 1999.
35. Urbanczyk, G.W.; Lipp-Symonowicz, B. The influence of processing terms of chitosan membranes made of differently deacetylated chitin on the crystalline structure of membranes. Journal of Applied Polymer Science **1994**, *51*, 2191–2194.
36. Ritthidej, G.C.; Phaechamud, T.; Koizumi, T. Moist heat treatment on physicochemical change of chitosan salt films. International Journal of Pharmaceutics **2002**, *232*, 11–22.

Drying Kinetics and β-Carotene Degradation in Carrot Undergoing Different Drying Processes

PEAMSUK SUVARNAKUTA, SAKAMON DEVAHASTIN, AND ARUN S. MUJUMDAR

ABSTRACT: Superheated steam drying, which is an airless drying technology, has recently received much attention as an alternative to conventional hot air drying, which is a relatively oxygen-rich drying process and causes much product quality degradation. However, because most food products are damaged when subjected to superheated steam at atmospheric or higher pressures, lowering the dryer operating pressure is preferred. In this study, the effects of a low-pressure superheated steam drying (LPSSD), vacuum drying, and hot air drying on the drying and degradation kinetics of β-carotene in carrot were investigated experimentally. LPSSD and vacuum drying led to less degradation of β-carotene in carrot than in the case of hot air drying. The empirical models, which can describe the experimental data of β-carotene degradation in carrot undergoing different drying techniques, were also proposed. β-Carotene degradation in carrot depended more on the carrot temperature than its moisture content in all cases.

Keywords: empirical correlations, hot air drying, low-pressure superheated steam drying, vacuum drying

Introduction

In recent years, the consumption of carrot and its related products has increased steadily due to the recognition of antioxidant and anticancer activities of β-carotene in carrot, which is also a precursor of vitamin A (Speizer and others 1999; Dreosti 1993). However, in food industry, especially instant food industry, carrot must usually be dried prior to its use. Several techniques have been used to dry carrot with the goal of maintaining its natural appearance as well as its nutritional values, including β-carotene, to the maximum level possible.

Many studies (Mulet and others 1989; Ratti 1994) were performed to study hot air drying of carrot of various shapes. It was found that hot air-dried carrot was characterized by the low porosity and the high apparent density nature (Krokida and Maroulis 1997). Khraisheh and others (1997) found that the increased density and shrinkage of carrot was dependent on the operating temperature of hot air drying. Significant color changes also occurred during hot air drying of carrot (Krokida and others 1998) and the change of its red color was attributed to the changing level of β-carotene (Lin and others 1998).

Vacuum drying is an alternative technique to improve the quality of dehydrated heat-sensitive products, including carrot. Krokida and others (1997) found that vacuum drying was able to yield higher porosity and redder carrot than that dried by hot air.

During the past decade, there has been considerable interest in applying superheated steam to dry various food products with some success (Seyed-Yagoobi and others 1999; Moreira 2001; Caixeta and others 2002). Despite the many advantages of near-atmospheric pressure superheated steam drying (Devahastin and Suvarnakuta 2004), there still exist some limitations, especially when applying it to drying heat-sensitive materials, for example, foods and bio-products (Mujumdar 2000). Because most foods or other heat-sensitive products are damaged at the saturation temperature of superheated steam corresponding to the atmospheric or higher pressures, one possible way to alleviate the above-mentioned problems is to operate the dryer at reduced pressure.

Recently, the concept of low-pressure (or sub-atmospheric pressure) superheated steam drying (LPSSD) has been applied to various types of heat-sensitive materials. Elustondo and others (2001) studied sub-atmospheric pressure superheated steam drying of shrimp, banana, apple, potato, and cassava slices both experimentally and theoretically. A semi-empirical mathematical model was developed, and it was found to predict the drying kinetics reasonably well. However, no mention about the quality of dried food products was given. More recently, Devahastin and others (2004) studied experimentally drying of carrot cubes both in low-pressure superheated steam and vacuum dryers. The effects of operating pressure and temperature on the drying characteristics as well as various physical properties, i.e., volume, shrinkage, apparent density, color and rehydration behavior, of the dried carrot subjected to the 2 processes were evaluated. It was observed that steam drying provided better rehydration and redder dried carrot than that obtained in vacuum drying although the drying time in the former case was slightly longer. No mention about the chemical (nutritional) quality changes of carrot during drying was given, however.

The objective of this study was, therefore, to investigate experimentally the effects of a low-pressure superheated steam drying as well as other drying techniques, hot air and vacuum drying, on the drying kinetics and degradation of β-carotene in carrot undergoing these drying operations. Simple relationships between the amount of β-carotene and the product moisture content as well as temperature were also developed for all drying processes studied.

Material and Methods

Experimental setup

A schematic diagram of the low-pressure superheated steam dryer and its accessories is shown in Figure 1. The dryer consists of a stainless steel drying chamber, insulated with rock wool; a steam reservoir, which received steam from a boiler; and a liquid ring vac-

MS 20050213 Submitted 4/7/05, Revised 5/16/05, Accepted 6/16/05. *Authors Suvarnakuta and Devahastin are with Dept. of Food Engineering, King Mongkut's Univ. of Technology Thonburi, 91 Pracha u-tid Rd., Bangkok 10140, Thailand. Author Mujumdar is with Dept. of Mechanical Engineering, Natl. Univ. of Singapore, Singapore. Direct inquiries to author Devahastin (E-mail: sakamon.dev@kmutt.ac.th).*

uum pump (Nash, model ET32030, Nuremberg, Germany), which was used to maintain the vacuum in the drying chamber. A steam trap was installed to reduce the excess steam condensation in the reservoir. An electric heater, which was controlled by a Proportional-Integral-Derivative (PID) controller (Omron, model E5CN, Tokyo, Japan), was installed in the drying chamber to control the steam temperature and to minimize the condensation of steam in the drying chamber during the start-up period. With the use of a heater, the initial steam condensation during the start-up period was reduced considerably. An electric fan was used to disperse steam throughout the drying chamber. The change of the weight of the sample was detected continuously using a load cell (Minebea, model Ucg-3kg, Nagano, Japan). The temperatures of the steam and of the sample were measured continuously using type K thermocouples. Thermocouple signals were then multiplexed to a data acquisition card (Omega Engineering, model no. CIO-DAS16Jr., Stamford, Conn., U.S.A.) installed in a PC. Labtech Notebook Software (version 12.1, Laboratory Technologies Corp., Middleboro, Mass., U.S.A.) was used to read and record the temperature data. More detailed experimental setup can be found in Devahastin and others (2004). For vacuum-drying experiments, the same experimental set-up was used but without the application of steam to the drying chamber. Hot air–drying experiments were performed in a lab-scale tray dryer with an installed balance to monitor the weight change of the drying sample. The temperatures of the air and of the sample were measured continuously using the above-mentioned measuring equipment. The air velocity through the dryer was maintained at 0.8 m/s.

Sample preparation

Fresh carrot (*Daucus carota var. sativa*) was obtained from a supermarket and stored at 4 °C. Prior to the start of each drying experiment, carrot was peeled and diced (only the cortex part) into 1 cm^3 cubes. The moisture content of the fresh carrot was determined by drying it at 105 °C for 12 h in a hot air oven (Memmert, model 800, Schwabach, Germany).

Drying experiments

Raw carrot cubes were dried using 3 different methods: LPSSD, vacuum drying, and hot air drying.

To perform an LPSSD experiment, approximately 35 cubes of carrot (about 40 g) were placed as singer layer on the sample holder.

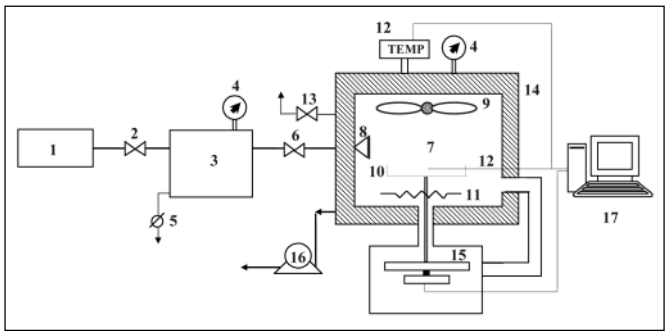

Figure 1—A schematic diagram of the low-pressure superheated steam dryer and associated units: 1, boiler; 2, steam valve; 3, steam reservoir; 4, pressure gauge; 5, steam trap; 6, steam regulator; 7, drying chamber; 8, steam inlet and distributor; 9, electric fan; 10, sample holder; 11, electric heater; 12, on-line temperature sensor and logger; 13, vacuum break-up valve; 14, insulator; 15, on-line weight indicator and logger; 16, vacuum pump; and 17, PC with installed data acquisition card.

More detailed procedures of an LPSSD experiment can be found in Devahastin and others (2004). Although only 40 g of the sample was used, the results reported here should be applicable to future commercial drying applications if care is made in maintaining the same drying conditions in an industrial dryer. The experiments were performed at the steam absolute pressure of 7 kPa and the steam temperatures of 60, 70, and 80 °C. The flow rate of steam into the drying chamber was maintained at about 26 kg/h and the speed of the fan was fixed at 1100 rpm.

For vacuum-drying experiments, the same operating conditions were used but without the application of steam to the chamber. For hot air drying, the experiments were performed at the drying temperatures of 60, 70, and 80 °C at an atmospheric pressure.

To determine the relationship between the β-carotene content of carrot and its moisture content as well as temperature, the drying carrot was sampled and its β-carotene content was measured at a predetermined sampling time; that particular experiment was ended at that time. A new experiment was then performed until the next predetermined sampling time was reached. The β-carotene content of the fresh sample was also measured, so a direct comparison could be made between the fresh and dried samples. The same procedure was repeated until the complete relationship, valid over the whole range of moisture content of interest, was obtained. All experiments were performed in duplicate.

β-Carotene analysis

Drying samples were sampled at different drying times and stored in sealed aluminum foil bags to protect them from light at –18 °C prior to the β-carotene analysis. The samples were thawed at room temperature before the analysis.

The β-carotene analysis method used was a modification of that suggested by AOAC (2000), and the high-performance liquid chromatography (HPLC) method described by Howard and others (1999). To extract β-carotene, dried carrot was prepared by grinding 5 to 8 g of the sample for 2 min using a stainless steel pulverizer (Waring, model SS110, Torrington, Conn., U.S.A.). The ground sample was then placed in a flask filled with 40 mL of ethanol. Forty milliliters of 2 N potassium hydroxide was added to saponify the solution at 70 °C for 30 min. The extract was then cooled to 0 °C. β-Carotene was then extracted twice with 5 mL diisopropyl ether and the aqueous layer was discarded. The extracted solution was diluted by a mobile phase and was filtered through a 0.45 μm filter before injecting 10 μL of the sample into the liquid chromatograph column.

Symmetry® C_{18} 5 μm (3.9 × 150 mm) HPLC column (Waters, Milford, Mass., U.S.A.) was used for β-carotene analysis. The HPLC system consists of a pump and a controller (Waters, model 600), a tunable absorbance detector (Waters, model 486), and an auto sampler (Waters, model 717 plus). A mixture of methanol and acetonitrile (90:10) was used as the mobile phase, and its flow rate was set at 1.5 mL/min. A ultraviolet spectrophotometer detector at a wavelength of 450 nm was used for detecting β-carotene. The mobile phase was degassed using an ultrasonic generator. An HPLC β-carotene standard (Sigma, C4582, Steinheim, Germany) was run daily with the samples to accurately characterize the retention time of β-carotene. Quantification of β-carotene was carried out based on the β-carotene standard curve. The concentration of β-carotene was calculated from the relative peak area of the β-carotene standard curve. The standard curve was prepared daily by injecting solutions of HPLC β-carotene standard in diisopropyl ether at 6 concentrations (0, 2, 4, 6, 8, and 10 μg/mL) and recording their respective absorbance values. All standard curves showed good linearity ($R^2 > 0.99$). A typical chromatogram of β-carotene is shown in Figure 2.

The measured total β-carotene content is expressed in this work

Table 1—Average drying times and losses of β-carotene of dried carrot (at moisture content of 0.1 kg/kg [d.b.]) that underwent different drying methods

Sample	Average drying time (min)	β-Carotene content[a] (mg/100 g)		β-Carotene Retention ratio (β_t/β_i)
		Wet basis	Dry basis	
Fresh carrot	—	4.86 ± 0.65	51.11 ± 6.89	—
LPSSD carrot				
T = 60 °C	420	54.92	43.94	0.83 ± 0.02a
T = 70 °C	330	50.32	41.24	0.76 ± 0.04b
T = 80 °C	210	38.81	31.55	0.74 ± 0.02b
Vacuum-dried carrot				
T = 60 °C	300	26.95	24.28	0.74 ± 0.03c
T = 70 °C	250	25.81	24.05	0.71 ± 0.03cd
T = 80 °C	180	31.61	27.85	0.68 ± 0.03d
Hot air-dried carrot				
T = 60 °C	420	22.56	21.46	0.62 ± 0.02e
T = 70 °C	300	35.66	23.3	0.62 ± 0.03e
T = 80 °C	240	36.26	22.05	0.58 ± 0.03e

[a]Mean ± SD. Different letters in the same column indicate that values are significantly different ($P < 0.05$).

in terms of the β-carotene retention ratio:

$$\beta\text{-carotene retention ratio} = \frac{\beta_t}{\beta_i} \quad (1)$$

where β_i and β_t are, respectively, the β-carotene contents of fresh carrot and dried carrot at the end of each drying experiment (mg/100 g dry solid). All β-carotene measurements were performed in duplicate, and the data presented are an average of the 2 measurements.

Statistical analysis

The data were analyzed and presented as mean values with standard deviations. Differences between mean values were established using Duncan's multiple range test. Values were considered at 95% level of significance ($P < 0.05$) and a statistical program SPSS (version 10.0, Chicago, Ill., U.S.A.) was used to perform the calculation.

Results and Discussion

Drying kinetics of carrot

The drying curves and temperature profiles of carrot (initial moisture contents of 9.5 to 10 kg/kg dry solid (dry basis) or 905 to 909 kg/kg sample (wet basis) undergoing different drying techniques at drying temperatures of 60 to 80 °C are shown in Figure 3**.** The chosen operating conditions were those of Devahastin and others (2004). The drying times needed to dry carrot to the final moisture content of about 0.1 kg/kg (d.b.) are listed in Table 1.

As illustrated in Figure 3, although vacuum drying was a faster drying process than LPSSD and hot air drying, previous studies (Devahastin and others 2004; Suvarnakuta and others 2005) have shown that the differences between the drying times of LPSSD and vacuum drying were smaller at higher drying temperatures. Raising the drying temperature further would eventually lead to equal rates of drying at the so-called inversion temperature due to the increased temperature difference between the steam and the surface temperature of carrot as well as a reduction of the initial steam condensation, which is inevitable in any superheated steam drying applications (Mujumdar 2000). Although LPSSD generally required longer drying time than vacuum drying, LPSSD provided better product physical properties, i.e., better rehydrated and redder dried carrot, than that obtained by vacuum drying over the operating temperature range of 60 to 80 °C and operating pressure of 7 kPa used in this work (Devahastin and others 2004).

In the case of hot air drying, it can be seen in Figure 3 that the drying rates during the 1st 80 min were higher than those of LPSSD. Although the hot air drying rates (slope of the drying curves) in the constant rate period were higher than those of LPSSD, hot air drying

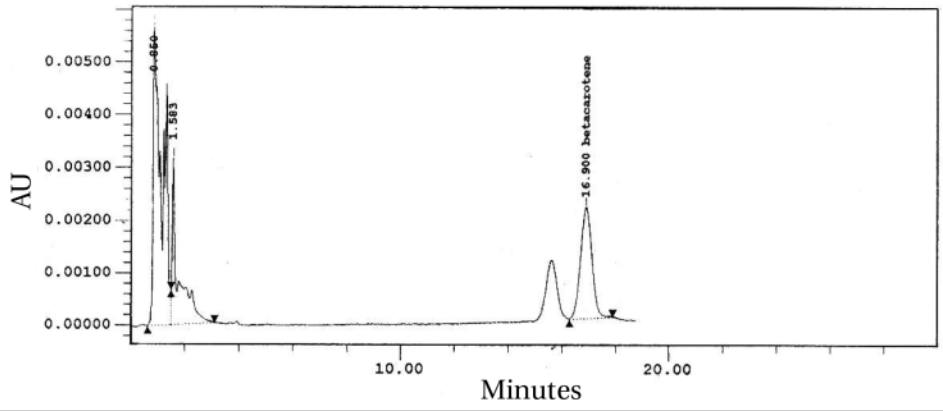

Figure 2—Chromatogram of β-carotene in dried carrot at a wavelength of 450 nm.

took as much time to dry carrot to the final desired moisture content as did LPSSD. This is because the falling rate period of hot air drying was longer than that of LPSSD. In the constant rate period, the water removal carried out by evaporation from the carrot surface in the case of LPSSD took longer time than in the case of hot air drying due to a smaller temperature difference between the drying medium (steam) and the carrot surface (if drying was carried out below the inversion temperature, as in this case). On the other hand, in the falling rate period, LPSSD was faster than hot air drying due to the more porous structure of carrot as well as the higher water diffusivity in the case of steam drying. Therefore, the 2 sets of overall drying times were not much different.

For more detailed information about the drying behavior of carrot cube undergoing LPSSD and vacuum drying the reader is referred to Devahastin and others (2004).

Degradation kinetics of β-carotene

The β-carotene retention in carrot during drying is presented in Table 1. The β-carotene content in fresh carrot on a dry solid basis (51.11 mg/100 g solid) was close to 54 mg/100 g solid documented by Chen and others (1993). The β-carotene content of fresh carrot varied slightly according to its maturity and initial moisture content. The ratio of the β-carotene content of fresh carrot and the dried one (β-carotene retention ratio) was then used to report the results in this study.

As seen in Table 1, all dried carrot cubes lost some β-carotene as compared with fresh ones. However, the loss of β-carotene in the case of hot air drying was significantly ($P < 0.05$) higher (about 21% to 25%) than those observed when drying carrot by other processes to a similar level of moisture content of 0.1 kg/kg (d.b.). LPSSD and vacuum drying could, therefore, reduce the loss of β-carotene to some extent. The ability of LPSSD to conserve heat and oxygen-sensitive products (such as vitamin C) has indeed been shown earlier (Methakhup and others 2005).

It is known that carotene is degraded by free radical oxidation mechanism and that the degree of oxidation depends on the heating time, heating temperature, and oxygen content. In this case, hot air drying was the only non-airless process and, hence, caused more aerobic degradation of β-carotene compared with the other drying processes. These results were similar to those reported by Lin and others (1998) who compared β-carotene contents of carrot slices at a moisture content of 10% (d.b.) underwent vacuum microwave, air drying, and freeze drying. They reported that air drying resulted in the highest loss of β-carotene and the rapid heating and depletion of oxygen offered by vacuum microwave could reduce the loss of β-carotene.

Based on the experimental data, it was found that the total β-carotene retention in the cases of LPSSD and vacuum drying was higher than in the case of hot air drying. This is because of the oxygen-free environment of the LPSSD drying chamber. In the case of vacuum drying, however, because the level of vacuum pressure used in this study was not that low (7 kPa absolute), there still existed some oxygen that could participate in an oxidation reaction. The effect of aerobic degradation of β-carotene could not, therefore, be negligible, although its extent was still lower than in the case of hot air drying.

The relationships between the β-carotene content and the moisture content of carrot undergoing LPSSD, vacuum drying, and hot air drying are shown in Figure 4. As mentioned earlier, the level of oxidation, which is the major cause of carotene losses, depends in part on

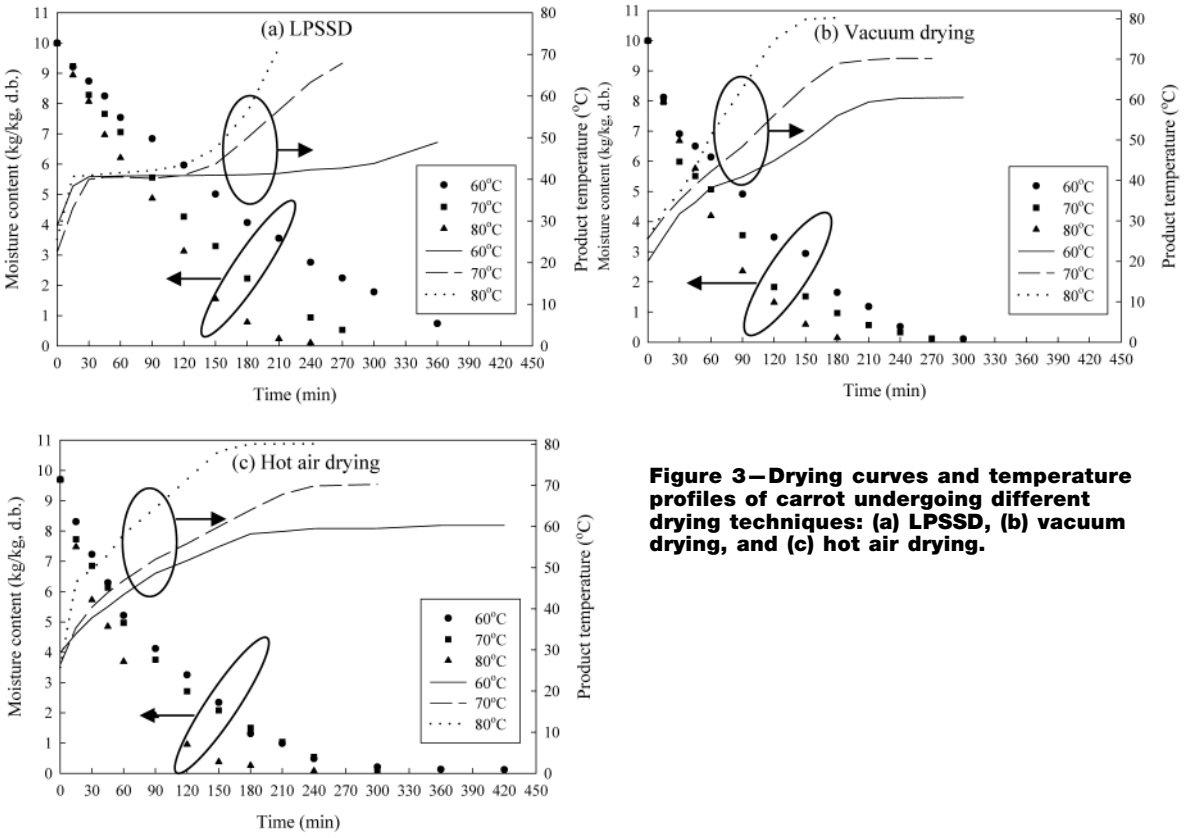

Figure 3—Drying curves and temperature profiles of carrot undergoing different drying techniques: (a) LPSSD, (b) vacuum drying, and (c) hot air drying.

the available oxygen content in the drying chamber. It can be seen from this figure that the level of β-carotene dropped rapidly during the start-up period of drying in all cases. This is due to the fact that moist carrot was immediately subjected to heat treatment, and there might still be some oxygen remained for oxidation initially.

It is seen from Figure 4c that the β-carotene content of carrot decreased continuously in the case of hot air drying while the levels of β-carotene in carrot undergoing LPSSD and vacuum drying remained relatively unchanged (Figures 4a and 4b) after the initial start-up period. This is due to the fact that in the case of hot air drying, lipoxygenase, and probably peroxidase, which are aerobic catalysts of an oxidation reaction, which are contained in unblanched carrot like the one used in this study, was activated significantly at temperatures in the range of 60 to 65 °C (Cui and others 2004). Therefore, it is seen that β-carotene degraded continuously in the case of hot air drying when product temperature increased to this range.

The negligible changes (until the moisture content of around 2 kg/kg [d.b.]) of β-carotene after the initial drop in the case of LPSSD might be explained by the fact that the activity of lipoxygenase and peroxidase, which are responsible for the oxidative degradation of β-carotene, was greatly reduced due to several possible effects, including the lower oxygen level in the drying chamber and the lower product temperature (see Figures 3a and 3c). After some period of time, the temperature of carrot undergoing LPSSD started to rise again. This rise induced additional degradation of β-carotene. At the drying temperature of 60°C, for example, this rise of temperature occurred after 300 min of drying or at moisture contents of less than 2 kg/kg (d.b.). The corresponding degradation of β-carotene can be seen clearly in Figure 4.

Comparison between vacuum drying and LPSSD revealed that the β-carotene retention differed slightly between the 2 processes although vacuum drying took much shorter time than LPSSD to dry the sample to the desired moisture content (Figures 3 and 4). This is because the LPSSD chamber was fully contained with superheated steam; therefore, the oxygen content remaining in the LPSSD chamber was less (none indeed) than in the case of vacuum drying chamber. In addition, the product temperature of all vacuum drying cases was higher than LPSSD cases (Figure 3), thus thermal stability of β-carotene was decreased in the case of vacuum drying. Moreover, the change of the shape of carrot undergoing LPSSD was much more uniform than in the case of vacuum drying. This result was consistent with our previous findings (Devahastin and other 2004). Thus, the LPSSD product had less surface area for heat transfer and hence had higher β-carotene retention.

Empirical models

Figure 5 illustrates the relationship between the β-carotene content and the product temperature during different drying processes. It is seen that β-carotene degraded continuously as the product temperature increased, especially in the case of hot air drying. Because there was no period of constant carrot temperature that corresponded to the constant rate of β-carotene degradation, the use of a kinetic model of β-carotene degradation that refers to an elementary reaction expression and the Arrhenius equation was not appropriate. Therefore, in this study, simple empirical models that enable prediction of the β-carotene degradation as a function of carrot moisture content and temperature were instead proposed. Although, as can be seen in Figure 5c, there were periods of rather constant temperature, which corre-

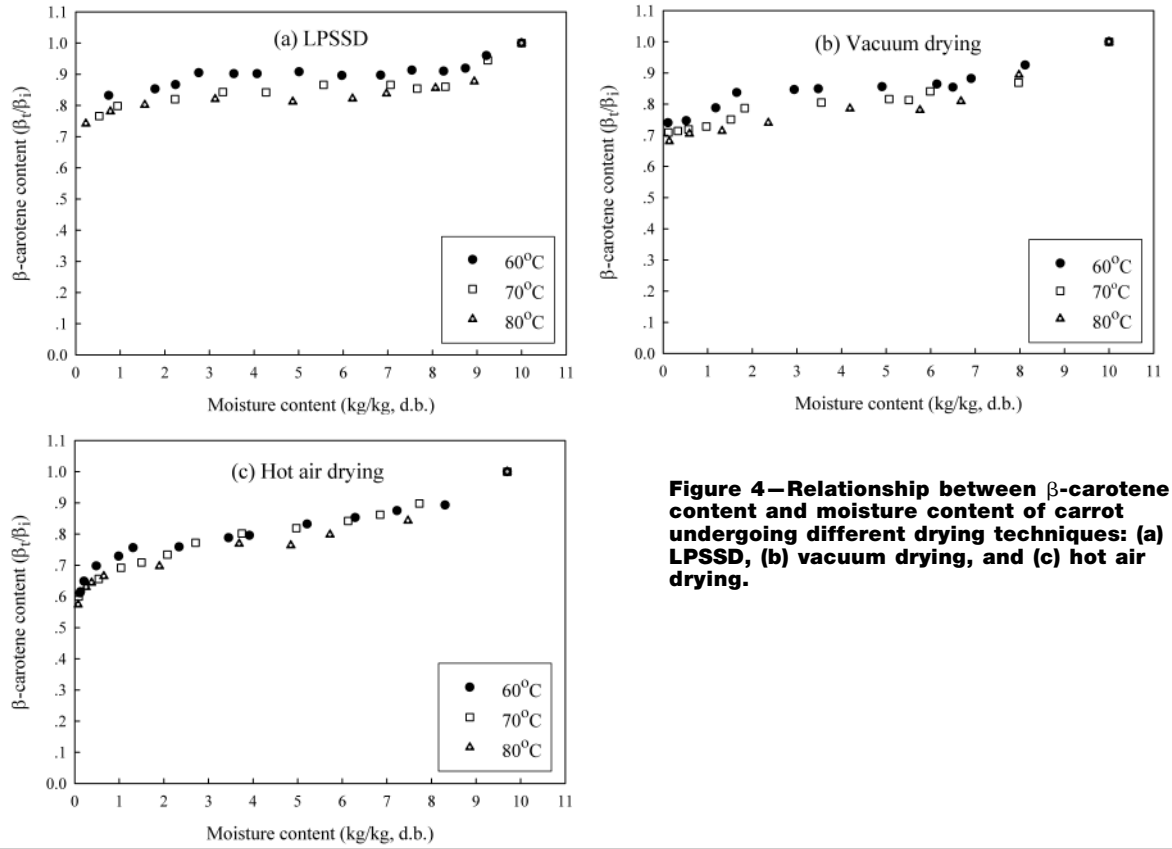

Figure 4—Relationship between β-carotene content and moisture content of carrot undergoing different drying techniques: (a) LPSSD, (b) vacuum drying, and (c) hot air drying.

sponded to the constant degradation rate of β-carotene toward the end of hot air drying, no attempt was made to consider only these rather short periods for a simple elementary reaction expression.

A simple empirical model that enables prediction of the β-carotene degradation as a function of carrot moisture content and temperature during LPSSD, vacuum and hot air drying was proposed in the following form:

$$\frac{\beta_t}{\beta_i} = a + b\frac{X_t}{X_i} + c\frac{T_p}{T_i} + d\left(\frac{X_t}{X_i}\right)^2 + e\left(\frac{T_p}{T_i}\right)^2 + f\left(\frac{X_t}{X_i}\right)^3 + g\left(\frac{T_p}{T_i}\right)^3 \quad (2)$$

where β_i and β_t are the initial and instantaneous β-carotene contents (mg/100 g solid), respectively. X_i and X_t are the initial and instantaneous moisture contents (kg/kg, d.b.), respectively. T_i and T_p are the initial and instantaneous temperatures of carrot (°C), respectively. *a*, *b*, *c*, *d*, *e*, *f*, *g* are empirical constants.

The following equations were fitted to the experimental data and the fitted equations were evaluated based on their R^2 and absolute mean error of estimation. The absolute mean error values are 0.015, 0.031, and 0.012 for the case of LPSSD, hot air drying, and vacuum drying, respectively.

For LPSSD:

$$\frac{\beta_t}{\beta_i} = 1.104 + 0.261\frac{X_t}{X_i} - 0.192\frac{T_p}{T_i} - 0.561\left(\frac{X_t}{X_i}\right)^2 - 6.61\times10^{-3}\left(\frac{T_p}{T_i}\right)^2 + 0.390\left(\frac{X_t}{X_i}\right)^3 + 0.011\left(\frac{T_p}{T_i}\right)^3 \quad R^2 = 0.911 \quad (3)$$

For vacuum drying:

$$\frac{\beta_t}{\beta_i} = 0.754 + 0.596\frac{X_t}{X_i} - 0.339\frac{T_p}{T_i} - 0.708\left(\frac{X_t}{X_i}\right)^2 + 0.221\left(\frac{T_p}{T_i}\right)^2 + 0.517\left(\frac{X_t}{X_i}\right)^3 - 0.038\left(\frac{T_p}{T_i}\right)^3 \quad R^2 = 0.90 \quad (4)$$

For hot air drying:

$$\frac{\beta_t}{\beta_i} = 0.663 + 0.742\frac{X_t}{X_i} + 0.165\frac{T_p}{T_i} - 1.400\left(\frac{X_t}{X_i}\right)^2 - 0.130\left(\frac{T_p}{T_i}\right)^2 + 0.941\left(\frac{X_t}{X_i}\right)^3 + 0.026\left(\frac{T_p}{T_i}\right)^3 \quad R^2 = 0.982 \quad (5)$$

It can be seen from the above simple empirical relationships that the β-carotene retention depends on both the product moisture content and temperature. It should be noted that these empirical equations are based on the experimental results and conditions used in this study only. It can be seen also that the carrot temperature was the main contributor of β-carotene degradation. It is observed from the values of the main parameters of these equations (the terms of 3rd order and $0 < \frac{X_t}{X_i} \le 1,\ 1 \le \frac{T_p}{T_i} \le 3.2$) that the effect of carrot temperature was larger than the effect of carrot moisture content on the β-carotene degradation of carrot during drying. This is because heat is the main reason for β-carotene degradation, especially in the low-oxygen system. Product temperature was,

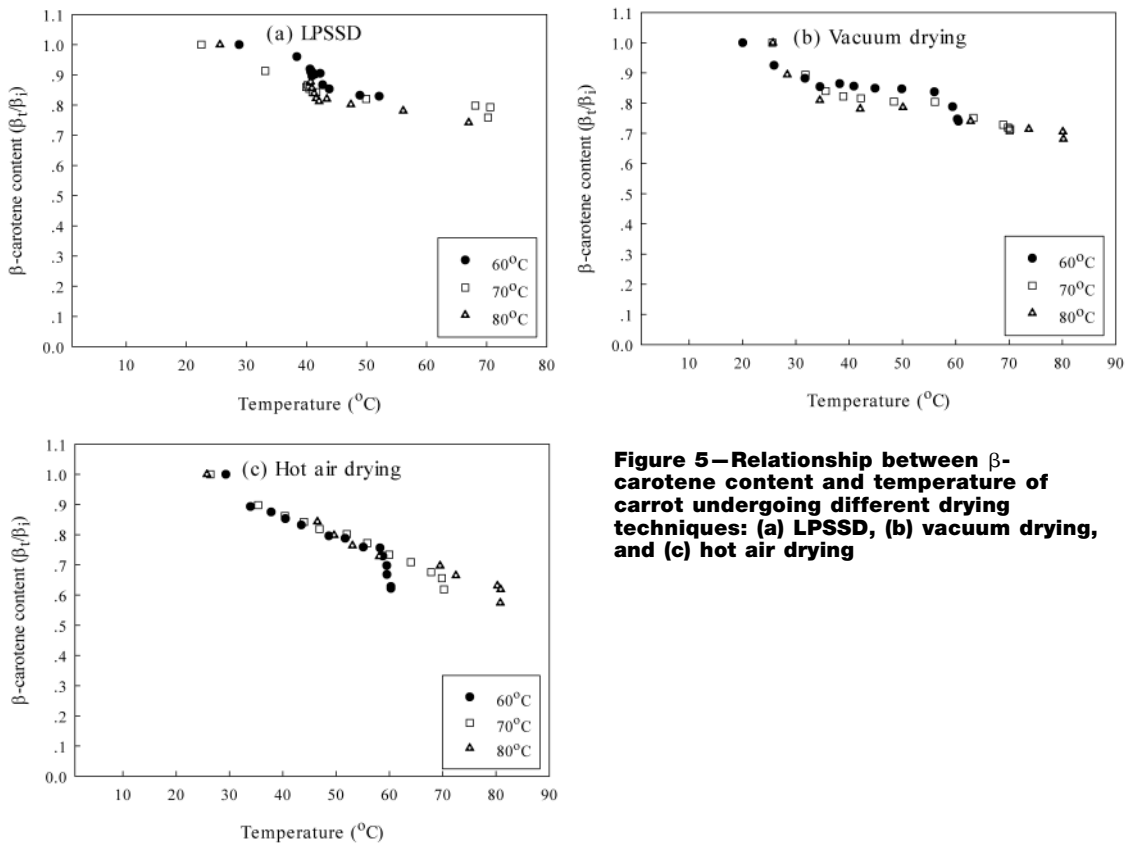

Figure 5—Relationship between β-carotene content and temperature of carrot undergoing different drying techniques: (a) LPSSD, (b) vacuum drying, and (c) hot air drying

therefore, the major player of the β-carotene degradation in the cases of LPSSD and vacuum. In the case of hot air drying, although the product temperature also affected more significantly the β-carotene degradation compared with the effect of moisture content, the effect of the product temperature was less obvious than in the cases of airless drying systems. This is due to the fact that for hot air drying the main cause of β-carotene degradation was the oxygen content available to an oxidative reaction of β-carotene in the drying chamber. Therefore, the effect of the product temperature was somehow overshadowed.

Conclusions

Comparison was made of the β-carotene degradation in carrot undergoing different drying techniques, such as LPSSD, vacuum drying, and conventional hot air drying. It was found that LPSSD and vacuum drying led to less degradation of β-carotene of carrot than in the case of hot air drying (up to 20% to 25% in the case of LPSSD). The empirical models, which can describe the experimental data of β-carotene degradation in carrot undergoing different drying techniques, were also proposed. The information obtained here can be used as a guideline in the design and operation of a system, which is suitable for drying heat- and/or oxygen-sensitive bio-products with the aim to minimize the quality losses of these products.

Acknowledgments

The authors express their sincere appreciation to Commission on Higher Education, the Thailand Research Fund (TRF), Natl. Science and Technology Development Agency (NSTDA), and the Intl. Foundation for Science (Sweden) for supporting this study financially.

References

[AOAC] Assn. of Official Analytical Chemists. 2000. Official methods of analysis. 17th ed., Gaithersburg, MD: AOAC.
Caixeta AT, Moreira R, Castell-Perez ME. 2002. Impingement drying of potato chips. J Food Process Eng 25(1):63–90.
Chen BH, Chuang JR, Lin JH, Chiu CP. 1993. Quantification of provitamin A compounds in Chinese vegetables by high-performance liquid chromatography. J Food Protect 53(12):1076–8.
Cui ZW, Xu SY, Sun DW. 2004. Effect of microwave-vacuum drying on the carotenoids retention of carrot slices and chlorophyll retention of Chinese chive leaves. Drying Technol 22(3):563–75.
Devahastin S, Suvarnakuta P. 2004. Superheated steam drying of food products. In: Mujumdar AS, editor. Dehydration of products of biological origin. Enfield, NH: Science Publishers. p 493–512.
Devahastin S, Suvarnakuta P, Soponronnarit S, Mujumdar AS. 2004. A comparative study of low-pressure superheated steam and vacuum drying of a heat-sensitive material. Drying Technol 22(8):1845–67.
Dreosti IE. 1993. Vitamins A, C, E and β-carotene as protective factors for some cancers. Asia Pacific J Clin Nutr 2(l):21–5.
Elustondo D, Elustondo MP, Urbicain MJ. 2001. Mathematical modeling of moisture evaporation from foodstuffs exposed to subatmospheric pressure superheated steam. J Food Eng 49(1):15–24.
Howard LA, Wong AD, Perry AK, Klein BP. 1999. β-Carotene and ascorbic acid retention in fresh and processed vegetables. J Food Sci 64(5):929–36.
Khraisheh MAM, Cooper TJR, Magee TRA. 1997. Shrinkage characteristics of potatoes dehydrated under combined microwave and convective air conditions. Drying Technol 15(3–4):1003–21.
Krokida MK, Maroulis ZB. 1997. Effect of drying method on shrinkage and porosity. Drying Technol 15(10):1145–55.
Krokida MK, Tsami E, Maroulis ZB. 1998. Kinetics on color changes during drying of some fruits and vegetables. Drying Technol 16(3–5):667–85.
Krokida MK, Zogzas NP, Maroulis ZB. 1997. Modelling shrinkage and porosity during vacuum dehydration. Int J Food Sci Tech 32(6):445–58.
Lin TM, Durance TD, Scaman CH. 1998. Characterization of vacuum microwave, air and freeze dried carrot slices. Food Res Int 31(2):111–7.
Methakhup S, Chiewchan N, Devahastin S. 2005. Effects of drying methods and conditions on drying kinetics and quality of Indian gooseberry flake. Lebensm Wiss Technol 38(6):579–87.
Moreira RG. 2001. Impingement drying of foods using hot air and superheated steam. J Food Eng 49(4):291-5.
Mujumdar AS. 2000. Superheated steam drying—technology of the future. In: Devahastin S, editor. Mujumdar's practical guide to industrial drying. Brossard, Canada: Exergex. p 115–38.
Mulet A, Berna A, Rosello C, Pinaga F. 1989. Drying carrots. II. Evaluation of drying models. Drying Technol 7(4):641–61.
Ratti C. 1994. Shrinkage during drying of foodstuffs. J Food Eng 23(1):91–5.
Seyed-Yagoobi J, Li YB, Moreira RG, Yamsaengsung R. 1999. Superheated steam impingement drying of tortilla chips. Drying Technol 17(1–2):191–213.
Speizer FE, Colditz GA, Hunter DJ, Rosner B, Hennekens C. 1999. Prospective study of smoking, antioxidant intake, and lung cancer in middle-aged women. Cancer Cause Control 10(5):475–82.
Suvarnakuta P, Devahastin S, Soponronnarit S, Mujumdar AS. 2005. Drying kinetics and inversion temperature in a low-pressure superheated steam drying system. Ind Eng Chem Res 44(6):1934–41.

Available online at www.sciencedirect.com
ScienceDirect
Journal of Food Engineering 85 (2008) 154–162
JOURNAL OF FOOD ENGINEERING
www.elsevier.com/locate/jfoodeng

Effect of far-infrared radiation assisted drying on microstructure of banana slices: An illustrative use of X-ray microtomography in microstructural evaluation of a food product

Angélique Léonard [a,*], Silvia Blacher [a], Chatchai Nimmol [b], Sakamon Devahastin [c]

[a] Laboratory of Chemical Engineering, Department of Applied Chemistry, University of Liège, FNRS, B6c, Sart Tilman, 4000 Liège, Belgium
[b] School of Energy, Environment and Materials, King Mongkut's University of Technology Thonburi, 126 Pracha u-tid Road, Bangkok 10140, Thailand
[c] Department of Food Engineering, King Mongkut's University of Technology Thonburi, 126 Pracha u-tid Road, Bangkok 10140, Thailand

Received 22 May 2007; received in revised form 11 July 2007; accepted 20 July 2007
Available online 3 August 2007

Abstract

X-ray microtomography coupled with image analysis represents a non-destructive technique, which allows scanning an entire sample to obtain such information as total pore volume and pore size distribution without the need of serial cuts as in the case of scanning electron microscopy (SEM). The technique has been applied successfully to obtain reliable microstructural information of many products undergoing different physical and chemical processes. However, the technique has still found limited use in food processing. To illustrate the use of X-ray microtomography the technique was applied to investigate the effect of far-infrared radiation (FIR) assisted drying on microstructure of a food product viz. banana. Two representative drying techniques, i.e., low-pressure superheated steam drying (LPSSD) and vacuum drying (VACUUM) were tested. Banana slices were dried by LPSSD–FIR at two different temperatures (80 and 90 °C) at a fixed pressure of 7 kPa. The total pore volume and pore size distribution of dried banana slices were then determined using X-ray microtomography. The results were also compared with those of products dried by LPSSD without FIR. Far-infrared radiation was found to modify the structure of the dried bananas by increasing their final porosity. The same effect of FIR was also observed in the case of vacuum drying with FIR (VACUUM–FIR). An increase of the drying temperature was also found to globally lead to an increase in the final porosity of the products.

Keywords: Image analysis; Low-pressure superheated steam drying; Microstructure; Porosity; X-ray microtomography; Vacuum drying

1. Introduction

Although scanning electron microscopy (SEM) is a significant means to analyse the microstructure of a sample, SEM does not give reliable information on the total pore volume and pore size distribution of the sample. Indeed, due to the small parts that can be investigated with this method, measurements must be largely repeated in order to give statistically relevant results. Moreover, this technique fails to describe the whole 3D morphology as only 2D information is obtained. X-ray microtomography, on the other hand, is a powerful technique that can be used to obtain the above information. The main advantage of X-ray microtomography lies in its non-destructive character, as opposed to SEM that requires cutting of the sample. With its large field of view, X-ray microtomography also allows scanning of the entire sample. This technique is quite new in the field of food engineering (Babin et al., 2006; Haedelt, Pyle, Beckett, & Niranjan, 2005; Lim & Barigou, 2004; van Dalen, Blonk, van Haalts, & Hendriks, 2003) but it has been successfully applied for the characterization of highly porous materials (Blacher et al., 2006; Blacher et al., 2004; Léonard et al., 2007), the follow-up

* Corresponding author. Tel.: +32 4 366 47 22; fax: +32 4 366 28 18.
E-mail address: a.leonard@ulg.ac.be (A. Léonard).

0260-8774/$ - see front matter © 2007 Elsevier Ltd. All rights reserved.
doi:10.1016/j.jfoodeng.2007.07.017

of shrinkage and crack formation (Job, Sabatier, Pirard, Crine, & Léonard, 2006; Léonard, Blacher, Marchot, Pirard, & Crine, 2004) as well as internal moisture profiles during drying (Léonard, Blacher, Marchot, Pirard, & Crine, 2005).

Porosity is one of the important properties of dried foods and is generally related to their texture. To obtain dried products with higher degree of porosity, several novel drying methods have been proposed and tested. Low-pressure superheated steam drying (LPSSD) is one of the drying techniques that has recently been applied to various products for the above-mentioned purpose. Due to the low-pressure environment and evolution of evaporated moisture within the products during LPSSD, high-pressure gradients within the products occur, leading to an expansion of the cells of the products. Consequently, LPSSD dried products have more porous structure than those obtained by conventional hot air drying or vacuum drying (Devahastin, Suvarnakuta, Soponronnarit, & Mujumdar, 2004). Despite the potential of LPSSD to provide dried products with higher degree of porosity, the process is rather slow. To accelerate the drying process, a drying system combining LPSSD and far-infrared radiation (FIR) has been developed and applied successfully to a heat-sensitive food material (Nimmol, Devahastin, Swasdisevi, & Soponronnarit, 2007). It was found in this latter work that when FIR was applied to the process as an additional heat source, not only the drying time was reduced but the dried product quality, as assessed by texture analysis and SEM, was also improved.

As an illustrative example of the use of X-ray microtomography to evaluate the microstructure of a food product undergoing drying, the effect of FIR on the microstructure of banana slices dried by the system combining LPSSD and FIR (or LPSSD–FIR) was analysed. The results were also compared with those obtained by only low-pressure superheated steam drying (LPSSD), vacuum drying (VACUUM), and combination of FIR with vacuum drying (VACUUM–FIR). Two drying temperatures, 80 and 90 °C, were investigated in this work.

2. Experimental set-up, materials and methods

2.1. Experimental set-up

Fig. 1 shows a schematic diagram of the far-infrared radiation assisted drying system (Nimmol et al., 2007). Depending on whether the steam injection was switched on or off, two operating modes were respectively realized, i.e., low-pressure superheated steam drying or vacuum drying. The dryer consists mainly of a stainless steel drying chamber with inner dimensions of $45 \times 45 \times 45$ cm^3; a boiler for steam production; a steam reservoir, which maintained a steam pressure at around 200 kPa; a liquid ring vacuum pump (Nash, ET32030, Trumball, CT), which was used to maintain vacuum in the drying chamber; a sample holder; a load cell (Minebea, Ucg-3 kg, Nagano, Japan) with an accuracy of ±0.2 g, which was used to record continuously the mass of the sample (at 1 min interval); a far-infrared radiator (Infrapara, A-2T-500, Selangor, Malaysia) rated at 500 W with a surface area of 60×120 mm^2, which was used to supply thermal radiation to the drying sample and the drying medium in the case of LPSSD–FIR and VACUUM–FIR experiments; and an electric heater rated at 1500 W, which was used to maintain the superheated steam and air temperature in the case of LPSSD and VACUUM experiments.

The operation of the far-infrared radiator was controlled through the temperature of the drying medium (air or superheated steam) measured at 30 mm above the sample surface via the use of a Proportional–Integral–Derivative (PID) controller (Shinko, JCS-33A-R/M, Osaka, Japan) with an accuracy of ±0.1 °C. Similar to the far-infrared radiator, the operation of the electric heater was also controlled by a PID controller (Omron, E5CN, Tokyo, Japan) with an accuracy of ±0.1 °C. The temperatures of the drying medium and of the drying sample were measured continuously using type K thermocouples. Thermocouple signals were multiplexed to a data acquisition card (Omega Engineering, CIO-DAS16Jr., Stamford, CT) installed in a PC. Labtech Notebook software (version

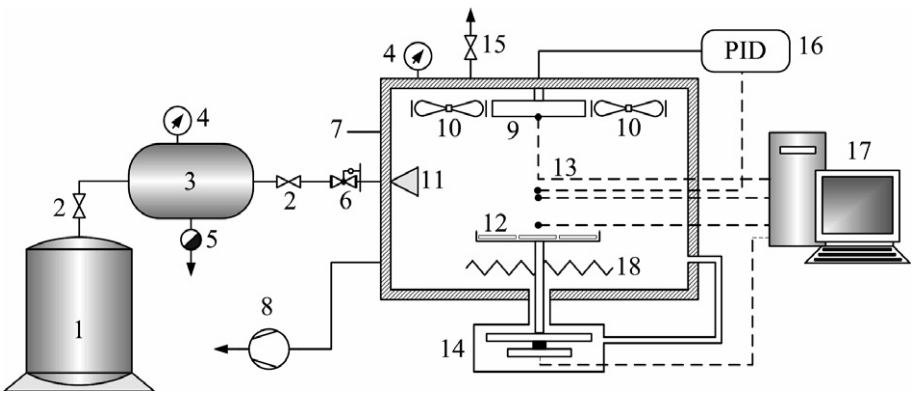

Fig. 1. A schematic diagram of the far-infrared radiation assisted drying system: (1) boiler; (2) steam valve; (3) steam reservoir; (4) pressure gauge; (5) steam trap; (6) steam regulator; (7) drying chamber; (8) vacuum pump; (9) far-infrared radiator; (10) electric fans; (11) steam inlet and distributor; (12) sample holder; (13) thermocouples; (14) load cell; (15); vacuum break-up valve; (16) PID controller; (17) PC with data acquisition card; (18) electric heater.

12.1, Laboratory Technologies Corp., Wilmington, MA) was then used to read and record the temperature data.

2.2. Material

Gros Michel banana (*Musa Sapientum* L.) was used as the tested material in this study. Fresh banana with initial moisture content (AOAC, 1984) in the range of 2.65–3.10 kg/kg (d.b.) and selected ripeness level of green tip (color index no. 5) was obtained from a local supermarket in Bangkok, Thailand and stored at 4 °C. Before each drying experiment, banana was peeled and sliced by an electric food slicer (Chef's Choice, 667 S, Aurora, NE) to 3 mm thick. The sliced samples were then cut into 30 mm diameter using a die.

2.3. Methods

In this study, approximately 16 pieces of prepared banana slices were used in each drying experiment. The experiments were carried out at the drying medium temperatures of 80 and 90 °C and absolute chamber pressure of 7 kPa. It should be noted that low-pressure superheated steam was the drying medium in the case of LPSSD–FIR and LPSSD experiments, while low-pressure air was the drying medium in the case of VACUUM–FIR and VACUUM experiments. Since the forced convection in the drying chamber led to lower temperatures of the far-infrared radiator and of the samples leading to lower drying rates, the electric fans were not used in the case of VACUUM–FIR experiments. Detailed methods of LPSSD–FIR and VACUUM–FIR experiments can be found in Nimmol et al. (2007), while detailed methods of LPSSD and VACUUM experiments are available in Devahastin et al. (2004). The drying experiments were performed until a moisture content of 0.035 kg/kg (d.b.) was obtained. This final moisture content was estimated from both the knowledge of the initial water content and the loss of mass, obtained through the drying curve. All experiments were performed in duplicate.

2.4. X-ray microtomography

X-ray microtomography is a powerful non-invasive technique allowing the visualization of the internal structure of a sample based upon local variation of the X-ray attenuation coefficient. During tomographic investigation an X-ray beam is sent to the sample and the transmitted beam is recorded by a detector. According to the Beer–Lambert's law the transmitted intensity is related to the integral of the X-ray attenuation coefficient (μ) along the path of the beam. This coefficient depends on the density (ρ), the atomic number (Z) of the material and on the energy of the incident beam (E) according to

$$\mu = \rho\left(a + \frac{bZ^{3.8}}{E^{3.2}}\right), \quad (1)$$

where a is a quantity with a relatively small energy dependence and b is a constant (Vinegar & Wellington, 1987).

Projections (assembling of transmitted beams) are recorded for several angular positions by rotating the sample between 0° and 180°. Then, a back-projection algorithm is used to reconstruct 2D or 3D images, depending on the method used. In the case of 2D images each pixel has a grey level value corresponding to the local attenuation coefficient.

The "Skyscan-1172 high-resolution desk-top micro-CT system" (Skyscan, Kontich, Belgium) was used in this study. A banana slice was placed vertically in a polystyrene holder, the latter being almost transparent to X-rays. In contrast to a classical medical scanner, the source and the detector were fixed, while the sample was rotated during the measurement. The cone beam source operated at 60 kV and 167 μA. The detector was a 2 D, 1048 × 2000 pixels, 16-bit X-ray camera. The distance source-object-camera was adjusted to produce images with a pixel size of 15 μm. Because of the sample height, three successive sub-scans, each corresponding to one third of the slice height, had to be performed. The rotation step was fixed at 0.4°. For each angular position, a radiograph of the sample, instead of a 1D-projection of a cross-section, was recorded by a 2D camera.

Fig. 2 shows a typical radiograph obtained after the three sub-scans were linked together. The acquisition time required for each of the three segments was close to 50 min. The Feldcamp back-projection algorithm was used to reconstruct 2D images of the cross-sections. For each banana slice about 200 cross-sections, separated by 150 μm, were reconstructed. Fig. 3a and b shows typical grey level cross-sections obtained for two vertical positions in the sample.

2.5. Image analysis and measurement

3D images of the samples were built by stacking ca. 200 cross-sections obtained by X-ray microtomography. The

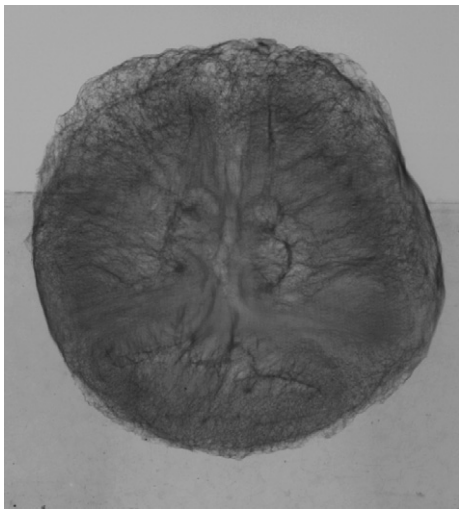

Fig. 2. Typical radiograph of a dried banana slice.

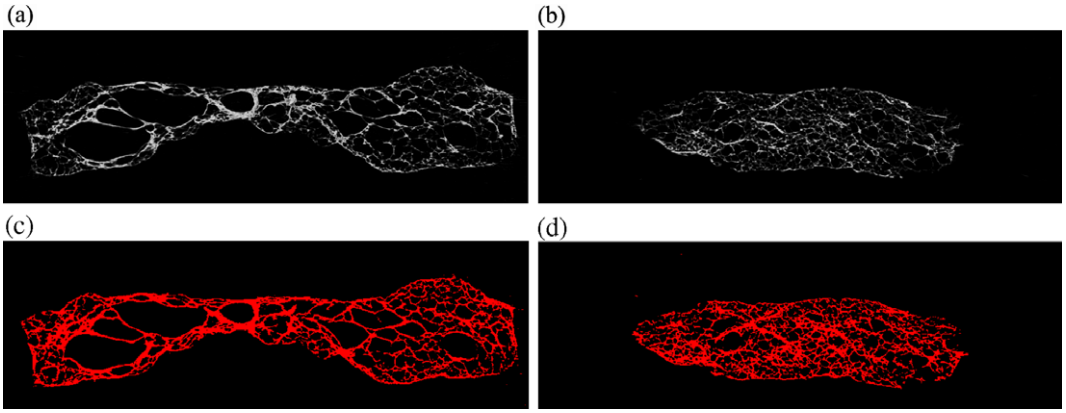

Fig. 3. Grey level cross-sections (a–b) and the corresponding binary images after thresholding (c–d).

resulting 3D grey level images were formed by two phases: the pore space at low grey levels (dark voxels), and the banana skeleton at high grey levels (bright voxels) (see Fig. 3a and b). To perform a measurement, the 3D image was preliminary segmented by assigning the value 1 to all pixels whose intensity was below a given grey tone value and 0 to the others, which implies fixing a threshold on the 3D grey level image. This threshold was determined as follows: an automatic threshold based on the entropy of the histogram (Sahoo, Soltani, Wong, & Chen, 1988) was calculated for each 2D cross-section. In this method, the inter-class entropy (S), defined by Eq. (2), was maximized.

$$S = -\sum p_i \times \log(p_i), \tag{2}$$

where p_i is the probability of a pixel grey scale value in the image.

Fig. 3c and d show the result of the segmentation process applied to Fig. 3a and b, respectively. The threshold values obtained from the entropy method for the set of cross-sections, which formed each 3D image, were very close indicating that skeleton tomograms had an homogeneous contrast. Then, a single threshold value for the 3D images was determined as an average of the cross-section thresholds. After this thresholding step, some small black holes were still present in the image and were removed by applying a closing filter (Soille, 1999).

From the 3D processed binary images the porosity (δ), defined as the fraction of voxels of the image that belong to the pores, was first measured. As the 3D images of banana slices presented a continuous and rather disordered pore structure in which it was not possible to assign to each pore a precise geometry, a standard granulometry measurement could not be applied. Therefore, to quantify the larger pore sizes, the opening size distribution (Soille, 1999), which allows assigning a size to both continuous and individual particles, was calculated. When an opening transformation was performed on a binary image with a structuring element (SE) of size λ, the image was replaced by an envelope of all SEs inscribed in its objects. For the sake of simplicity spheres of increasing radii λ (approximated by octahedra) were used. When an image was opened by a sphere whose diameter was smaller than the smallest features of its objects it remains unchanged. As the size of the sphere increased, larger parts of the objects were removed by the opening transformation. Therefore, opening could be considered as equivalent to a physical sieving process. This procedure was applied to the reversed 3D images of the foams, i.e., to the 3D images in which pores correspond to white measurable voxels and the matrix to black voxels. Image processing and measurements were performed with software Aphelion 3.2 (Adsis, Meythet, France) on a PC.

3. Results and discussion

3.1. Temperature evolution of banana slices during drying

Because the temperature of the samples during drying is an important factor influencing their pore structure, the temperature of banana slices undergoing different drying methods and conditions is first discussed. As revealed by Fig. 4a and b the temperature of the samples undergoing the process applying FIR (LPSSD–FIR and VACUUM–FIR) was much higher than that of samples undergoing LPSSD and VACUUM. This is due to an extra heating. In the cases of LPSSD and LPSSD–FIR, the periods of constant sample temperature, which were consistent with the period of constant drying rates, were observed after a rapid increase of the sample temperature during the first 10 min of drying. For LPSSD the level of constant sample temperature was the boiling point of water corresponding to the chamber pressure. However, for LPSSD–FIR the level of constant sample temperature was higher than the boiling point of water because FIR was present. For the processes without the application of superheated steam (VACUUM and VACUUM–FIR) no periods of constant sample temperature were observed because no constant drying rate periods were observed (Nimmol et al., 2007). It should also be noted from Fig. 4 that the temperatures of LPSSD–FIR and VACUUM–FIR samples during the later stages of drying rose to levels higher than the set medium temperatures and remained rather constant until the end of the processes. This is again due to the influence of

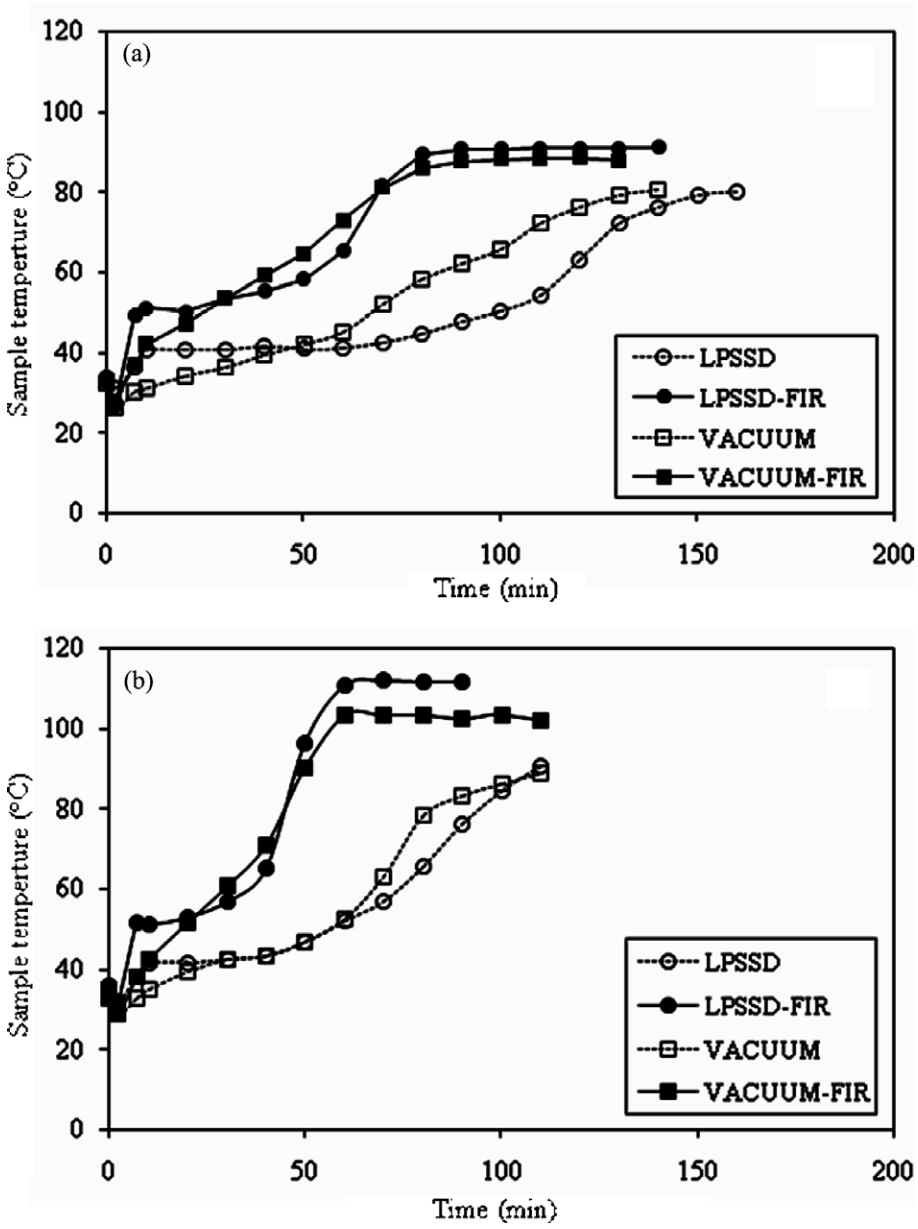

Fig. 4. Temperature evolution of banana slices dried at (a) 80 °C and (b) 90 °C.

additional energy obtained from FIR. These results are in contrast to those of LPSSD and VACUUM for which the sample temperature approached the drying medium temperature toward the end of drying. It was also observed that the sample temperature during the later stage of LPSSD–FIR was higher than that in the case of VACUUM–FIR. This is because in the case of LPSSD–FIR the far-infrared radiator was used more often due to the fact that the far-infrared absorptivity of superheated steam is higher than that of air (Nimmol et al., 2007). More detailed explanation of the temperature evolutions during drying using methods employed in this study is available in Nimmol et al. (2007) and Thomkapanish, Suvarnakuta, and Devahastin (2007).

Table 1
Total porosity of banana slices undergoing various drying methods at different drying conditions

Drying method	Drying temperature (°C)	Porosity
LPSSD	80	0.42 ± 0.05
	90	0.53 ± 0.06
LPSSD–FIR	80	0.55 ± 0.06
	90	0.70 ± 0.08
VACUUM	80	0.54 ± 0.05
	90	0.46 ± 0.05
VACUUM–FIR	80	0.57 ± 0.06
	90	0.63 ± 0.07

3.2. Pore structure characterization

The total porosity obtained from the 3D reconstructed images of banana slices are listed in Table 1. The porosity

values indicated that an increase in the drying temperature generally led to an increase in the porosity of the samples. This is because drying at a higher temperature resulted in a higher sample temperature and hence higher pressure gradients within the sample. These gradients in turn led to stronger evolution of moisture within the sample during drying resulting in higher values of the sample porosity.

At the same drying temperature, the use of FIR clearly resulted in an increase of the sample porosity in all cases. For example, at 90 °C a relative augmentation of about 32% and 37% was observed in the case of LPSSD and VACUUM, respectively, when FIR was used. This is due to the fact that during the processes applying FIR higher sample temperature was developed (see again Fig. 4). Consequently, the internal pressure gradients increased more

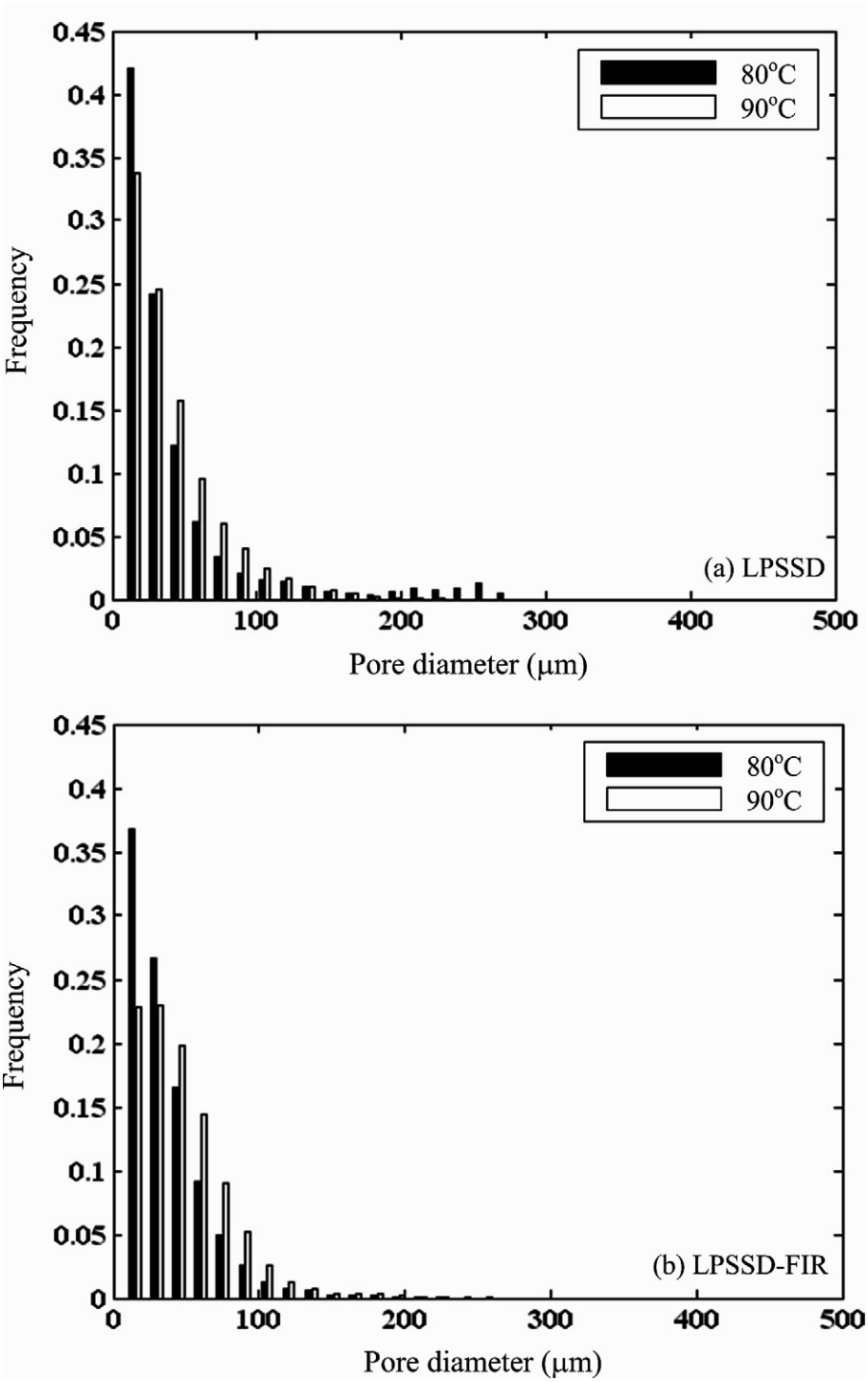

Fig. 5. Pore size distributions of the samples dried at 80 and 90 °C with (a) LPSSD and (b) LPSSD–FIR.

intensely leading to high-porosity products. It is also found from Table 1 that drying at a higher temperature led to the dried products with higher porosity in almost all cases, except for VACUUM. This may probably be due to the fact that, in the case of VACUUM, the stresses developed during drying at a higher temperature were larger and this led to a higher degree of microstructural deformation and collapse of structure leading to denser structure of the product (Devahastin et al., 2004). No additional effect of FIR was also present to help expanding the sample structure as well in the case of VACUUM.

It should be noted from Table 1 that when drying was performed at a higher temperature (90 °C) the porosity values of LPSSD and LPSSD–FIR samples were higher than those of VACUUM and VACUUM–FIR samples, respectively. This is due to a rapid increase of the sample temper-

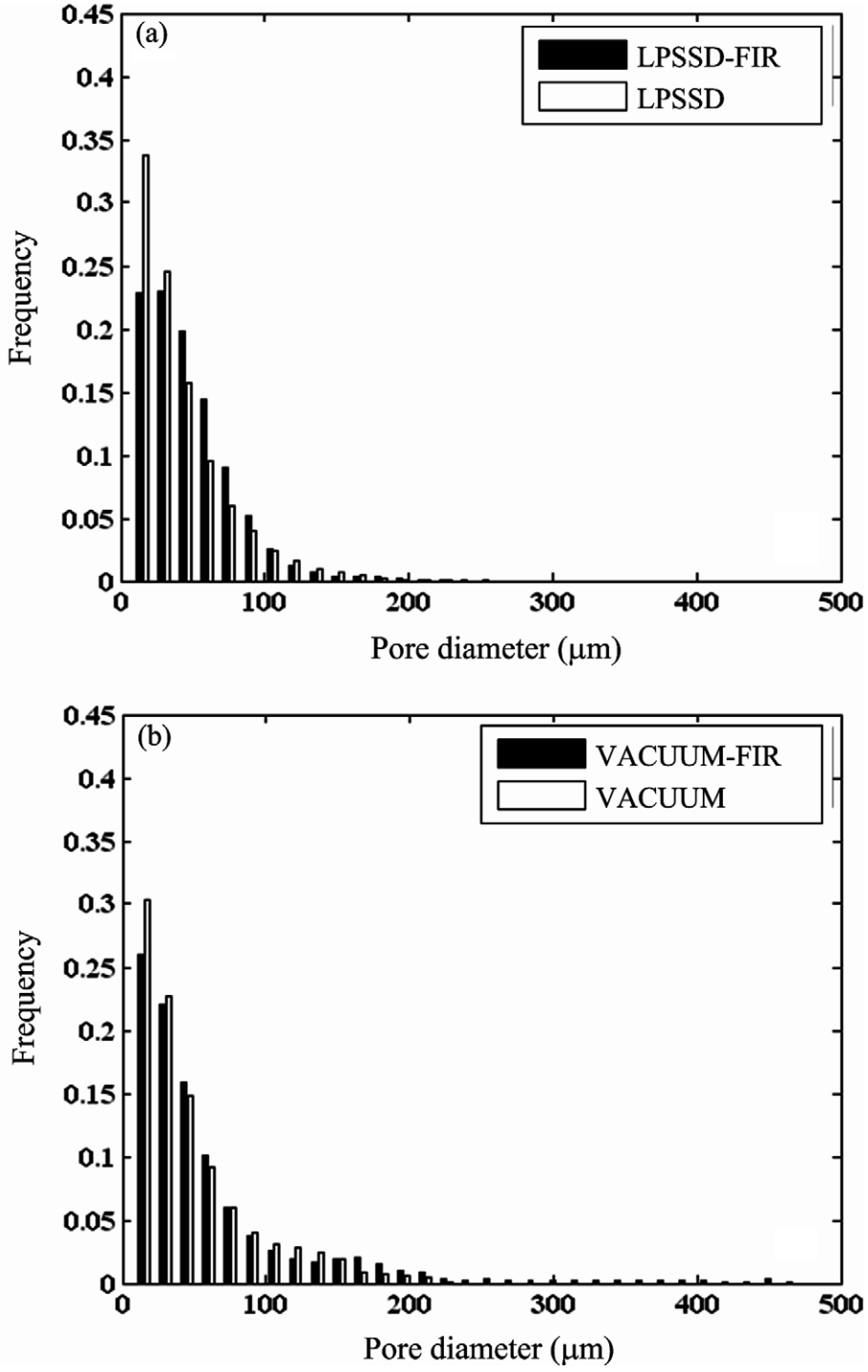

Fig. 6. Pore size distributions of the samples dried at 90 °C: (a) comparison between LPSSD–FIR and LPSSD dried samples and (b) comparison between VACUUM–FIR and VACUUM dried samples.

ature during initial stages of LPSSD and LPSSD–FIR (see Fig. 4b) resulting in rigorous boiling of moisture within the samples. However, the results were opposite when drying was performed at a lower temperature (80 °C). This may probably be due to the effect of an inversion phenomenon (Suvarnakuta, Devahastin, Soponronnarit, & Mujumdar, 2005), which happened somewhere between 80 and 90 °C in this case (Nimmol et al., 2007; Thomkapanish, et al., 2007). This effect could also be viewed from the evolution of the sample temperature. Although a rapid increase of the sample temperature during an initial stage was also observed in the cases of LPSSD and LPSSD–FIR at 80 °C, the period of constant sample temperature occurring afterwards was clearly found to be longer than that at 90 °C (see Fig. 4a). Consequently, moisture within the samples had less chance to boil rigorously leading to lower degrees of porosity.

The observed changes of porosity could be attributed to a modification of the pore size distribution. Fig. 5a and b show the histograms comparing the pore size distribution of the samples obtained at 80 and 90 °C with LPSSD and LPSSD–FIR, respectively. Fig. 6a and b show the histograms representing the pore size distribution of the samples obtained at 90 °C with LPSSD–FIR and LPSSD as well as VACUUM–FIR and VACUUM, respectively. These four figures clearly show that the pore sizes were non-normally distributed but that pores with sizes lower than 100 μm prevailed. The use of FIR as well as a higher drying temperature resulted in a shift of the distribution towards larger pore sizes for both drying techniques; the frequency of pores whose sizes were smaller than 50 μm clearly decreased. Moreover, for LPSSD experiments, there was a frequency increase of pores with sizes between 50 and 150 μm when the drying conditions were more intense, while for VACUUM experiments large pores appeared, especially in the case of VACUUM–FIR for which pores with diameters up to 450 μm were created.

4. Conclusions

X-ray microtomography coupled with 3D image analysis was used to study the effect of a combination of far-infrared radiation (FIR) with low-pressure superheated steam drying or vacuum drying. The results clearly showed that FIR and higher drying temperature led to an increase in the total porosity and the displacement of pore size towards larger sizes. The knowledge of the pore structure is essential in order to relate the quality of the product (e.g., shrinkage, rehydration and texture) to the drying conditions and hence the ability to optimize the drying processes better.

Regarding its possibilities and advantages in comparison with classical characterization techniques, X-ray microtomography will surely find a lot of applications in food engineering research. It is important to note here, however, that this measurement was limited to micron-size pores although submicron and even nano-size pores can be as important.

Acknowledgements

A. Léonard is grateful to the FRS-FNRS (Fund for Scientific Research, Belgium) for a Postdoctoral Researcher position. S. Devahastin and C. Nimmol express their appreciation to the Commission on Higher Education, the Thailand Research Fund (TRF), the National Research Council of Thailand and the International Foundation for Science (IFS) in Sweden for their financial support.

References

AOAC (1984). *Official methods of analysis* (14th ed.). Washington, DC, USA: Association of Official Analytical Chemists.

Babin, P., Della Valle, G., Chiron, H., Cloetens, P., Hoszowska, J., Pernot, P., et al. (2006). Fast X-ray tomography analysis of bubble growth and foam setting during breadmaking. *Journal of Cereal Science, 43*, 393–397.

Blacher, S., Calberg, C., Kerckhofs, G., Léonard, A., Wevers, M., Jérôme, R., et al. (2006). The porous structure of biodegradable scaffolds obtained with supercritical CO_2as foaming agent. *Studies in Surface Science and Catalysis, 160*, 681–688.

Blacher, S., Léonard, A., Heinrichs, B., Tcherkassova, N., Ferauche, F., Crine, M., et al. (2004). Image analysis of X-ray microtomograms of Pd–Ag/SiO_2 xerogel catalysts supported on Al_2O_3 foams. *Colloids and Surfaces A: Physicochemical and Engineering Aspects, 241*, 201–206.

Devahastin, S., Suvarnakuta, P., Soponronnarit, S., & Mujumdar, A. S. (2004). A comparative study of low-pressure superheated steam and vacuum drying of a heat-sensitive material. *Drying Technology, 22*, 1845–1867.

Haedelt, J., Pyle, D. L., Beckett, S. T., & Niranjan, K. (2005). Vacuum-induced bubble formation in liquid-tempered chocolate. *Journal of Food Science, 70*, E159–E164.

Job, N., Sabatier, F., Pirard, J. P., Crine, M., & Léonard, A. (2006). Towards the production of carbon xerogel monoliths by optimizing convective drying conditions. *Carbon, 44*, 2534–2542.

Léonard, A., Blacher, S., Marchot, P., Pirard, J. P., & Crine, M. (2004). Measurement of shrinkage and cracks associated to convective drying of soft materials by X-ray microtomography. *Drying Technology, 22*, 1695–1708.

Léonard, A., Blacher, S., Marchot, P., Pirard, J. P., & Crine, M. (2005). Moisture profiles determination during convective drying using X-ray microtomography. *Canadian Journal of Chemical Engineering, 83*, 127–131.

Léonard, A., Guiot, L., Pirard, J. P., Crine, M., Balligand, M., & Blacher, S. (2007). Non-destructive characterization of deer antlers by X-ray microtomography coupled with image analysis. *Journal of Microscopy, 225*, 258–263.

Lim, K. S., & Barigou, M. (2004). X-ray micro-computed tomography of cellular food products. *Food Research International, 37*, 1001–1012.

Nimmol, C., Devahastin, S., Swasdisevi, T., & Soponronnarit, S. (2007). Drying of banana slices using combined low-pressure superheated steam and far-infrared radiation. *Journal of Food Engineering, 81*, 624–633.

Sahoo, P. K., Soltani, S., Wong, K. C., & Chen, Y. C. (1988). A survey of thresholding techniques. *Computer Vision, Graphics, and Image Processing, 41*, 233–260.

Soille, P. (1999). *Morphological Image Analysis – Principles and Applications*. New York: Springer-Verlag.

Suvarnakuta, P., Devahastin, S., Soponronnarit, S., & Mujumdar, A. S. (2005). Drying kinetics and inversion temperature in a low-pressure

superheated steam-drying system. *Industrial and Engineering Chemistry Research, 44*, 1934–1941.

Thomkapanish, O., Suvarnakuta, P., & Devahastin, S. (2007). Study of intermittent low-pressure superheated steam and vacuum drying of banana. *Drying Technology, 25*, 205–223.

van Dalen, G., Blonk, H., van Haalts, H., & Hendriks, C. L. (2003). 3-D imaging of foods using X-ray microtomography. *G.I.T. Imaging and Microscopy, 3*, 18–21.

Vinegar, H. J., & Wellington, S. L. (1987). Tomographic imaging of three-phase flow experiments. *Review of Scientific Instruments, 58*, 96–107.

Available online at www.sciencedirect.com
SCIENCE DIRECT®
Journal of Food Engineering 77 (2006) 635–643
JOURNAL OF FOOD ENGINEERING
www.elsevier.com/locate/jfoodeng

Drying kinetics and quality of potato chips undergoing different drying techniques

Namtip Leeratanarak, Sakamon Devahastin *, Naphaporn Chiewchan

Department of Food Engineering, King Mongkut's University of Technology Thonburi, 91 Pracha u-tid Road, Bangkok 10140, Thailand

Received 1 May 2005; accepted 4 July 2005
Available online 26 August 2005

Abstract

Potato slices were dried using both low-pressure superheated steam drying (LPSSD) and hot air drying in this study. The effects of blanching as well as the drying temperature on the drying kinetics as well as various quality attributes of potato slices viz. color, texture, and brown pigment accumulation were also investigated. It was found that LPSSD took shorter time to dry the product to the final desired moisture content than that required by hot air drying when the drying temperatures were higher than 80 °C. Longer blanching time and lower drying temperature resulted in better color retention and led to chips of lower browning index. Blanching also reduced the hardness and shrinkage of the product; however, the use of different blanching periods did not significantly affect the product hardness. Drying methods had no obvious effect on the product quality except the browning index.

Keywords: Blanching; Browning index; Color; Hardness; Hot air drying; Low-pressure superheated steam drying

1. Introduction

Potato chips have been popular snacks for more than a century (Pedreschi, Moyano, Kaack, & Granby, 2005) and its production is indeed a more competitive industry than other snack products (Garayo & Moreira, 2002). Currently, there are demands for low-fat or fat-free snack products, which have been the driving force of the snack food industry (Moreira, 2001). Drying as one of the most common preservation methods could therefore be a feasible alternative for production of low-fat or fat-free potato chips with desirable color and textural characteristics.

Many works have been performed to study hot air drying of potato pieces of various shapes (e.g., Krokida, Tsami, & Maroulis, 1998; McMinn & Magee, 1996; Wang & Brennan, 1995). Generally, it is found that hot air drying causes much quality degradation (in terms of nutritional values, color, shrinkage and other organoleptic properties). Krokida, Maroulis, and Saravacos (2001) investigated the effects of drying methods on the color of dried potato and found that the conventional air drying caused extensive browning with a significant drop of the lightness and an increase in the redness and yellowness of dried potato. Khraisheh, McMinn, and Magee (2004) studied the quality and structural changes (in terms of vitamin C destruction, shrinkage and rehydration) of potato during microwave and convective drying. They reported that air drying led to higher vitamin C destruction than in the case of microwave drying. The rehydration potential of the air-dried sample was also lower than that of microwave-dried sample. Moreover, case hardening of the surface developed in the case of air-dried sample at higher temperatures and thus reduced the degree of shrinkage.

During the past decade the idea of using superheated steam to dry foods has been derived from other industries, e.g., paper and wood industries (Mujumdar,

* Corresponding author. Tel.: +662 470 9246; fax: +662 470 9240.
E-mail address: sakamon.dev@kmutt.ac.th (S. Devahastin).

0260-8774/$ - see front matter © 2005 Elsevier Ltd. All rights reserved.
doi:10.1016/j.jfoodeng.2005.07.022

1995), and has been applied as well to drying of potato. Caixeta, Moreira, and Castell-Perez (2002) studied the effects of impinging superheated steam temperature and convective heat transfer coefficient on the drying rate and quality attributes of potato chips. They found that the samples dried at higher steam temperatures and high convective heat transfer coefficients had less shrinkage, higher porosity, darker color, and lower vitamin C content. Unlike superheated steam drying (SSD) hot air drying produced less shrinkage because the air-dried samples developed hardened surfaces that increased the resistance to volume change. However, hot air drying led to chips of lower porosity, darker color, and lower vitamin C content. Moreira (2001) studied the use of superheated steam and hot air impingement drying for tortilla and potato chips. It was found that impingement drying with superheated steam could produce potato chips with less color deterioration and less vitamin C losses than drying with hot air. Iyota, Nishimura, Onuma, and Nomura (2001) experimentally determined the drying kinetics, surface conditions as well as color changes of potato slices using atmospheric-pressure SSD and hot air drying. They found that the samples dried by superheated steam were more glossy and there were no starch granules remain on the surface. On the other hand, starch gelatinization of the samples dried by hot air occurred more slowly than in the case of SSD. Non-gelatinized starch granules still remained on the surface of the product after the hot air drying process was completed.

Recently, a concept of using low-pressure superheated steam drying has been proposed as an alternative to dry heat-sensitive products (Chen, Chen, & Mujumdar, 1992; Devahastin, Suvarnakuta, Soponronnarit, & Mujumdar, 2004; Elustondo, Elustondo, & Urbicain, 2001) since it can combine the advantages of drying at reduced temperature to those of conventional atmospheric-pressure superheated steam drying (Mujumdar & Devahastin, 2000). Elustondo et al. (2001) studied sub-atmospheric pressure superheated steam drying of foodstuffs both experimentally and theoretically. Wood slab, shrimp, banana, apple, potato and cassava slice were dried using the steam pressures of 10,000–20,000 Pa, the steam temperatures of 60–90 °C and the steam circulating velocities of 2–6 m/s. However, no mention about the dried product quality is given.

Prior to drying most food products are usually subjected to one form of pretreatments; among other methods hot water blanching is one of the most common techniques. Potato blanching helps inactivate enzymes that lead to some quality degradations (Moreno-Perez, Gasson-Lara, & Ortega-Rivas, 1996). Blanching also facilitates starch gelatinization that leads to the change of internal structure and influences the drying rate and quality of the dried product (Senadeera, Bhandari, Young, & Wijesinghe, 2000). The combined effects of blanching and drying on the drying behavior and quality of the dried product are thus the interesting issues.

The present work is aimed at studying the effects of pretreatment (i.e., hot water blanching), drying methods and conditions on the drying kinetics and quality of potato chips in terms of color, texture, and browning index, which can be used as an indicator of quality deterioration causing from excessive heat treatment (Cohen, Birk, Mannheim, & Saguy, 1998). Low-pressure superheated steam drying (LPSSD) and the conventional hot air drying were selected for this comparative purpose.

2. Materials and methods

2.1. Materials

Fresh potato was obtained from a local supermarket and stored at 4 °C. Prior to starting of each experiment it was washed, peeled, and sliced into chips of 3.5 ± 0.3 mm thickness. The sliced potato chips were blanched in hot water at 90 ± 2 °C for 0, 1, 3, and 5 min with the ratio of potato to water of 0.015 g/g. Chips were then immediately cooled down in cold water (4 °C) and placed on a paper towel to remove excess water prior to drying.

2.2. Experimental set-up and methods

A schematic diagram of the hot air dryer used is illustrated in Fig. 1. It consists of a stainless steel drying chamber, which is connected to an electric heater rated at 6.6 kW, which was used to heat up the air to the desired drying temperature; the heater was controlled by a PID temperature controller. The air velocity was controlled by a fan speed controller. In each experiment approximately 28 slices of potato were placed on the tray with a dimension of 30×40 cm^2. Samples from the tray were collected at every 15 min interval for moisture content determination. Drying temperatures used were 70, 80, and 90 °C while the constant inlet air velocity of 0.8 m/s was used.

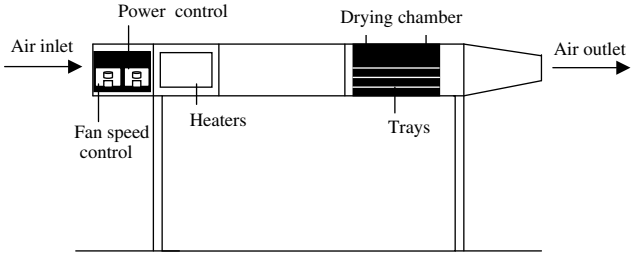

Fig. 1. A schematic diagram of hot air dryer and associated units.

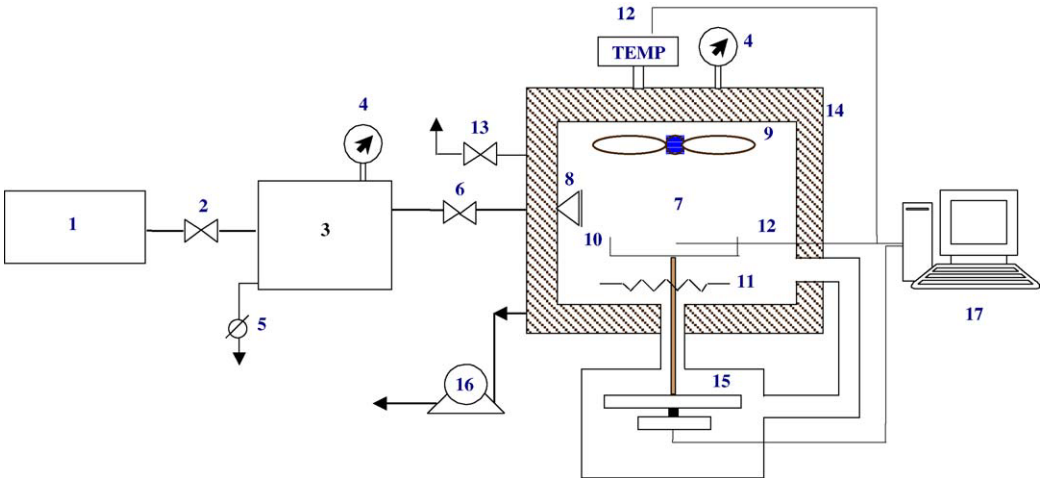

Fig. 2. A schematic diagram of the low-pressure superheated steam dryer and associated units: (1) boiler; (2) steam valve; (3) steam reservoir; (4) pressure gauge; (5) steam trap; (6) steam regulator; (7) drying chamber; (8) steam inlet and distributor; (9) electric fan; (10) sample holder; (11) electric heater; (12) on-line temperature sensor and logger; (13) vacuum break-up valve; (14) insulator; (15) on-line weight indicator and logger; (16) vacuum pump and (17) PC with installed data acquisition card.

A schematic diagram of the low-pressure superheated steam dryer and its accessories is shown in Fig. 2. The dryer consists of a stainless steel drying chamber, insulated with rock wool; a steam reservoir, which received steam from the boiler; and a liquid ring vacuum pump (Nash, ET32030, Trumball, CT), which was used to maintain the vacuum in the drying chamber. Steam trap was installed to reduce the excess steam condensation in the reservoir. The steam inlet was made into a cone shape and was covered with a screen to help distributing the steam in the chamber. An electric fan was used to disperse steam throughout the drying chamber. An electric heater, rated at 1.5 kW, which was controlled by a PID controller (Omron, E5CN, Tokyo, Japan), was installed in the drying chamber to control the steam temperature and reduce steam condensation during the start-up period. The change of the mass of the sample was detected continuously using a load cell (Minebea, Ucg-3 kg, Nagano, Japan). The temperatures of the steam and of the drying sample were measured continuously using type K thermocouples. Thermocouple signals were multiplexed to a data acquisition card (Omega Engineering, CIO-DAS16Jr., Stamford, CT) installed in a PC. LABTECH NOTEBOOK software (version 12.1, Laboratory Technologies Corp., MA) was then used to read and record the temperature data. More detailed experimental set-up could be referred in Devahastin et al. (2004).

To perform a drying experiment approximately seven slices of potato were placed on the sample holder. Drying experiments were performed at the drying temperatures of 70, 80, and 90 °C and at an absolute pressure of 7 kPa. During drying mass of samples was recorded at every 1 min interval. The samples were dried until reaching the final moisture content of around 3.5% (d.b.) (Caixeta et al., 2002), which is similar to that of commercially available potato chips (Pringle™ and Lay™) of 2–3% (d.b.).

Moisture content (AOAC, 1984), color, browning index, and hardness of the samples were measured. Preliminary test was also performed to evaluate the peroxidase activity and the degree of starch gelatinization of chips after blanching. The qualitative method described by Raganna (1982) was used to determine peroxidase activities of raw and blanched potato slices. All experiments were performed in duplicate and the mean values with standard deviations are reported.

2.3. Degree of starch gelatinization

Degree of starch gelatinization was evaluated using the differential scanning calorimetry method. Approximately 15 mg of sample was placed in an aluminum pan. The sample was then scanned from 25 to 160 °C at a heating rate of 10 °C/min by a differential scanning calorimeter (DSC) (Mettler Toledo DSC 822^e, Schwerzenbach, Switzerland). The degree of starch gelatinization was calculated using Eq. (1).

$$\mathrm{DG} = \left(1 - \frac{\Delta H_g}{\Delta H_{raw}}\right) \times 100 \quad (1)$$

where DG is the degree of starch gelatinization (%), ΔH_g is the enthalpy of gelatinization of the sample (J/g), ΔH_{raw} is the enthalpy of gelatinization of the raw sample (J/g).

2.4. Color measurement

The color of samples were analyzed by measuring the reflectance using a colorimeter (JUKI, model JP7100,

Tokyo, Japan). Two degree North skylight was used as the light source. The colorimeter was calibrated against a standard white plate before each actual color measurement. For each sample at least five measurements were performed at different positions and the measured values (mean values) were compared with those of the same sample prior to drying. Three Hunter parameters, namely, L (lightness), a (redness/greenness), and b (yellowness/blueness) were measured and color changes were calculated by

$$\Delta L = \frac{L - L_0}{L_0}, \quad \Delta a = \frac{a - a_0}{a_0}, \quad \text{and} \quad \Delta b = \frac{b - b_0}{b_0} \qquad (2)$$

where L, a, b represent the lightness, redness and yellowness of the dried samples, respectively, while L_0, a_0, b_0 represent the initial values of the lightness, redness and yellowness of the sample prior to drying, respectively.

2.5. Browning index

The browning index was determined using the procedure described by Hendel, Silveira, and Harrington (1955). The samples were ground and 2 g portion was extracted with 20 ml of 2% acetic acid solution (Carlo Erba, Val de Reuil, Italy) and then filtered through a filter paper (Whatman No. 3, Maidstone, England). An aliquot of the filtrate was mixed with an equal volume of acetone (Carlo Erba, Val de Reuil, Italy) and filtered again. The absorbance of the extracted color solution was measured at 420 nm using a spectrophotometer (Shimadzu, Model UV 2101 PC, Tokyo, Japan) using a 1 cm cell. The results are expressed in terms of the optical density.

2.6. Texture analysis

The texture of potato chips was evaluated by a compressive test using a texture analyzer (Instron 4301, Buckinghamshire, England). The test involved applying a direct force to the sample, which was placed on the hollow planar base. A 3 mm cylindrical probe was inserted at a constant rate of 2 mm/s until it cracked the sample (Moreno-Perez et al., 1996). The maximum compression force of a rupture test of each sample was used to describe the sample texture (in terms of hardness).

2.7. Statistical analysis

All data were analyzed using the analysis of variance (ANOVA). The Duncan's test was used to establish the multiple comparisons of mean values. Mean values were considered at 95% significance level ($\alpha = 0.05$). A statistical program SPSS was used to perform all statistical calculations.

3. Results and discussion

3.1. Effect of blanching on potato slices

From peroxidase activity determination the results showed that peroxidase did not exist after blanching, even for 1 min. Thus, the effect of enzymatic browning during subsequent drying could be neglected in the case of blanched samples. Potato slices blanched at various periods also had different degrees of starch gelatinization, which are shown in Table 1.

3.2. Drying kinetics of potato chips

Raw and blanched potato slices with initial moisture contents in the range of 445.41–599.3% (d.b.) (or 81.67–85.7% (w.b.)) were dried until reaching their equilibrium moisture contents. Fig. 3 shows the drying curves of potato chips undergoing hot air drying at various conditions. It was found that drying at higher temperature took shorter time to reach the desired moisture content because of a larger driving force for heat transfer. Moisture diffusivity is also higher at higher drying temperature. Similar results were observed for chips underwent any blanching conditions. However, it was found that the blanched samples dried faster than the unblanched one. This behavior was probably due to structure softening due to blanching that might facilitate water removal (Severini, Baiano, Pilli, Carbone, & Derossi, 2005; Potter & Hotchkiss, 1998). When the tissue was blanched or cooked the cells might become more permeable to moisture. However, excessive blanching time decreased the rate of moisture removal. This might be due to the effect of starch gelatinization, structural changes, and water content absorbed during blanching. Higher degree of starch gelatinization might affect the cell structure and increase the internal resistance to moisture movement, which resulted in lower diffusivity (Maté, Quartaert, Meerdink, & van't Riet, 1998). Therefore, the samples blanched for 1 min resulted in the highest drying rates followed by those blanched for 3 and 5 min, respectively; unblanched potato chips had the lowest drying rates for all drying conditions. However, it was found that, at higher drying temperatures, the drying rates of samples treated with different

Table 1
Degree of starch gelatinization of potato slices blanched for various periods

Blanching time (min)	Enthalpy (J/g)	Degree of starch gelatinization (%)
0	5.48	0.00
1	1.98	63.96
3	1.87	65.88
5	0.99	81.93

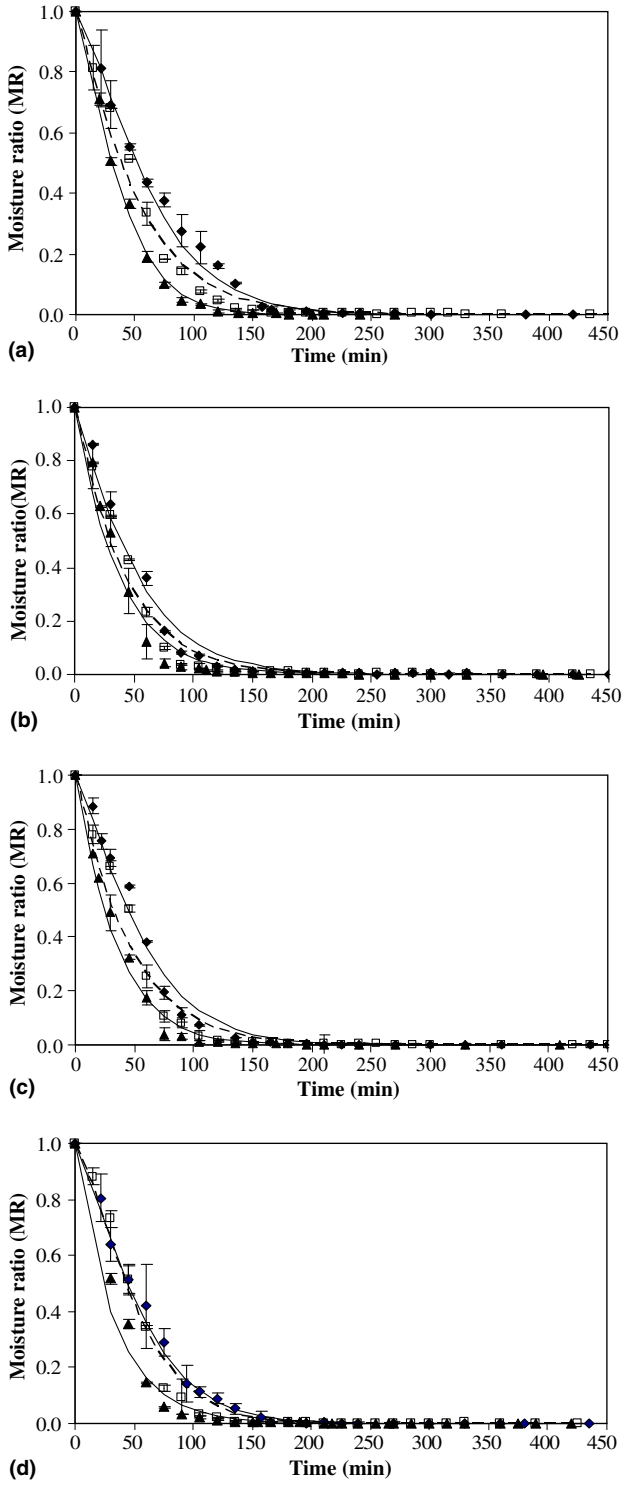

Fig. 3. Drying curves of potato chips underwent blanching at (a) 0, (b) 1, (c) 3, and (d) 5 min in a hot air dryer at 70 °C (◆), 80 °C (□), 90 °C (▲).

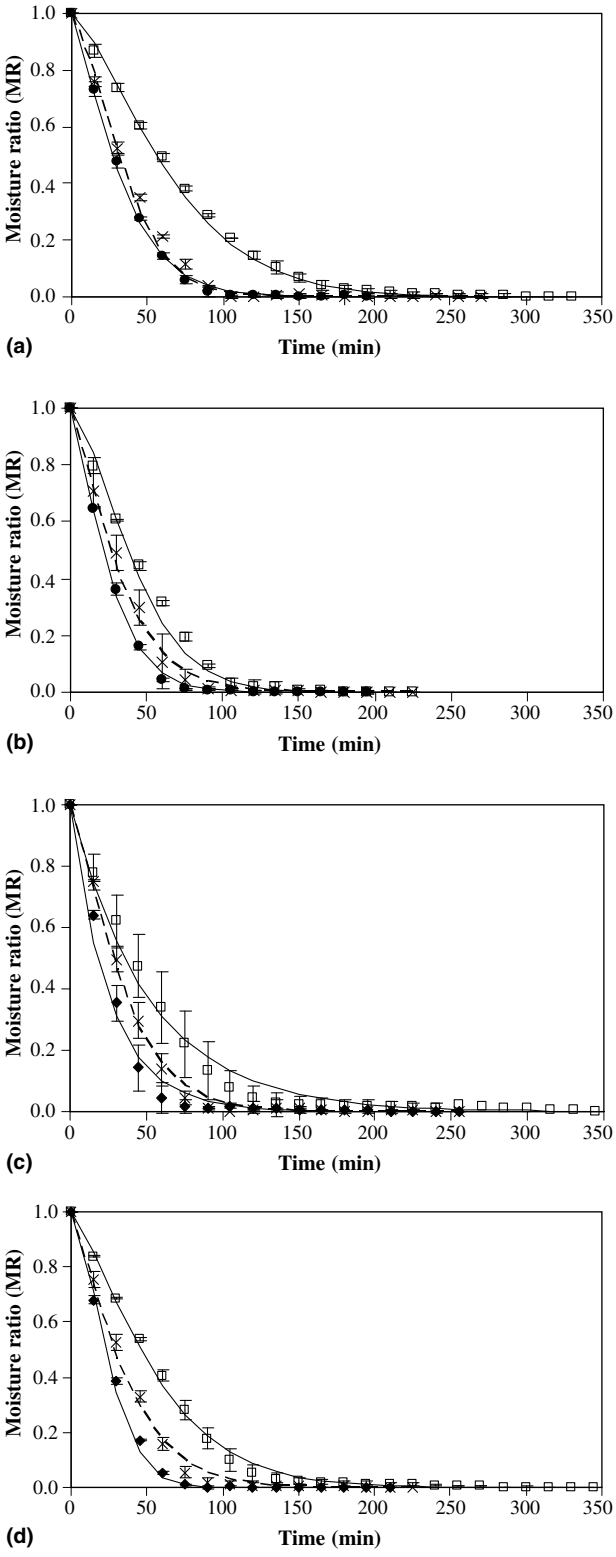

Fig. 4. Drying curves of potato chips underwent blanching at (a) 0, (b) 1, (c) 3, and (d) 5 min in a low-pressure superheated steam dryer at 70 °C (□), 80 °C (×), 90 °C (◆).

blanching periods were not obviously different. So, the effect of drying temperature was greater than the effect of blanching time at higher drying temperatures.

Fig. 4 shows the drying curves of potato slices undergoing low-pressure superheated steam drying at various conditions. Similar to hot air drying higher drying temperature resulted in a faster reduction of moisture

content. Blanching time also had an effect on the drying rates at all drying temperatures as observed in the case of hot air drying. The blanched sample again dried faster than the unblanched one; the effect of blanching time was again smaller at higher drying temperatures.

Considering the drying rates of hot air drying and LPSSD it was found that the drying rates of the two drying methods were not different at a low drying temperature (70 °C). However, LPSSD yielded higher drying rates when the drying temperature was higher than 80 °C for all blanching conditions. This suggests that the effective inversion temperature calculated from the overall drying rates is somewhere between 70 and 80 °C (Suvarnakuta, Devahastin, Soponronnarit, & Mujumdar, 2005). Fig. 5 illustrates the drying curves of the samples blanched for 5 min undergoing both drying methods. The results of samples treated with different blanching periods (e.g., 0, 1, and 3 min) were similar to that of 5 min.

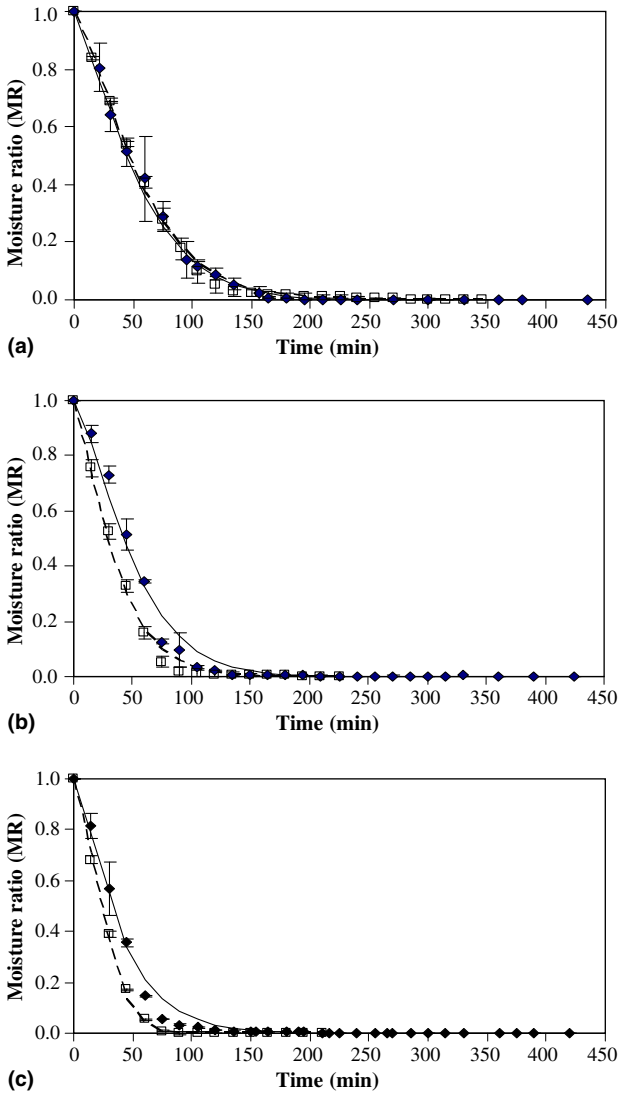

Fig. 5. Drying curves of potato chips undergoing hot air drying (◆), and LPSSD (□) at drying temperatures of (a) 70 °C, (b) 80 °C, and (c) 90 °C.

4. Quality of dried potato chips

4.1. Color

Table 2 illustrates the color changes of potato chips in terms of color differences, $\Delta L/L_0$, $\Delta a/a_0$, and $\Delta b/b_0$. Since the enzymes that caused the quality degradation were destroyed during blanching, the non-enzymatic browning was considered a major cause of color changes of dried potato chips. In the case of lightness it was found that the drying method and drying temperature did not as significantly affect the change of lightness as blanching time did. However, the reduction of lightness ($\Delta L/L_0$) was greater at higher drying temperatures for both drying methods although the results were not significantly different.

Regarding the change of redness of dried potato chips the drying temperature, blanching time and their interaction had significant influences on this color parameter under certain conditions. It was observed that all dried potato chips were redder than the fresh potato, however. LPSSD led to smaller increase of a value than hot air drying but the results were again not significantly different. Regarding the effect of the drying temperature higher drying temperature led to an increase of a value for both drying methods at all blanching conditions. The above results were due to Maillard reaction or heat damage that occurred more at higher drying temperatures. The changes of redness of blanched chips treated at 90 °C were significantly higher than those at 70 °C but did not statistically differ from those at 80 °C for both drying methods.

For the effect of blanching unblanched chips had higher a values than those of blanched samples and thus resulted in greater changes of $\Delta a/a_o$ values at all drying temperatures. Blanching reduced the a value of potato chips due to the leaching out of reducing sugars, which are the substrates of Maillard reaction, prior to drying and thus minimized the non-enzymatic browning reaction and led to less red chips. These results are similar to those reported by Pedreschi et al. (2005).

The yellowness (b value) of dried potato chips was affected by blanching while the drying method and drying temperature did not show any significant influence on the b value. The unblanched potato chips showed an obvious reduction of the yellowness (lower $\Delta b/b_0$ values) after drying. In other words, blanched potato chips showed relative stability of yellowness. Potato chips dried at lower temperatures tended to have higher values of yellowness than those dried at higher temperatures. It was also observed that shorter blanching time led to

Table 2
Effects of drying method, drying temperature, and blanching time on color changes and browning index of dried potato chips

Drying method	Drying temp (°C)	Blanching time (min)	$\Delta L/L_0$	$\Delta a/a_0$	$\Delta b/b_0$	Browning index
Hot air drying	70	0	-0.769 ± 0.004^{a}	1.305 ± 0.067^{abcde}	-0.797 ± 0.085^{d}	0.076 ± 0.019^{ab}
		1	-0.085 ± 0.047^{cd}	0.483 ± 0.087^{f}	0.603 ± 0.097^{ab}	0.071 ± 0.008^{ab}
		3	-0.037 ± 0.002^{d}	0.536 ± 0.076^{f}	0.542 ± 0.033^{abc}	0.063 ± 0.003^{a}
		5	-0.146 ± 0.066^{cd}	0.556 ± 0.003^{f}	0.546 ± 0.072^{abc}	0.039 ± 0.005^{a}
	80	0	-0.792 ± 0.048^{a}	1.336 ± 0.048^{abcde}	-0.810 ± 0.045^{d}	0.256 ± 0.058^{g}
		1	-0.143 ± 0.014^{cd}	0.845 ± 0.053^{def}	0.563 ± 0.037^{abc}	0.207 ± 0.017^{efg}
		3	-0.113 ± 0.047^{cd}	0.998 ± 0.076^{cdef}	0.435 ± 0.030^{abc}	0.184 ± 0.005^{de}
		5	-0.145 ± 0.078^{cd}	1.028 ± 0.022^{bcdef}	0.697 ± 0.069^{ab}	0.14 ± 0.007^{cd}
	90	0	-0.812 ± 0.073^{a}	1.897 ± 0.020^{a}	-0.826 ± 0.023^{d}	0.755 ± 0.043^{m}
		1	-0.221 ± 0.020^{bcd}	1.471 ± 0.025^{abcd}	0.259 ± 0.027^{bc}	0.557 ± 0.041^{l}
		3	-0.197 ± 0.013^{bcd}	1.573 ± 0.073^{abc}	0.179 ± 0.063^{bc}	0.436 ± 0.028^{k}
		5	-0.223 ± 0.033^{bcd}	1.448 ± 0.070^{abcd}	0.239 ± 0.028^{bc}	0.360 ± 0.023^{hi}
LPSSD	70	0	-0.655 ± 0.073^{a}	1.220 ± 0.010^{bcde}	-0.604 ± 0.020^{d}	0.075 ± 0.001^{ab}
		1	-0.021 ± 0.063^{d}	0.722 ± 0.062^{ef}	1.069 ± 0.098^{a}	0.070 ± 0.001^{ab}
		3	0.005 ± 0.058^{d}	0.497 ± 0.016^{f}	0.710 ± 0.006^{ab}	0.062 ± 0.006^{a}
		5	-0.117 ± 0.006^{cd}	0.540 ± 0.044^{f}	0.903 ± 0.014^{ab}	0.045 ± 0.008^{a}
	80	0	-0.707 ± 0.021^{a}	1.283 ± 0.012^{abcde}	-0.669 ± 0.077^{d}	0.246 ± 0.008^{fg}
		1	-0.214 ± 0.094^{bcd}	1.261 ± 0.012^{abcde}	0.631 ± 0.089^{ab}	0.193 ± 0.012^{def}
		3	-0.211 ± 0.068^{bcd}	0.960 ± 0.043^{cdef}	0.484 ± 0.067^{abc}	0.166 ± 0.043^{cde}
		5	-0.101 ± 0.025^{cd}	0.971 ± 0.090^{cdef}	0.769 ± 0.054^{ab}	0.124 ± 0.007^{bc}
	90	0	-0.726 ± 0.088^{a}	1.676 ± 0.029^{ab}	-0.679 ± 0.032^{d}	0.564 ± 0.011^{l}
		1	-0.427 ± 0.007^{b}	1.417 ± 0.047^{abcd}	-0.149 ± 0.02^{cd}	0.429 ± 0.025^{jk}
		3	-0.292 ± 0.047^{bc}	1.472 ± 0.089^{abcd}	0.245 ± 0.048^{bc}	0.381 ± 0.040^{ij}
		5	-0.303 ± 0.028^{bc}	1.486 ± 0.051^{abcd}	0.294 ± 0.038^{bc}	0.322 ± 0.038^{h}

Different superscripts in the same column mean that the values are significantly different at 95% confidence level ($\alpha = 0.05$).

higher b values but the results were again not significantly different.

4.2. Browning index

The effects of blanching, drying method and drying temperature on the browning index of potato chips are shown in Table 2. The results were significantly different between the two drying methods at high drying temperatures. Hot air drying resulted in higher browning index than did LPSSD at higher drying temperatures but there was no difference between the two methods at low temperatures. This is due to the difference in surface temperature of potato during drying. In the constant drying rate period the surface temperature of potato chips undergoing hot air drying at 70, 80, and 90 °C were equal to the wet-bulb temperature, which was 41, 44, and 48 °C, respectively. In the case of LPSSD the surface temperature of potato chips was equal to the saturation temperature at the operating pressure (i.e., 7 kPa) or about 40 °C. As the drying temperature increased, of course, the wet-bulb temperature also increased. This increase in turn led to larger differences in browning index between the chips treated with different drying methods at higher drying temperatures. The highest value of browning index was obtained in the case of air-dried sample at 90 °C. A higher degree of non-enzymatic browning occurring during hot air drying might be due to both Maillard reaction and ascorbic acid oxidation. In the case of LPSSD there was no oxygen left in the drying chamber and the main cause of non-enzymatic browning could be only Maillard reaction.

The results of the browning index were also related to the color changes, especially the change of redness. The results showed similar trends for both physical and chemical changes. From the results of color changes and browning index it might be concluded that hot air drying resulted in more severe chemical damage of potato chips than did LPSSD. Browning occurring in hot air drying was due to Maillard reaction and ascorbic acid oxidation while LPSSD possible led to only Maillard reaction. It might be implied that LPSSD could better preserve quality, especially nutrients, than hot air drying at the same drying temperature.

4.3. Texture

The texture of dried potato chips is reported in terms of hardness, which is the maximum breaking force, and the results are shown in Table 3. It was found that blanching and drying temperature significantly affected the hardness of potato chips under certain conditions while the drying method did not show any significant influence on the hardness. Generally, blanching caused starch gelatinization, softening of structure and led to less hardness of dried starchy products. It was observed in this work that unblanched chips had the maximum hardness in all cases; blanching only led to significantly

Table 3
Effects of drying method, drying temperature, and blanching time on hardness of dried potato chips

Drying method	Drying temp (°C)	Blanching time (min)	Maximum force (N)
Hot air drying	70	0	6.256 ± 0.914^{ab}
		1	4.890 ± 0.671^{bcde}
		3	4.843 ± 0.417^{bcde}
		5	4.537 ± 1.267^{bcde}
	80	0	6.283 ± 1.163^{ab}
		1	4.633 ± 0.257^{bcde}
		3	4.769 ± 0.632^{bcde}
		5	4.810 ± 0.743^{bcde}
	90	0	5.446 ± 0.263^{bcd}
		1	3.191 ± 0.474^{cde}
		3	3.136 ± 0.067^{de}
		5	3.121 ± 0.244^{de}
LPSSD	70	0	7.956 ± 0.600^{a}
		1	5.520 ± 0.215^{bc}
		3	5.670 ± 0.503^{b}
		5	5.518 ± 0.155^{bc}
	80	0	5.859 ± 0.124^{ab}
		1	4.721 ± 1.682^{bcde}
		3	4.588 ± 0.484^{bcde}
		5	4.603 ± 1.086^{bcde}
	90	0	4.796 ± 0.578^{bcde}
		1	2.991 ± 0.349^{e}
		3	2.834 ± 0.413^{e}
		5	2.814 ± 0.163^{e}

Different superscripts in the same column mean that the values are significantly different at 95% confidence level ($\alpha = 0.05$).

less hard chips only in the case of LPSSD at low temperature (70 °C), however. This might be due to the effect of casehardening developed during moisture removal. In the case of hot air drying casehardened skin occurred in all cases and overshadowed the effect of blanching on the hardness of the chips. As a result, no statistical difference between blanched and unblanched air-dried chips was observed. On the other hand, LPSSD tended to protect the integrity of the surface better and casehardening seemed to occur only at higher drying temperatures (i.e., 80 and 90 °C). This similar behavior has also been reported by other workers who studied superheated steam in general (Mujumdar, 1995). Different blanching periods did not seem to alter the hardness of the chips in all cases.

Although potato chips underwent LPSSD, which led to puffing at higher drying temperatures, were obviously less hard than those treated with hot air drying based on human perception, the results were not statistically different between the two drying methods. This could be due to a large variation of the experimental results caused by the non-uniform or heterogeneous nature of raw potato.

Fig. 6 illustrated the maximum breaking force of steam-dried chips treated with different blanching periods and drying temperatures in comparison with those of commercial products. The maximum breaking forces

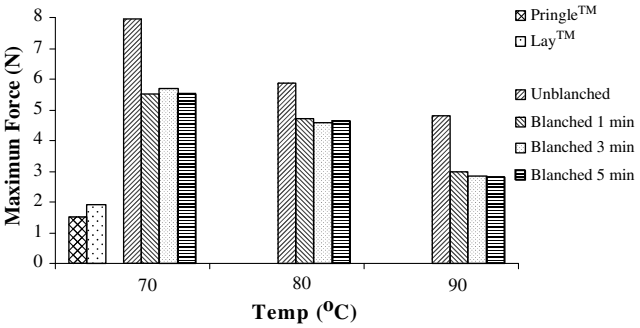

Fig. 6. Hardness of potato chips blanched for different periods and underwent LPSSD at different drying temperatures compared with the commercial products.

of the commercially available potato chips, which are Lay™ and Pringle™, are 1.919 ± 0.248 and 1.517 ± 0.338 N, respectively. It was found that potato chips treated with LPSSD at 90 °C (with 5 min blanching time), which puffed more than those treated with other conditions and consequently required the lowest force of compression (Table 3), were still harder than the commercial products.

5. Conclusions

The effects of blanching time, drying methods and conditions on the drying kinetics and quality of potato chips were examined in this study. In terms of drying kinetics blanching time as well as drying temperature were found to have effects on the moisture reduction rate of samples, both in cases of hot air drying and LPSSD. It was found that blanching could increase the drying rates of both hot air drying and LPSSD. Moreover, LPSSD took shorter time to dry the product to the final desired moisture content than that of hot air drying when the drying temperatures were higher than 80 °C.

The quality study showed that blanching led to better color retention, less hardness and lower degree of browning of chips. Regarding the drying method, LPSSD provided better quality chips than hot air drying in terms of the browning index, especially at high drying temperatures. No significant effect of the drying method on the hardness was observed, however. Casehardening seemed to overshadow the effect of blanching on the hardness of the chips at all drying conditions except in the case of LPSSD at low temperature.

A blanching time of 5 min followed by LPSSD at 90 °C at an absolute pressure of 7 kPa was proposed as the best condition for drying potato chips in this study. These conditions gave puffed product, less hard with moderate browning index, which corresponded to less nutrients and other heat damages. These conditions

also provided potato chips that had small changes of colors from their natural values and required shortest drying time. However, the best condition proposed still led to chips of inferior quality compared with the commercially available potato chips, especially in terms of hardness. The study of the combined effects of blanching and/or freezing pretreatments with higher drying temperature is recommended for future work.

Acknowledgement

The authors express their sincere appreciation to the Commission on Higher Education, the Thailand Research Fund (TRF) and the International Foundation for Science (IFS), Sweden for supporting this study financially.

References

AOAC (1984). *Official method of analysis* (14th ed.). Washington DC: Association of Official Agricultural Chemists.

Caixeta, A. T., Moreira, R., & Castell-Perez, M. E. (2002). Impingement drying of potato chips. *Journal of Food Process Engineering, 25*, 63–90.

Chen, S. R., Chen, J. Y., & Mujumdar, A. S. (1992). Preliminary study of steam drying of silkworm cocoons. *Drying Technology, 10*, 251–260.

Cohen, E., Birk, Y., Mannheim, C. H., & Saguy, I. S. (1998). A rapid method to monitor quality of apple juice during thermal processing. *Lebensmittel-Wissenschaft und-Technologie, 31*, 612–616.

Devahastin, S., Suvarnakuta, P., Soponronnarit, S., & Mujumdar, A. S. (2004). A comparative study of low-pressure superheated steam and vacuum drying of a heat-sensitive material. *Drying Technology, 22*, 1845–1867.

Elustondo, D., Elustondo, M. P., & Urbicain, M. J. (2001). Mathematical modeling of moisture evaporation from foodstuffs exposed to sub-atmospheric pressure superheated steam. *Journal of Food Engineering, 49*, 15–24.

Garayo, J., & Moreira, R. (2002). Vacuum frying of potato chips. *Journal of Food Engineering, 55*, 181–191.

Hendel, C. E., Silveira, V. G., & Harrington, W. O. (1955). Rates of non-enzymatic browning of white potato during dehydration. *Food Technology, 9*, 433–438.

Khraisheh, M. A. M., McMinn, W. A. M., & Magee, T. R. A. (2004). Quality and structural changes in starchy foods during microwave and convective drying. *Food Research International, 37*, 497–503.

Krokida, M. K., Maroulis, Z. B., & Saravacos, G. D. (2001). The effect of the method of drying on the colour of dehydrated products. *International Journal of Food Science and Technology, 36*, 53–59.

Krokida, M. K., Tsami, E., & Maroulis, Z. B. (1998). Kinetics on color changes during drying of some fruits and vegetables. *Drying Technology, 16*, 667–685.

Iyota, H., Nishimura, N., Onuma, T., & Nomura, T. (2001). Drying of sliced raw potatoes in superheated steam and hot air. *Drying Technology, 19*, 1411–1424.

McMinn, W. A. M., & Magee, T. R. A. (1996). Air drying kinetics of potato cylinders. *Drying Technology, 14*, 2025–2040.

Maté, J. I., Quartaert, C., Meerdink, G., & van't Riet, K. (1998). Effect of blanching on structural quality of dried potato slices. *Journal of Agricultural and Food Chemistry, 46*, 676–681.

Moreira, R. G. (2001). Impingement drying of food using hot air and superheated steam. *Journal of Food Engineering, 49*, 291–295.

Moreno-Perez, L. F., Gasson-Lara, J. H., & Ortega-Rivas, E. (1996). Effect of low temperature-long time blanching on quality of dried sweet potato. *Drying Technology, 14*, 1839–1857.

Mujumdar, A. S. (1995). Superheated steam drying (Second ed.. In A. S. Mujumdar (Ed.). *Handbook of industrial drying* (Vol. 2, pp. 1071–1086). New York: Marcel Dekker.

Mujumdar, A. S., & Devahastin, S. (2000). Fundamental principles of drying. In S. Devahastin (Ed.), *Mujumdar's practical guide to industrial drying* (pp. 1–22). Brossard: Exergex.

Pedreschi, F., Moyano, P., Kaack, K., & Granby, K. (2005). Color changes and acrylamide formation in fried potato slices. *Food Research International, 38*, 1–9.

Potter, N. M., & Hotchkiss, J. H. (1998). In *Food science* (5th ed., pp. 207–211). Gaithersburg: Aspen Publisher.

Raganna, S. (1982). *Manual of analysis of fruit and vegetable products*. New Delhi: Tata McGraw-Hill.

Senadeera, W., Bhandari, B., Young, G., & Wijesinghe, B. (2000). Physical property changes of fruits and vegetables during hot air drying. In A. S. Mujumdar (Ed.), *Drying technology in agriculture and food sciences* (pp. 159–161). Enfield: Science Publishers.

Severini, C., Baiano, A., Pilli, T. D., Carbone, B. F., & Derossi, A. (2005). Combined treatments of blanching and dehydration: Study on potato cubes. *Journal of Food Engineering, 68*, 289–296.

Suvarnakuta, P., Devahastin, S., Soponronnarit, S., & Mujumdar, A. S. (2005). Drying kinetics and inversion temperature in a low-pressure superheated steam drying system. *Industrial & Engineering Chemistry Research, 44*, 1934–1941.

Wang, N., & Brennan, J. G. (1995). Changes in structure, density and porosity of potato during dehydration. *Journal of Food Engineering, 24*, 61–76.

Drying Technology
An International Journal
Publication details, including instructions for authors and subscription information:
http://www.informaworld.com/smpp/title~content=t713597247

Errata

Online Publication Date: 01 June 2007
To cite this Article: , (2007) 'Errata', Drying Technology, 25:6, 1127
To link to this article: DOI: 10.1080/07373930701402622
URL: http://dx.doi.org/10.1080/07373930701402622

Drying Technology, 25: 1137, 2007

ISSN: 0737-3937 print/1532-2300 online
DOI: 10.1080/07373930701402622

Taylor & Francis
Taylor & Francis Group

Errata

The following text provides errata for the publication noted below.

Kerdpiboon, S.; Devahastin, S. Fractal characterization of some physical properties of a food product under various drying conditions. Drying Technology **2007**, *25*, 135–146.

The authors regret any inconvenience caused.

On page 145, right column:

The normalized change of fractal dimension could be used to monitor the physical property changes of carrot during drying. For example, at ΔFD/FDo of around 0.06, the percentage of shrinkage was around 70–80% in all HAD and LPSSD cases (Figs. 12 and 13). This kind of relationship was also observed at other ΔFD/FDo and percentage of shrinkage values. These results are supported by results presented in Fig. 14, which illustrates the microstructure of the samples at ΔFD/FDo of 0.06 when drying with HAD at 60°C, 1 m/s, 150 min; 70°C, 1 m/s, 120 min; 80°C, 1 m/s, 90 min; LPSSD at 60°C, 7 kPa, 210 min; 70°C, 7 kPa, 150 min; and 80°C, 7 kPa, 90 min. All of the samples had similar levels of shrinkage although they had different microstructure. However, they all had the same ΔFD/FDo values. The deviations in the percentage of shrinkage might arise from the errors that occurred during the collection of the experimental data.

On the other hand, values of the rehydration ratio at the same ΔFD/FDo were quite different. For instance, at ΔFD/FDo of around 0.06, the rehydration ratio was around 2.8–3.0 at all conditions of HAD while the rehydration ratio was around 2.0–2.2 at all conditions of LPSSD (Figs. 12 and 13). However, ΔFD/FDo could be used to correlate the rehydration behavior of samples dried using the same type of dryer.

5 Low-pressure superheated steam drying of food products

Sakamon Devahastin and Peamsuk Suvarnakuta

5.1 INTRODUCTION

Although the concept of superheated steam drying (SSD) was originally proposed over a century ago and the first industrial applications were reported some 60 years ago (Mujumdar, 2000, 2007), SSD has only recently re-emerged as an alternative drying technology for a wider array of products including woods (Pang, 1997; Pang and Dakin, 1999), paper (Douglas, 1994) as well as foods and biomaterials (Devahastin and Suvarnakuta, 2004). SSD involves the use of superheated steam in a direct (convective) dryer in place of hot air, combustion, or flue gases as the drying medium to supply heat for drying and to carry away the evaporated moisture. Any direct or direct/indirect (e.g. combined convection/conduction) dryer can be, in principle, operated as a superheated steam dryer although, in practice, this conversion may not always be straightforward.

In addition to the energy-related advantages reported by many researchers (Mujumdar, 2000; Devahastin and Suvarnakuta, 2004), SSD also possesses many other advantages that are of special interest to processors of foods and biomaterials. Generally, no oxidative reactions, e.g. enzymatic browning (Nimmol *et al*., 2007; Thomkapanish *et al*., 2007), lipid oxidation or aerobic degradation of vitamins (Suvarnakuta *et al*., 2005a), are possible in SSD due to lack of oxygen.

SSD can also help decontaminate micro-organisms, toxins and spores due to its normally high-temperature environment, even during an early stage of drying (Pronyk *et al*., 2006; Cenkowski *et al*., 2007). A combination of drying with other thermal treatments, for example, blanching (Iyota *et al*., 2001; Prachayawarakorn *et al*., 2002; Namsanguan *et al*., 2004; Sotome *et al*., 2006), deodorization (Furukawa and Akao, 1983), parboiling (Soponronnarit *et al*., 2006), pasteurization and sterilization (Abe and Miyashita, 2006) as well as popping (Iyota *et al*., 2005) is also possible.

Another advantage of SSD is that, for certain foods or vegetables, the porosity of the products dried in superheated steam is higher than that dried in hot air. This is due to the evolution of steam within the product, which decreases the bulk density of the product while enhancing its rehydration characteristics. This feature is especially attractive for the instant food as well as confectionary industries (Devahastin *et al*., 2004).

Higher drying rates (comparing with hot air drying or in the case of the low-pressure superheated steam drying, vacuum drying) are possible in both constant and falling rate periods of SSD, depending on the steam temperature. The higher thermal conductivity and heat capacity of superheated steam leads to higher rates of surface moisture removal above the so-called inversion temperature (Schwartze and Brocker, 2002; Suvarnakuta *et al*., 2005b). Below the inversion temperature drying in air is faster. In the falling rate period the higher

product temperature in SSD (over 100°C at 1 bar) and lack of diffusional resistance to water vapor lead to faster drying rates.

On the other hand, since most foods and biomaterials are damaged or degraded at the saturation temperature of superheated steam corresponding to atmospheric or higher pressures, these products cannot suitably be dried in SSD even if they contain only surface moisture. Lowering the dryer operating pressure is clearly a feasible option that could lead to preservation of the quality of dried products and additionally, in some cases, to enhanced drying rates as well.

In the following section a short description of the basic principles of SSD and low-pressure superheated steam drying (LPSSD) is first illustrated. This is followed by a review of the recent advances in LPSSD of foods and biomaterials. For superheated steam drying of foods at near-atmospheric pressure the reader is referred to Devahastin and Suvarnakuta (2004).

5.2 BASIC PRINCIPLES OF SUPERHEATED STEAM DRYING

A simple schematic sketch of a superheated steam drying system is shown in Figure 5.1. Saturated steam from a boiler or a steam generator is heated up in a heater (steam superheater) and becomes superheated steam. Drying takes place through direct contact between superheated steam and the product to be dried. As mentioned earlier, the exhaust of the dryer is also steam, albeit at lower specific enthalpy. Steam may be recirculated and reheated in a closed loop; only the amount of steam that corresponds to the amount of evaporated water is removed from the closed loop and used either directly or indirectly after its energy is recovered via a heat exchanger. The closed loop of SSD implies that emissions coming from the drying product are not emitted to the environment but are included in the condensate; toxic or expensive organic liquids can therefore be recovered more easily than in the case of hot air drying.

In the case of LPSSD the same basic concept applies except for the fact that an external steam superheater may not be required. As the saturated steam is introduced to

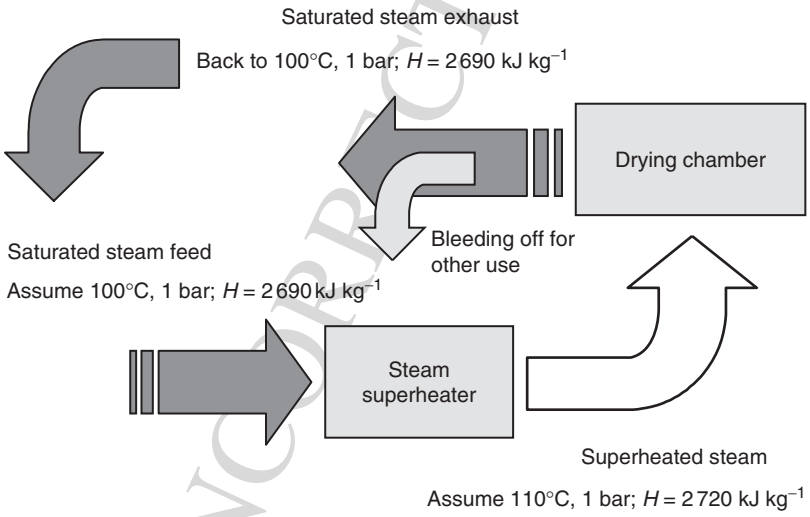

Fig. 5.1 A schematic sketch of a superheated steam drying system.

the low-pressure drying chamber, saturated steam becomes low-pressure superheated steam since its temperature is already well above the saturation temperature at the reduced pressure of the drying chamber. To minimize the effect of adiabatic expansion of steam that may occur in the low-pressure drying chamber, a heater is generally installed in the drying chamber to help control the low-pressure superheated steam temperature at a desired value (Devahastin *et al*., 2004).

Since there is no resistance to diffusion of the evaporated water in its own vapor, the drying rate in the constant rate period is dependent only on the heat transfer rate q. If sensible heat effects, heat losses and other modes of heat transfer are neglected, the rate at which surface moisture evaporates in steam is given simply by:

$$N = \frac{q}{\lambda} = \frac{h(T_{steam} - T_s)}{\lambda} \tag{5.1}$$

where N is the evaporation rate, h is the convective heat transfer coefficient, T_s is the drying surface temperature which corresponds to the saturation temperature at the dryer operating pressure, T_{steam} is the temperature of the superheated steam and λ is the latent heat of vaporization. In hot air drying, $T_s = T_{wet-bulb}$ and hence at lower drying temperatures, ΔT is higher in air drying but h is lower since air has heat transfer properties inferior to superheated steam at the same temperature. It turns out that these counter-acting effects lead to the phenomenon of inversion; a temperature beyond which the superheated steam drying rate is greater than hot air drying rate (see Figure 5.2). This is confirmed experimentally as well as numerically for water as well as several organic solvent systems (superheated vapor drying). It is observed that the inversion temperature is in the order of 160–200°C for evaporation of water in superheated steam for various flow configurations and flow regimes, for example, laminar/turbulent boundary layer flows, impinging jet flows, free convective flow over complex geometries (Chow and Chung, 1983; Wu *et al*., 1987, 1989; Haji and Chow, 1988; Sheikholeslami and Watkinson, 1992; Bond *et al*., 1994).

Strictly speaking, the inversion temperature is defined only for surface moisture evaporation and not for internal moisture removal, although some researchers do not make this distinction

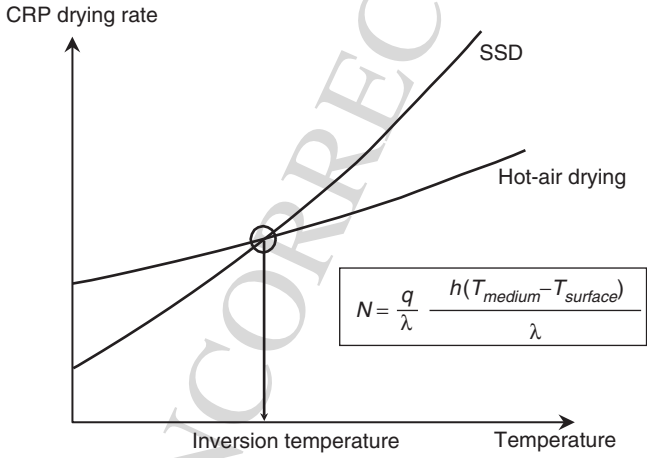

Fig. 5.2 An inversion phenomenon.

clear when reporting their results. However, the values of the inversion temperature calculated only from the surface moisture evaporation rates are obviously not the same as those calculated from the combined constant rate and falling rate drying rates (Suvarnakuta *et al*., 2005b).

The convective heat transfer coefficient, h, between steam and the solid material surface can either be estimated using standard correlations for inter-phase heat transfer (Incropera and Dewitt, 2002) or from the experimental drying rates data. The following example illustrates how the values of the convective heat transfer coefficient are calculated from the experimental low-pressure superheated steam drying rates.

Example 1: Based on the data of Suvarnakuta *et al*. (2005b) who experimentally determined the drying rates of molecular sieve beads undergoing LPSSD at various operating pressures (see Figure 5.3), it is possible, through the use of equation (5.1), to determine the values of the convective heat transfer coefficient. First of all, it is recognized that equation (5.1) can be rewritten as:

$$h = \frac{N\lambda}{A(T_{steam} - T_{surface})} \tag{5.2}$$

As an illustrative case, consider the case at the drying temperature of 80°C and absolute pressure of 7 kPa (Figure 5.3a). Since the drying rates reported by Suvarnakuta *et al*. (2005b) are in kg kg^{-1} (d.b.) min^{-1}, it is necessary to multiply the reported drying rates by the bone-dry mass of the sample (approximately 24 g). Hence, $N = 1.4 \times 10^{-2}$ kg kg^{-1} (d.b.) min$^{-1} \times 0.024$ kg $= 3.36 \times 10^{-4}$ kg min^{-1}. In this case, A is the surface area of all molecular sieve particles used in each experiment and is equal to 0.044 m^2.

At the pressure of 7 kPa the surface temperature is around 40°C, which corresponds to the saturation temperature at 7 kPa. Also at this pressure $\lambda = 2406.0$ kJ kg^{-1}. Hence, $h = [3.36 \times 10^{-4}$ kg min$^{-1} \times 2406.0$ kJ kg$^{-1}]/[0.044$ m$^2 \times (80 - 40)$ K$] = 0.4593$ kJ min^{-1} m^{-2} K^{-1} or 7.66 W m^{-2} K^{-1}.

The values of the heat transfer coefficient at other conditions are listed in Table 5.1. As expected, the values of the heat transfer coefficient increase with the operating pressure of the dryer as there is more mass (steam) available for convection heat transfer in the dryer.

5.3 LOW-PRESSURE SUPERHEATED STEAM DRYING OF FOODS AND BIOMATERIALS

Although there exist a number of publications on low-pressure superheated steam drying of other products, both from the fundamental (e.g. Shibata *et al*., 1988, 1990; Sano *et al*., 2005; Shibata, 2006; Tatemoto *et al*., 2007) and application-oriented points of view (e.g. Chen *et al*., 1992; Pang and Dakin, 1999; Defo *et al*., 2004), this section is focused only on a more limited pool of information on LPSSD of foods and biomaterials. Near-atmospheric pressure superheated steam drying is not included either; the reader is referred to Devahastin and Suvarnakuta (2004) for a review on near-atmospheric pressure superheated steam drying and also to the literature for some recent advances of this drying technique applied to foods and biomaterials (e.g. Taechapairoj *et al*., 2004; Rordprapat *et al*., 2005; Prachayawarakorn *et al*., 2006; Nathakaranakule *et al*., 2007; Jamradloedluk *et al*., 2007).

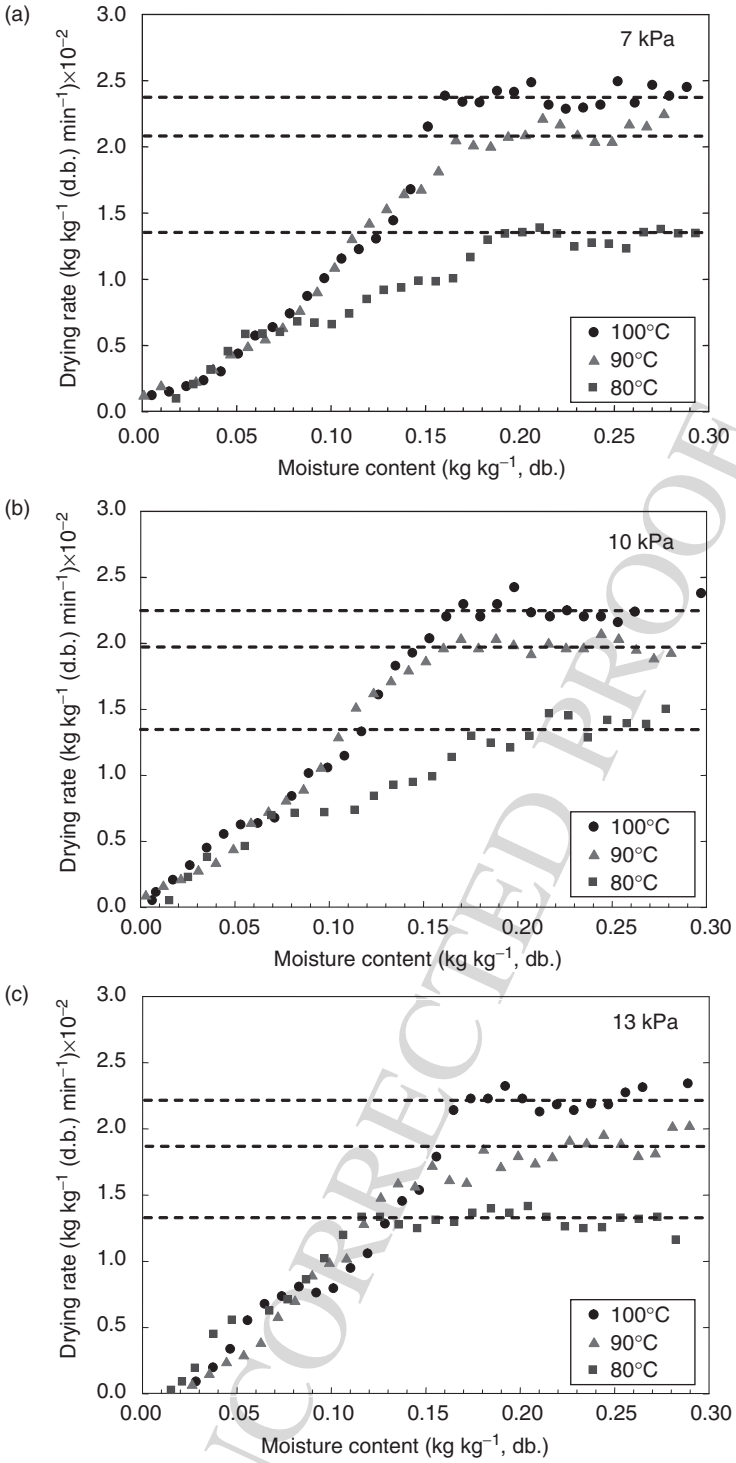

Fig. 5.3 Drying rate curves of molecular sieve beads undergoing LPSSD at various operating pressures. Reproduced with permission from Suvarnakuta *et al*. (2005b). Copyright 2005 American Chemical Society.

Table 5.1 Values of heat transfer coefficient ($W\,m^{-2}\,K^{-1}$) calculated from equation (5.2).

Absolute pressure					
7 kPa		**10 kPa**		**13 kPa**	
Mean	**SD**	**Mean**	**SD**	**Mean**	**SD**
7.661	0.61	8.353	0.44	9.168	0.33

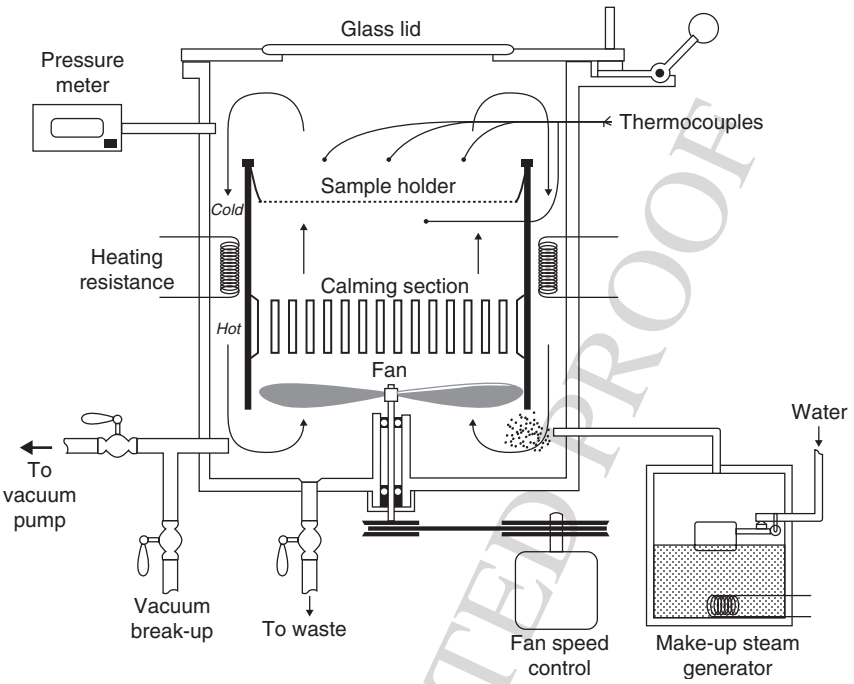

Fig. 5.4 Schematic of the experimental set up of Elustondo *et al*. (2001). Copyright 2001, reproduced with permission from Elsevier.

Among the first reported works on LPSSD of foods and biomaterials is the work of Elustondo *et al*. (2001) who studied LPSSD of foodstuffs both experimentally and theoretically. Wood slabs, shrimp, banana, apple, potato and cassava were dried using the steam pressures of 10 000–20 000 Pa, the steam temperatures of 60–90°C and the steam circulating velocities of 2–6 $m\,s^{-1}$ in a set up shown schematically in Figure 5.4. A mathematical model was also developed based on a theoretical drying mechanism, which assumes that the water removal is carried out by evaporation in a moving boundary allowing the vapor to flow through the dry layer built as drying proceeds to predict the drying characteristics of foodstuffs undergoing this drying operation. A simplified expression, which has two experimentally determined parameters, was derived and used to predict the drying rate of test samples.

An example of the dimensionless drying rate curve is shown in Figure 5.5. The constant drying rate period cannot be observed in this figure (and all other experiments conducted).

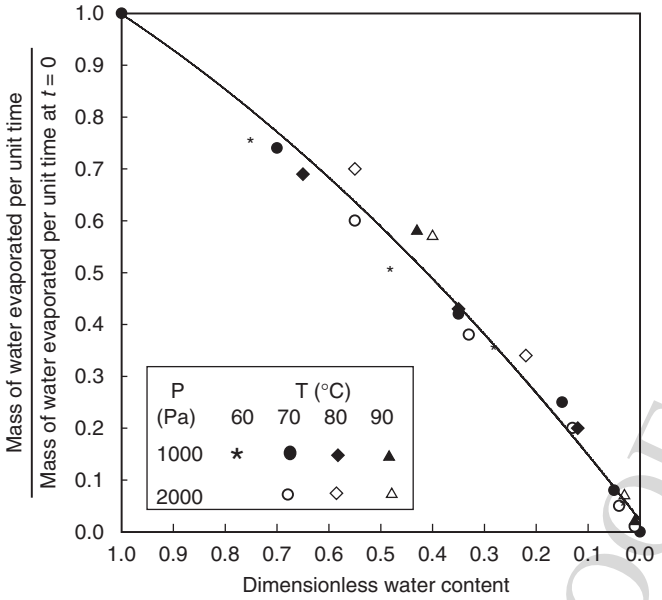

AQ: Please check the labelling of y-axis if any change is required for figure 5.5.

Fig. 5.5 Dimensionless drying rate of banana slices as a function of the instantaneous moisture content (Elustondo *et al*., 2001). Copyright 2001, reproduced with permission from Elsevier.

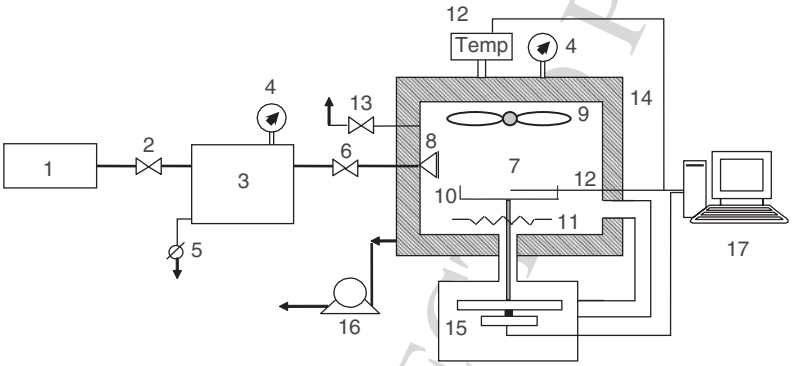

Fig. 5.6 A schematic diagram of the low-pressure superheated steam dryer and associated units (Devahastin *et al*., 2004). 1, boiler; 2, steam valve; 3, steam reservoir; 4, pressure gauge; 5, steam trap; 6, steam regulator; 7, drying chamber; 8, steam inlet and distributor; 9, electric fan; 10, sample holder; 11, electric heater; 12, on-line temperature sensor and logger; 13, vacuum break-up valve; 14, insulator; 15, on-line weight indicator and logger; 16, vacuum pump; 17, PC with installed data acquisition card.

An approximately linear relationship between the dimensionless drying rate and moisture content could be observed during an early stage of drying, whereas the slope of the curve increased toward the end of the drying process. A model proposed was found to predict the drying kinetics reasonably well. No mention about product quality was given, however.

Devahastin *et al*. (2004) developed another version of a low-pressure superheated steam dryer, which can be operated by using steam supplied from a typical boiler available in a food plant. A schematic diagram of this dryer is shown in Figure 5.6.

By using carrot as a model heat-sensitive material, experiments were conducted to examine the drying kinetics and various quality parameters of the product undergoing LPSSD. For comparison experiments were also performed under a vacuum condition (by using the same set-up but without the application of steam to the dryer) at the same operating conditions, that is, absolute pressures of 7, 10 and 13 kPa and temperatures of 60, 70 and 80°C. Based on the experimental drying data it was observed that all samples undergoing LPSSD gained a small amount of moisture during the first few minutes of drying. Nevertheless, the condensation of steam was rather negligible if the operating pressure was low. It was also observed that the effect of temperature on the drying rates was greater than the effect of pressure in the case of LPSSD, especially at higher drying temperatures. The effect of operating pressure was less clear even at lower temperature (60°C) for the case of vacuum drying, however. This is probably due to the fact that the steam thermal properties were affected by temperature to a larger extent than those of air, especially at lower drying temperatures. No initial condensation was also observed, as expected, in the case of vacuum drying. It was also reported that the moisture content decreased faster, especially in the case of LPSSD at lower drying temperatures, at lower pressures since water boiled and evaporated at lower temperatures. It was found that the drying times of vacuum drying were shorter than those of LPSSD (at the same pressure) for all conditions tested. This is probably due to the fact that the electric heater was used more often during vacuum drying since it was the only source of energy for drying. This might increase the amount of radiation absorbed by the carrot surfaces, thus explaining the higher drying rate during vacuum drying. The initial steam condensation on the product surface might also contribute to the longer drying times for the case of LPSSD. The differences between the two sets of drying times, however, were smaller at higher drying temperatures. Raising the drying temperature further would eventually lead to equal rates of drying at an inversion temperature (due to increased temperature difference between the steam and the product as well as a reduction of the initial steam condensation).

Figure 5.7 illustrates changes of moisture content and temperature of carrot undergoing LPSSD at some selected conditions. It can be seen in this figure that the shapes of the drying and temperature curves were affected by both the drying temperature and pressure. At lower drying temperatures the temperature of carrot changed suddenly from its initial value and remained rather constant at the boiling temperature of water corresponding to the operating pressure until the first falling rate period drying ended (drying rate data are not shown here for the sake of brevity). Beyond this point, the carrot temperature rose again and finally approached the temperature of the drying medium. As the medium temperature increased (at the same operating pressure) it can be seen (for example, from Figure 5.7c) that the period of constant product temperature was shorter; the product temperature rose almost steadily from its initial value to the medium temperature. At the same drying temperature, however, increasing the operating pressure led to a lower rate of drying but a longer period of constant product temperature (as can be seen from Figures 5.7c and 5.7d). It may depend both on the characteristics of the drying product and on these effects to determine the optimum operating conditions of an LPSSD.

Figure 5.8 shows the evolutions of moisture content and temperature of carrot undergoing vacuum drying at the same operating as those used for LPSSD shown in Figure 5.7. It can be seen from this figure that the drying and heat transfer behavior of carrot undergoing vacuum drying was quite different from that of LPSSD; the product temperature, in this case, rose almost steadily from its initial value to the medium temperature. However, the rates of moisture reduction in the case of vacuum drying were higher than those belonged to LPSSD, especially at lower drying temperatures as mentioned earlier.

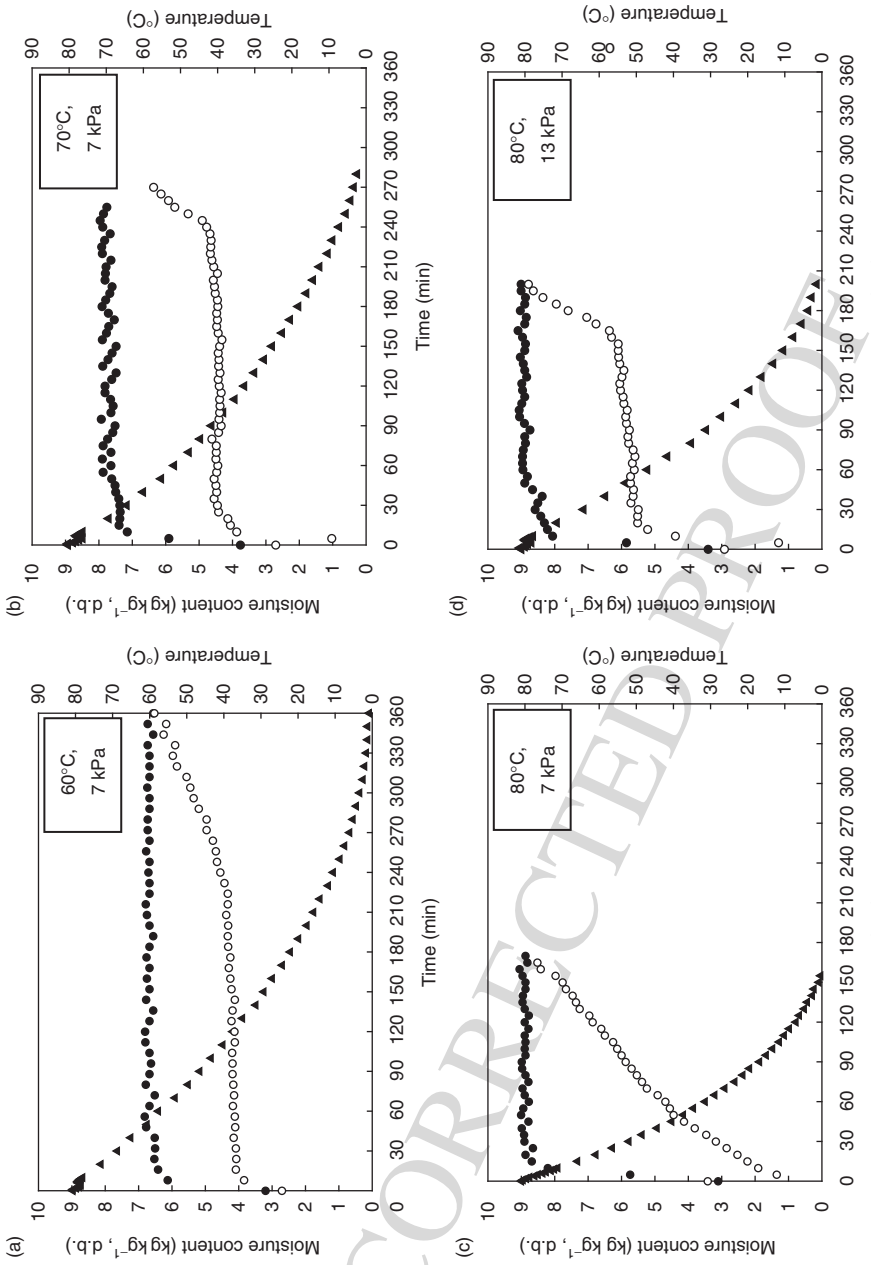

Fig. 5.7 Changes in moisture content and temperature of carrot undergoing LPSSD at different operating conditions. (▲), Moisture content; (●), steam temperature; (○), simple temperature.

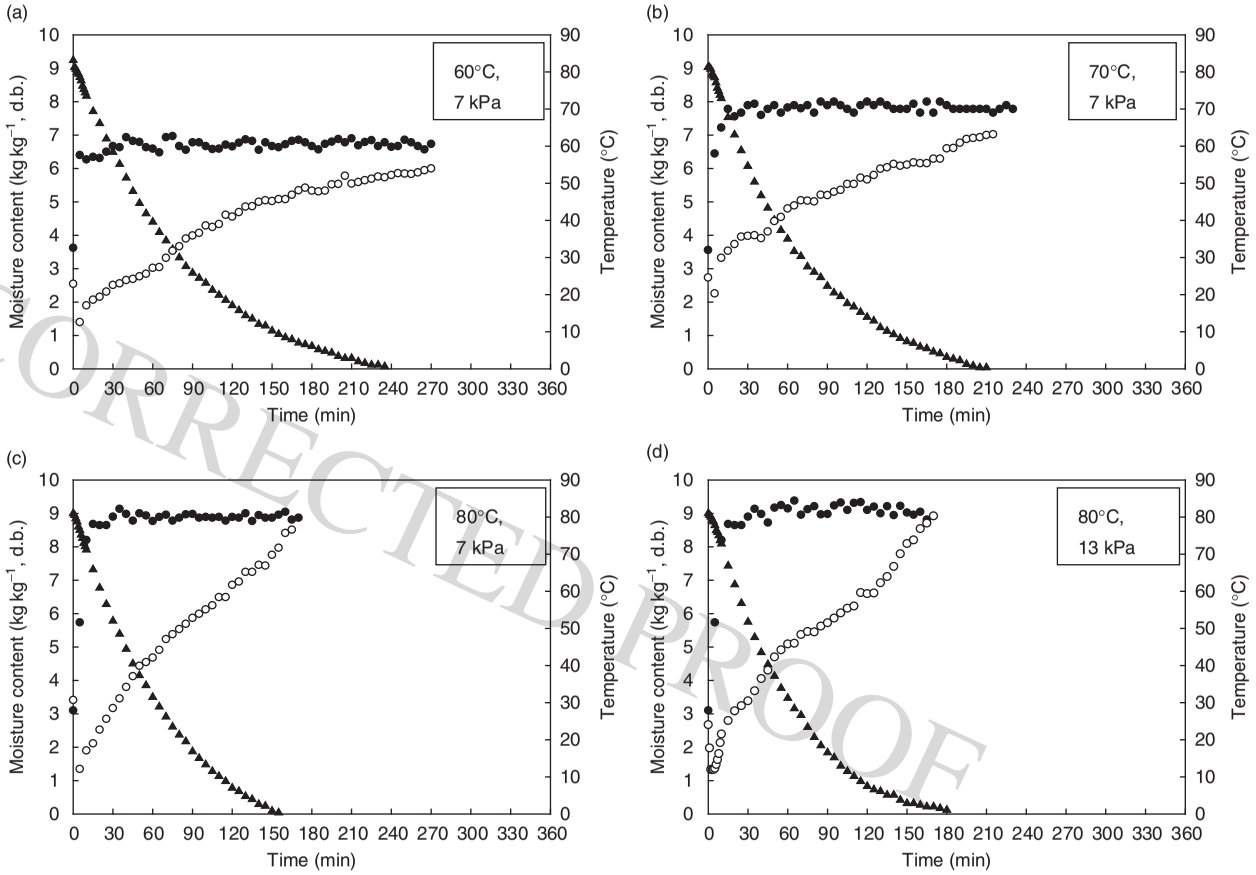

Fig. 5.8 Changes in moisture content and temperature of carrot undergoing vacuum drying at different operating conditions. (▲), moisture content; (●), steam temperature; (○), sample temperature.

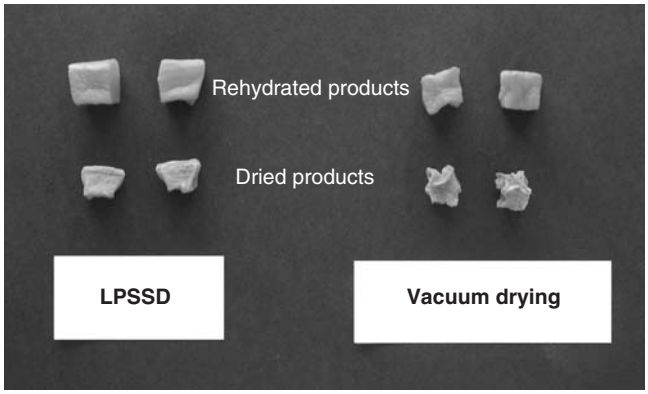

Fig. 5.9 Photographs of carrot cubes both after drying and after rehydration.

In terms of quality it was reported that the volume and apparent density of dried carrot undergoing both drying techniques slightly decreased and increased, respectively, as the operating pressure increased; both properties changed only slightly in this case, however, because of the narrow range of operating pressures tested. It was noted, however, that although the values of shrinkage of carrot that underwent LPSSD and vacuum drying were similar, the shrinkage patterns resulting from the two different drying processes were quite different. Carrot that underwent vacuum drying tended to shrink non-uniformly. In a more rapid drying (as in the case of vacuum drying when compared with LPSSD) the surface of the drying product became dry and rigid long before the center had dried out; the center dried and shrank much later than the outer surface did and hence pulled away from the rigid surface layers and caused a non-uniform shrinkage. Drying carrot in LPSSD, however, led to a more uniform shrinkage; in this case shrinkage seemed to occur because the carrot structure could not support its own weight and hence collapsed under gravitational force in the absence of moisture (Achanta and Okos, 2000). This is because LPSSD offered a milder drying condition (since the drying chamber was moister than in the case of vacuum drying). Dense or rigid large formations might not be formed as much in the case of LPSSD as in the case of vacuum drying. The photographs of carrot cubes both after drying and after rehydration are shown in Figure 5.9. These results are supported by the SEM photographs of Figures 5.10a and 5.10b, which show the micro-structure of LPSSD and vacuum dried carrot, respectively. It is seen from these figures that carrot that underwent vacuum drying developed a rather dense layer and its pore distribution was rather non-uniform compared to carrot that underwent LPSSD.

A simple technique has indeed been proposed to monitor deformation of a food product undergoing different drying techniques and conditions (Panyawong and Devahastin, 2007). The use of such a technique has confirmed the above-mentioned argument that the product undergoing LPSSD suffered less irregular deformation than the product undergoing vacuum drying although the percentage of the volumetric shrinkage of the two products was not significantly different.

Many studies were also performed to study the capability of LPSSD to retain some heat-sensitive chemical properties (e.g. various vitamins, flavors and aromas) of food products. Barbieri *et al*. (2004) compared the effects of hot air drying (40–60°C) and LPSSD (at a temperature of 50°C and pressure of around 5 kPa) on the retention of some volatile compounds in basil (*Ocimum basilicum*). It was found that the original aroma profiles were

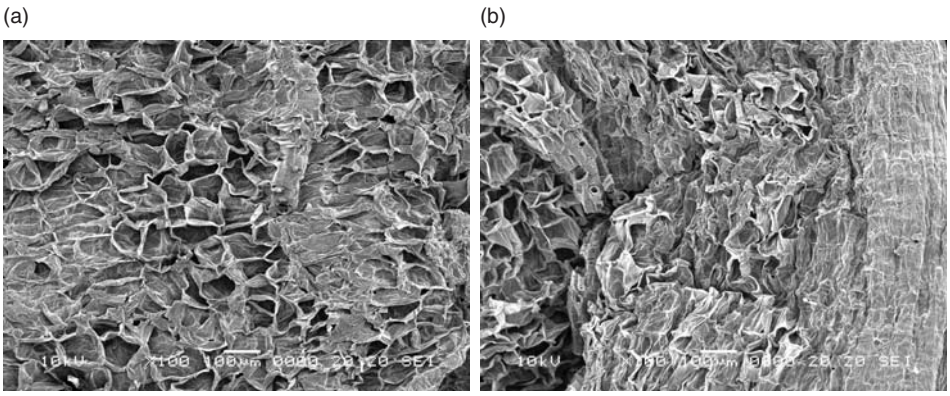

Fig. 5.10 SEM photographs of carrot undergoing (a) LPSSD and (b) vacuum drying.

kept almost constant in the case of basil dried by LPSSD. On the other hand, air-dried basil suffered significant variations in the relative proportions of aroma compounds.

Methakhup *et al*. (2005) dried Indian gooseberry (*Phyllanthus emblica* L.) flakes in both LPSSD and vacuum conditions using the same set-up as that used by Devahastin *et al*. (2004). Although vacuum drying took a shorter time to dry the product than did LPSSD at all drying conditions tested (temperatures in the range of 65–75°C and absolute pressures in the range of 7–13 kPa), it was found that LPSSD could retain ascorbic acid better than vacuum drying in almost all cases studied. In addition, LPSSD could preserve the colors of the sample better than vacuum drying at all drying conditions tested. In vacuum drying, temperature had a significant effect on ascorbic acid content and colors of the product while absolute pressure did not significantly affect the quality. In low-pressure superheated steam drying, on the other hand, the drying conditions did not affect the ascorbic acid and colors of the dried product. The quality results of their study are summarized in Tables 5.2 and 5.3.

From Table 5.2 it is seen that all dried Indian gooseberry flakes tended to lose some ascorbic acid as compared to fresh. The ascorbic acid retention was in the ranges of 64–94% for vacuum drying and 93–96% for LPSSD. For vacuum drying it was found that the ascorbic acid retention of the sample increased as the drying temperature increased. This may be due to the shorter drying time required to dry the samples to the desired moisture content. However, the pressure had only a little effect on the ascorbic acid retention. This may be explained by the fact that the drying time was not much affected by the operating pressure and that the level of oxygen content (which caused the aerobic degradation of vitamin C) was not much different at different pressures.

In LPSSD the ascorbic acid retention was not significantly different at different drying conditions even though the drying time was different. The results implied that no oxygen was available in the drying system and thus presented no effect on the ascorbic acid degradation during drying. The ability of the superheated steam drying system to maintain vitamin C has, in fact, been reported earlier by other investigators (e.g. Moreira, 2001)

From Table 5.3 it was found that LPSSD and vacuum drying at every condition resulted in a decrease of an L value and an increase of an a value of the dried sample compared with the fresh. However, b value of the dried sample was similar to that of the fresh sample. These results implied that the browning reaction and pigment destruction occurred in the dried sample. When considering the color retention of samples between two different drying

Table 5.2 Total ascorbic acid content of fresh and dried Indian gooseberry samples.

Drying method	Condition		Ascorbic acid (g per 100 g)		
	T (°C)	P_{ab} (kPa)	Fresh	Dried	% Retention
VD[1]	65	7	1.08 ± 0.07	3.67 ± 0.13	$71.52^{ab} \pm 1.97$
		10	1.06 ± 0.09	3.50 ± 0.25	$66.89^{a} \pm 2.51$
		13	0.94 ± 0.05	3.07 ± 0.30	$64.84^{a} \pm 6.01$
	75	7	0.96 ± 0.02	3.84 ± 0.18	$94.46^{cd} \pm 2.57$
		10	0.99 ± 0.02	3.72 ± 0.11	$89.46^{c} \pm 2.78$
		13	0.98 ± 0.11	3.34 ± 0.03	$78.13^{b} \pm 2.83$
LPSSD[2]	65	7	1.05 ± 0.06	3.99 ± 0.22	$93.46^{cd} \pm 1.58$
		10	—	—	—
		13	—	—	—
	75	7	1.06 ± 0.04	4.04 ± 0.08	$95.35^{d} \pm 3.49$
		10	1.09 ± 0.08	4.03 ± 0.11	$95.67^{d} \pm 2.10$
		13	$1.04 + 0.08$	3.99 ± 0.11	$94.96^{cd} \pm 2.14$

Means in the same column having the same letter are not significantly different ($\alpha < 0.05$).
[1] VD stands for vacuum drying.
[2] LPSSD stands for low-pressure superheated steam drying.

Table 5.3 Hunter parameters and total color difference (ΔE) of dried samples.

Drying method	Conditions					
	T (°C)	P_{ab} (kPa)	$\Delta L/L_o$	$\Delta a/a_o$	$\Delta b/b_o$	ΔE
VD[1]	65	7	0.06 ± 0.00	-0.91 ± 0.01	0.01 ± 0.01	$3.83^{b} \pm 0.09$
		10	0.08 ± 0.00	-1.39 ± 0.07	0.02 ± 0.02	$5.40^{cd} \pm 0.10$
		13	0.07 ± 0.01	-0.98 ± 0.22	0.00 ± 0.04	$4.99^{c} \pm 1.04$
	75	7	0.08 ± 0.00	-0.71 ± 0.01	-0.02 ± 0.01	$5.61^{cd} \pm 0.28$
		10	0.09 ± 0.00	-1.11 ± 0.01	-0.02 ± 0.00	$6.42^{d} \pm 0.26$
		13	0.07 ± 0.01	-1.56 ± 0.58	0.03 ± 0.02	$5.38^{cd} \pm 0.66$
LPSSD[2]	65	7	0.04 ± 0.00	-0.88 ± 0.97	0.04 ± 0.01	$3.09^{ab} \pm 0.19$
		10	—	—	—	—
		13	—	—	—	—
	75	7	0.03 ± 0.01	-0.64 ± 0.04	0.04 ± 0.02	$2.48^{a} \pm 0.44$
		10	0.04 ± 0.00	-0.49 ± 0.18	0.04 ± 0.01	$2.88^{ab} \pm 0.18$
		13	0.04 ± 0.04	-0.64 ± 0.23	0.02 ± 0.04	$2.93^{ab} \pm 0.39$

Means in the same column having the same letter are not significantly different ($\alpha < 0.05$).
[1] VD stands for vacuum drying.
[2] LPSSD stands for low-pressure superheated steam drying.

methods it was found that LPSSD could retain the colors better than the vacuum drying system. This is because the degree of ascorbic acid and, probably, chlorophyll degradation of LPSSD was much lower than that of the vacuum drying system.

The drying methods were also found to affect the degradation and release of vitamin C (evaluated in terms of the total ascorbic acid, TAA) from Indian gooseberry flakes during preparation of Indian gooseberry tea (Kongsoontornkijkul *et al*., 2006). LPSSD was indeed found to help retain TAA in dried gooseberry flakes better than hot air and vacuum drying.

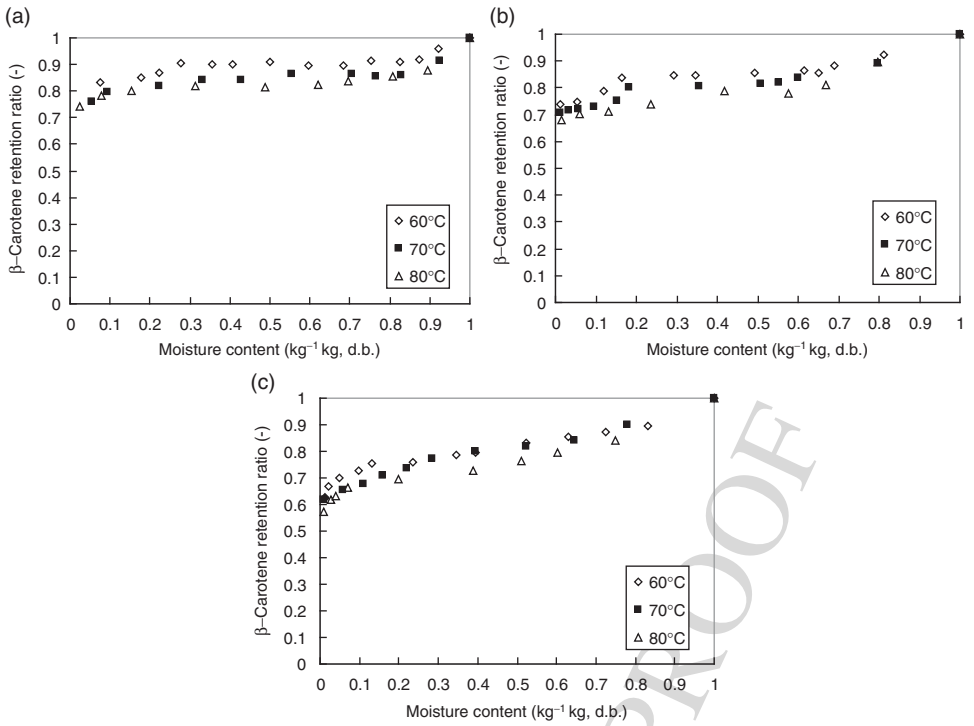

Fig. 5.11 Relationship between β-carotene content and moisture content of carrot undergoing different drying techniques: (a) LPSSD; (b) vacuum drying; (c) hot air drying.

Suvarnakuta *et al*. (2005a) experimentally studied the effects of LPSSD, vacuum and hot air drying on the drying and degradation kinetics of β-carotene in carrot. It was found that LPSSD and vacuum drying led to less degradation of β-carotene in carrot than in the case of hot air drying (see Figure 5.11 and Table 5.4). This is again due to the oxygen-free environment of LPSSD.

In terms of the texture of dried products (e.g. snacks) Leeratanarak *et al*. (2006) reported that the drying methods, in their case hot air drying (70–90°C) and LPSSD (at temperatures of 70–90°C and pressure of 7 kPa), had no significant effect on the texture (in terms of hardness) of dried potato chips. Hot-water blanching (95°C) of potato slices prior to drying, on the other hand, led to improved drying kinetics (due to structural softening leading to easier migration of moisture), colors (due to lower extents of browning reactions) and texture of the products. The degree of browning was also lowered. However, the use of different blanching periods (1–5 min) did not significantly affect the hardness of the chips.

Although blanching has been proved to enhance the quality of potato chips, the chips of Leeratanarak *et al*. (2006) were still observed to be of inferior quality to those available commercially. Pimpaporn *et al*. (2007) therefore investigated the use of different combined pretreatments prior to LPSSD (at temperatures of 70–90°C and pressure of 7 kPa) to improve the quality of potato chips, especially in terms of their texture. Both physical pre-treatments, such as blanching, combined blanching and freezing, as well as chemical pre-treatments, such as dipping raw potato slices in several chemicals including glycerol and monoglyceride, were evaluated. In terms of the drying kinetics it was noted (see Figure 5.12) that the combination

Table 5.4 Average drying times and losses of β-carotene of dried carrot (at moisture content of 0.1 kg kg^{-1} d.b.) undergoing different drying methods.

Sample	Average drying time (min)	β-Carotene content* (mg per 100)		β-Carotene retention ratio (β_t/β_i)
		Wet basis	Dry basis	
Fresh carrot	—	4.86 ± 0.65	51.11 ± 6.89	—
LPSSD carrot				
$T = 60°C$	420	54.92	43.94	0.83 ± 0.02^{a}
$T = 70°C$	330	50.32	41.24	0.76 ± 0.04^{b}
$T = 80°C$	210	38.81	31.55	0.74 ± 0.02^{b}
Vacuum-dried carrot				
$T = 60°C$	300	26.95	24.28	0.74 ± 0.03^{c}
$T = 70°C$	250	25.81	24.05	0.71 ± 0.03^{cd}
$T = 80°C$	180	31.61	27.85	0.68 ± 0.03^{d}
Hot air-dried carrot				
$T = 60°C$	420	22.56	21.46	0.62 ± 0.02^{e}
$T = 70°C$	300	35.66	23.30	0.62 ± 0.03^{e}
$T = 80°C$	240	36.26	22.05	0.58 ± 0.03^{e}

Means in the same column having the same letter are not significantly different ($\alpha < 0.05$).

AQ:Please provide explanation for '*' which is appearing in Table 5.4 column head.

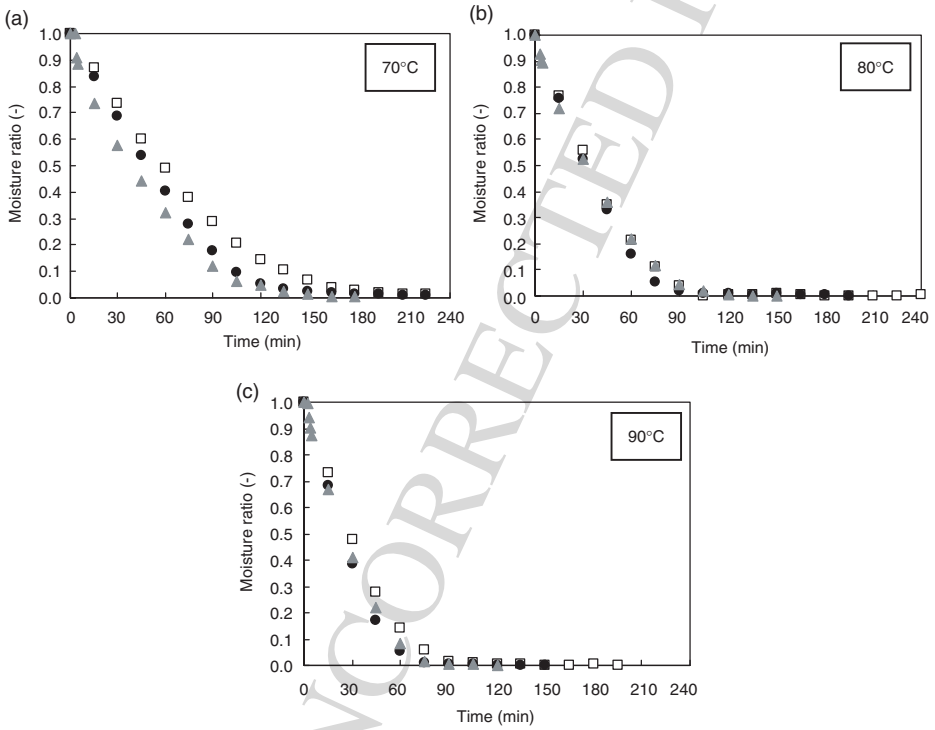

Fig. 5.12 Drying kinetics of unblanched (□), blanched (●) and blanched-frozen (▲) potato slices.

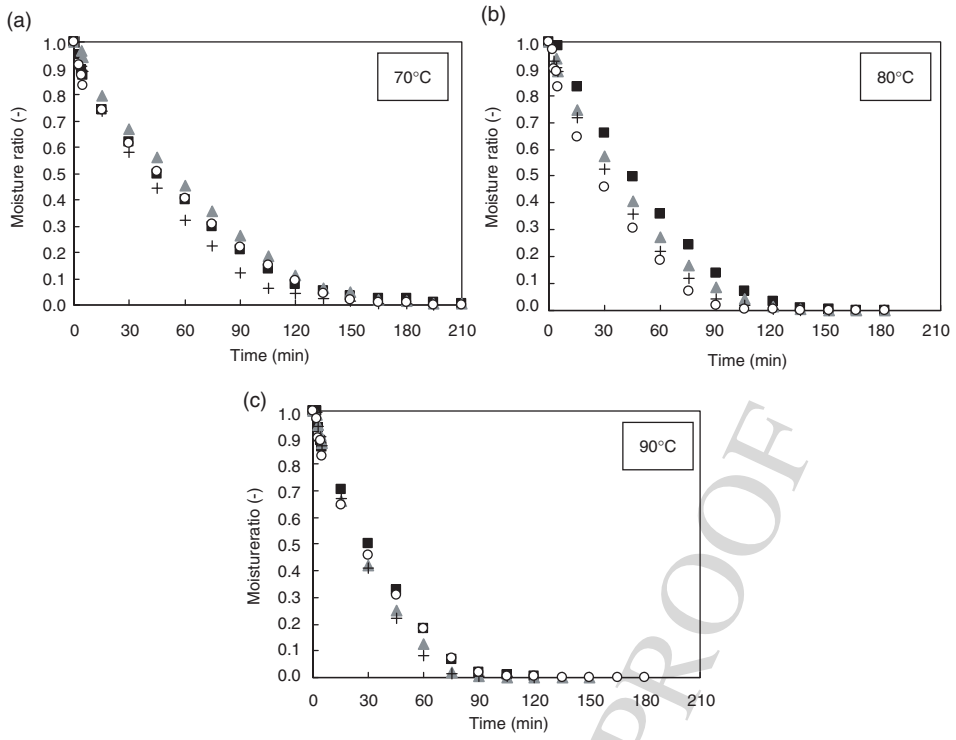

Fig. 5.13 Drying kinetics of blanched potato slices with glycerol immersion at concentrations of 0% (+), 1% (■), 3% (▲), and 5% (○) followed by freezing at different drying temperatures.

of blanching and freezing led to a shorter drying time compared to that of unblanched samples at all drying temperatures. This is probably due to structure softening during blanching. In addition, freezing affects the physical tissue of potato due to the large size of ice crystals formed during slow freezing. The ice crystals might cause openings of the cell wall and semi-permeable membrane that could facilitate moisture transfer during drying. Chemically treated samples showed different drying behavior, however. As can be seen in Figure 5.13, which shows the drying curves of glycerol-treated samples, all glycerol-treated samples needed a longer time to reach their desired final moisture contents than those that underwent blanching and freezing pre-treatment. This is because glycerol has three hydroxyl groups that form hydrogen bonds with water in potato slices. Therefore, evaporation of free water on the surface of sliced potato becomes more difficult. However, the effect of glycerol was reduced at high drying temperatures, especially at 90°C. The drying time of each case was nearly the same as that of combined blanched-frozen samples. However, the results showed an unclear effect of monoglyceride on the drying kinetics of the samples.

In terms of quality it was found that the lightness of dried potato chips was improved by the use of freezing pre-treatment; nevertheless, the lightness values were not significantly different among all freezing pre-treated samples. Redness and yellowness of dried potato chips were not significantly affected by drying temperature but were significantly affected by the methods of pre-treatment.

The hardness of dried potato chips was not significantly influenced by the pre-treatment methods but was better at higher drying temperatures. However, in the cases of crispness

Table 5.5 Effects of pre-treatments and drying temperature on final thickness, hardness, crispness and toughness of LPSSD potato chips.

Pretreatment method	Drying temperature (°C)	Hardness (N)	Toughness ($N\,mm^{-1}$)	Crispness ($N\,mm^{-1}$)
Blanching	70	12.75 ± 2.38^{efg}	18.81 ± 4.46^{f}	3.43 ± 1.65^{ab}
	80	8.59 ± 2.30^{cdef}	17.59 ± 1.87^{f}	6.22 ± 0.94^{abcde}
	90	8.21 ± 0.64^{bcdef}	16.22 ± 0.21^{ef}	5.07 ± 0.43^{abcd}
Blanching + freezing	70	10.21 ± 0.58^{def}	9.13 ± 1.38^{bcde}	14.82 ± 2.86^{fghi}
	80	8.00 ± 2.60^{bcdef}	4.14 ± 1.97^{ab}	13.00 ± 0.67^{fghi}
	90	6.77 ± 0.25^{abcd}	3.35 ± 1.37^{ab}	15.98 ± 3.58^{fghi}
B + I (0.1% monoglyceride) + F	70	9.94 ± 1.30^{fg}	14.28 ± 1.38^{def}	11.37 ± 0.84^{defgh}
	80	9.60 ± 0.74^{cdef}	8.38 ± 0.92^{bcd}	12.54 ± 3.94^{efghi}
	90	7.03 ± 0.67^{abcd}	3.59 ± 2.08^{ab}	14.96 ± 3.02^{fghi}
B + I (0.3% monoglyceride) + F	70	10.34 ± 3.87^{def}	13.25 ± 1.02^{cdef}	9.26 ± 1.44^{bcdef}
	80	8.73 ± 0.13^{cdef}	7.88 ± 1.70^{abcd}	10.55 ± 1.47^{cdefg}
	90	4.72 ± 0.48^{abc}	3.49 ± 2.05^{ab}	13.08 ± 2.68^{fghi}
B + I (0.5% monoglyceride) + F	70	10.33 ± 0.39^{def}	16.34 ± 0.72^{ef}	11.00 ± 1.19^{defg}
	80	9.47 ± 1.70^{cdef}	5.75 ± 2.49^{abc}	13.09 ± 2.34^{fghi}
	90	7.54 ± 2.17^{abcde}	5.06 ± 2.41^{ab}	16.49 ± 1.15^{ghi}
B + I (1% glycerol) + F	70	11.30 ± 2.10^{def}	18.95 ± 4.59^{f}	2.25 ± 0.18^{a}
	80	9.40 ± 1.03^{cdef}	14.75 ± 1.68^{def}	13.10 ± 1.38^{fghi}
	90	7.48 ± 1.25^{abcde}	3.28 ± 1.44^{ab}	14.47 ± 2.57^{fghi}
B + I (3% glycerol) + F	70*	9.92 ± 0.51^{h}	18.63 ± 0.96^{f}	9.10 ± 2.97^{bcdef}
	80	8.13 ± 1.87^{bcdef}	14.08 ± 1.61^{def}	12.39 ± 1.50^{efghi}
	90	7.59 ± 0.76^{abcde}	3.07 ± 1.01^{ab}	18.34 ± 2.99^{i}
B + I (5% glycerol) + F	70*	17.52 ± 0.59^{g}	34.09 ± 6.92^{g}	4.29 ± 0.64^{abc}
	80	9.47 ± 2.06^{cdef}	13.35 ± 2.27^{cdef}	6.28 ± 2.42^{abcde}
	90	7.41 ± 2.06^{abcde}	6.30 ± 2.12^{abc}	14.96 ± 1.41^{hi}

B: blanching, I: immersion in solution and F: freezing
Different superscripts in the same column mean that the values are significantly different ($p \pm 0.05$).
*Denotes the cases where the final moisture content of 3.5% (d.b.) was not achievable.

and toughness, the drying temperature affected these parameters significantly, especially at 90°C. More importantly, freezing pre-treatment could improve the crispness and also toughness of dried chips. The crispness increased as the drying temperature increased but the toughness decreased with increased drying temperature. The textural results are summarized in Table 5.5.

A micro-structural evaluation of the potato chips was also performed. It was noted that the drying temperature significantly affected the micro-structure of dried potato chips. On the other hand, the effects of pre-treatments on the micro-structure were only that combined blanching and freezing pre-treatments led to the best integrity of micro-structure (in terms of pore size, pore distribution and also less formation of rigid dense layer). This superior integrity of the micro-structure might lead to the favorable texture of dried potato chips as summarized earlier.

Based on the aforementioned arguments, combined blanching and freezing without any chemical pre-treatments, followed by drying in LPSSD at a higher temperature (90°C in this

case) was recommended. It is important to note, however, that a sensory study is needed prior to being able to make a definitive conclusion on the validity of the results.

5.4 SOME ADVANCES IN LPSSD OF FOODS AND BIOMATERIALS

In addition to drying foods and biomaterials in LPSSD tray dryers, some researchers have applied LPSSD to other types of dryers. It should be noted that the concept of combining different modes of drying by itself is obviously not new.

Kozanoglu *et al*. (2006) dried coriander and pepper seeds in a low-pressure (in the range of 40–66 kPa) superheated steam fluidized-bed dryer over the temperature range of 90–110°C. General trends of drying kinetics were observed. At a given temperature lowering the operating pressure led to a higher degree of steam superheat and higher fluidizing air velocity. The degree of steam superheat was found to have the most important effect on the drying behavior of both types of seeds.

Nimmol *et al*. (2007) combined LPSSD and far-infrared radiation (FIR) as an external heat source to enhance the rates of the drying process. The combined process (LPSSD-FIR) was also compared with combined vacuum drying and FIR (VACUUM-FIR) for banana slices, both in terms of the drying kinetics and quality of the dried chips (in terms of color, shrinkage, rehydration behavior, texture and micro-structure), over the temperature range of 70–90°C and pressures of 7 and 10 kPa. Moreover, the quality of dried banana chips was compared with that of banana slices undergoing LPSSD alone.

The changes in moisture ratio and temperature of banana slices undergoing LPSSD-FIR and VACUUM-FIR at some selected conditions are shown in Figures 5.14 and 5.15, respectively. After a slight drop of the sample temperature due to the rapid reduction of the chamber pressure, which led to some flash evaporation of surface moisture, the temperature of the sample (in the case of LPSSD-FIR) rose rapidly to a level close to the boiling point of water corresponding to the chamber pressure (not at the boiling point, as is seen in Figure 5.7, since far-infrared radiation was also present in this case) and then remained unchanged at this level until the surface of the sample started to dry. Another important aspect is that the temperature of the sample rose steadily to a level higher than the pre-determined medium temperature because heat transfer, in the case of LPSSD-FIR, simultaneously took place by radiation from the far-infrared radiator and by convection from superheated steam. After this period the temperature of the sample remained almost unchanged because during the later stage of the process moisture content within the sample was smaller leading to lower absorptivity of the sample.

Comparing the changes in the temperature of banana slices undergoing LPSSD-FIR and VACUUM-FIR reveals that, at the same pre-determined medium temperature, the sample temperature during the later stage of LPSSD-FIR was higher than that in the case of VACUUM-FIR. This is due to the fact that in the case of LPSSD-FIR, radiation intensity at the position of the thermocouple used for sending the signal to the temperature controller (30 mm above the sample surface) was less intense due to the higher absorptivity of superheated steam compared to that of air. The far-infrared radiator was thus used more often during LPSSD-FIR to maintain the desired level of drying medium temperature, leading to a higher surface temperature of the far-infrared radiator. Consequently, the radiation intensity, which depends on the surface temperature of the far-infrared radiator, experienced by LPSSD-FIR samples was greater, hence higher levels of the sample temperature.

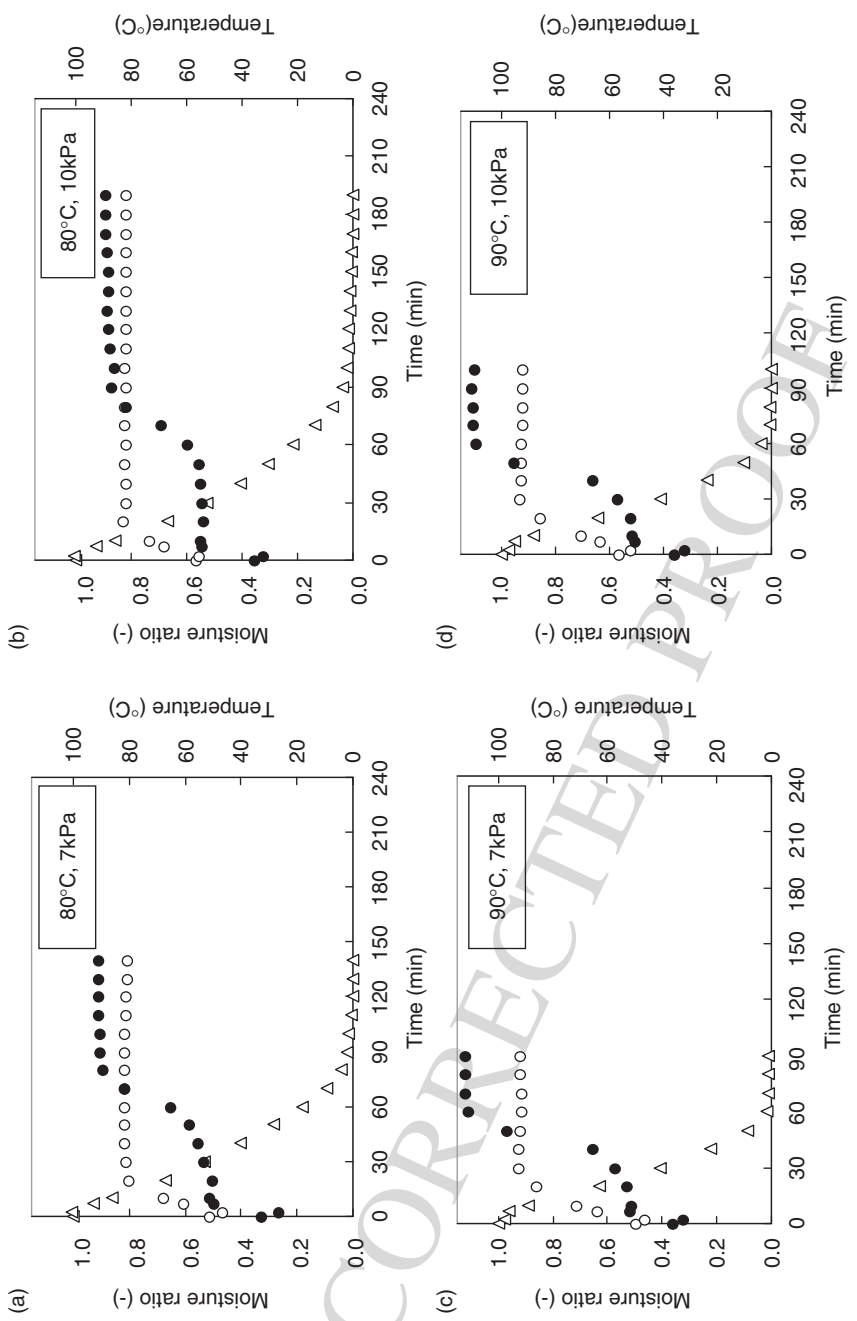

Fig. 5.14 Changes in moisture ratio and temperature of banana slices undergoing LPSSD-FIR. (○), Drying medium temperature; (●), sample temperature; (△), moisture ratio.

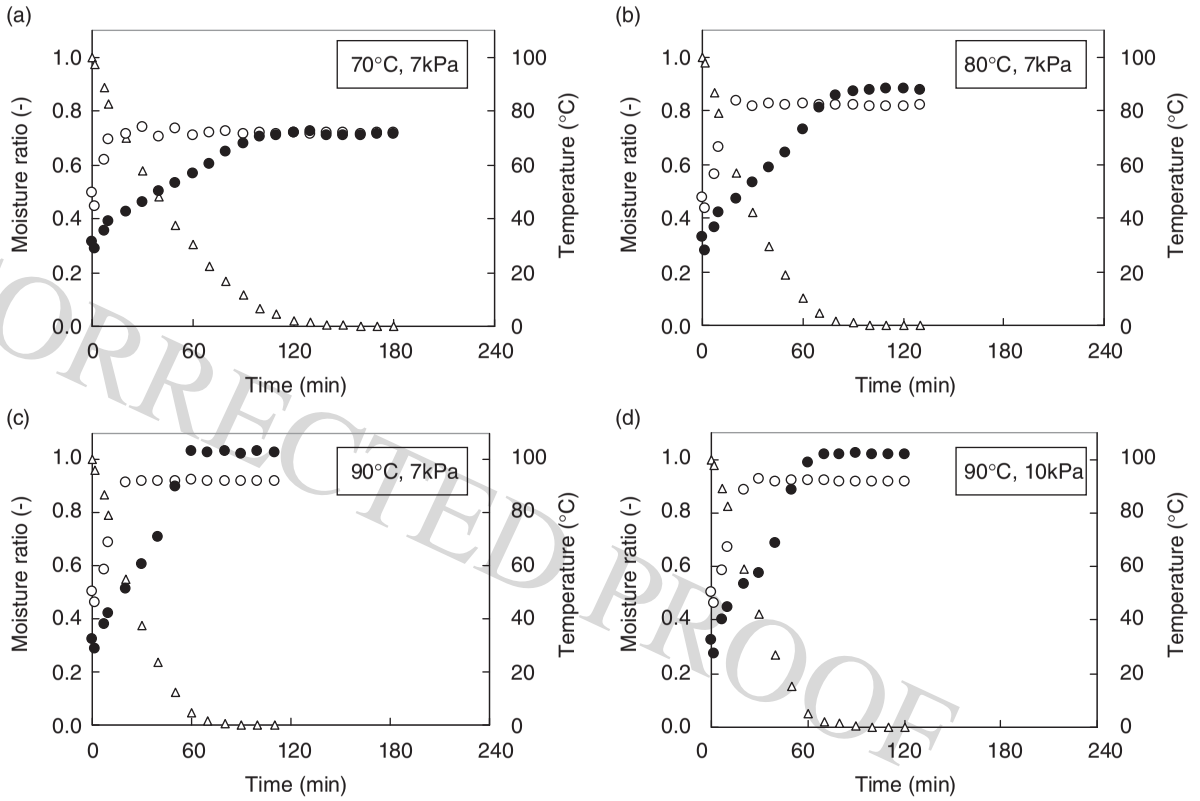

Fig. 5.15 Changes in moisture ratio and temperature of banana slices undergoing VACUUM-FIR. (○), drying medium temperature; (●), sample temperature; (△), moisture ratio.

In terms of quality it was observed that banana dried by LPSSD-FIR was significantly darker and redder than that dried by VACUUM-FIR at all drying conditions. This is because the temperature of banana slices undergoing LPSSD-FIR increased more rapidly and stayed at higher levels than that of samples dried by VACUUM-FIR as mentioned earlier.

When comparing the colors of banana chips dried either by LPSSD-FIR or VACUUM-FIR with those of banana chips dried only by LPSSD (Thomkapanish *et al*., 2007) it is noted that bananas dried by FIR-assisted processes had higher values of color changes, especially in the case of lightness and redness. This is due to the fact that banana slices undergoing LPSSD-FIR and VACUUM-FIR were subjected to the higher temperature for a longer period than those dried by LPSSD, especially during the later stage of the process.

In terms of shrinkage it was noted that drying at lower temperatures (70° and 80°C in this case) yielded dried products with lower degrees of area shrinkage because case hardening (rigid layers) on the sample perimeter, which retarded shrinkage (surface area change) of the samples, occurred less at these conditions. Case hardening also developed faster during LPSSD-FIR and VACUUM-FIR compared with the case of LPSSD alone due to the higher sample temperatures mentioned earlier. Regarding the rehydration behavior, it was noted that banana slices dried at higher temperatures had higher rehydration ability than those dried at lower temperatures. This is because higher drying temperatures led to dried banana slices with a more porous structure, thus facilitating rehydration ability. It was also noted that banana slices dried by LPSSD-FIR generally had higher rehydration ability than those dried by VACUUM-FIR. This is due to the fact that the temperature of bananas dried by LPSSD-FIR suddenly rose to a level close to boiling temperature (as can be seen in Figure 5.14). Consequently, moisture in the banana rapidly boiled leading to rigorous evolution of steam within the samples. Larger and more pores were developed compared with the samples dried by VACUUM-FIR (see Figure 5.16, which clearly shows that when drying was performed at lower temperature banana slices dried by LPSSD-FIR had larger and more pores compared with those dried by VACUUM-FIR). However, the rehydration ability of banana slices dried by LPSSD-FIR and VACUUM-FIR was not significantly different in the case of drying at 90°C. This is probably due to the fact that moisture within the samples dried by VACUUM-FIR boiled as rigorously as in the case of LPSSD-FIR at this higher temperature. This hypothesis was confirmed by the fact that the micro-structure of banana slices dried by both methods was similar in the case of drying at 90°C (see Figures 5.16c and 5.16d).

Table 5.6 shows the results of the texture of banana chips in terms of the maximum force (hardness) and the number of peaks in the force-deformation curve (crispness). In the case of hardness it was found that banana slices dried by VACUUM-FIR were harder than those dried by LPSSD-FIR, as indicated by the higher value of the maximum force. This is probably due to the fact that VACUUM-FIR, especially at a lower drying temperature (80°C in this case), yielded dried banana slices with a more dense structure (smaller and less pores), as can be seen in Figures 5.16a and 5.16b. However, the statistical analysis showed that the effects of drying temperature and drying pressure as well as drying methods on the hardness were not significant. It should be noted that, at the same drying temperature, the hardness of banana chips was lower than that of samples dried by LPSSD alone.

In terms of crispness it can be seen again from Table 5.6 that LPSSD-FIR yielded banana chips with a larger number of peaks (hence indicating that the products were crispier) compared with VACUUM-FIR, especially at 80°C. This might be due to the larger and more numerous pores that occurred during LPSSD-FIR. Comparing these results with those obtained using LPSSD it was found that LPSSD-FIR and VACUUM-FIR provided banana

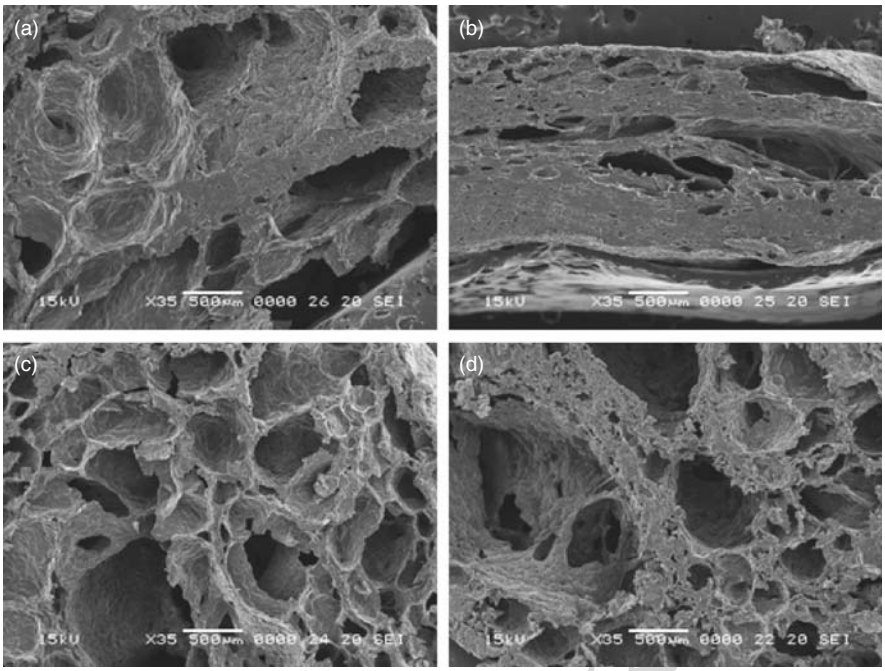

Fig. 5.16 SEM photographs showing cross section of banana slices dried by (a) LPSSD-FIR at 80°C–7 kPa, (b) VACUUM-FIR at 80°C–7 kPa, (c) LPSSD-FIR at 90°C–7 kPa, (d) VACUUM-FIR at 90°C–7 kPa.

Table 5.6 Effects of drying methods, drying temperature and pressure on maximum force and number of peaks of dried banana slices.

Drying method	Drying temperature (°C)	Drying pressure (kPa)	Maximum force (N)	Number of peaks
LPSSD-FIR	70	7	N/A	N/A
		10	N/A	N/A
	80	7	17.09 ± 3.15^{a}	37 ± 3^{d}
		10	17.30 ± 3.60^{a}	36 ± 4^{d}
	90	7	16.39 ± 3.57^{a}	38 ± 4^{d}
		10	16.89 ± 4.58^{a}	38 ± 5^{d}
VACUUM-FIR	70	7	18.44 ± 3.80^{a}	22 ± 4^{ab}
		10	19.12 ± 4.07^{a}	21 ± 5^{a}
	80	7	19.95 ± 3.55^{a}	25 ± 5^{bc}
		10	18.16 ± 4.51^{a}	26 ± 5^{c}
	90	7	16.72 ± 3.19^{a}	36 ± 3^{d}
		10	17.81 ± 3.63^{a}	36 ± 4^{d}
LPSSD[a]	70	7	N/A	N/A
	80	7	21.52 ± 2.23	27 ± 3
	90	7	24.09 ± 1.26	28 ± 6

[a] Data obtained from Thomkapanish *et al*. (2007).
N/A implies that the final moisture content of 0.035 kg kg^{-1} (d.b.) was not obtainable at this condition.
Values in the same column with different superscripts mean that the values are significantly different ($p < 0.05$).

chips with a slightly larger number of peaks. This is again due to the larger and more numerous pores presented during LPSSD-FIR and VACUUM-FIR.

Instead of supplying thermal energy (via the application of low-pressure superheated steam or via the use of an electric heater) and vacuum condition continuously, Thomkapanish *et al*. (2007) implemented intermittent LPSSD of a food product (banana slices). Two intermittent modes, namely, intermittent temperature and intermittent pressure LPSSD, were tested. The effects of intermittent drying schemes, along with the other drying parameters viz. drying temperature (70–90°C) and pressure as well as the intermittency (on/off) period (10:5, 10:10 and 10:20 min in the case of intermittent supply of energy and 5:0, 5:5 and 5:10 min in the case of intermittent supply of vacuum) on the drying kinetics and various quality attributes (color, shrinkage, texture and ascorbic acid retention) of the dried banana chips were evaluated. The energy consumption values for intermittent LPSSD were also monitored through the effective (or net) drying time at various intermittent drying conditions and the results compared to those using continuous LPSSD.

In the case of intermittent temperature LPSSD the overall drying rates of intermittent and continuous LPSSD were not significantly different. However, the effective or net drying time of intermittent drying was significantly shorter than that of continuous drying, especially with a longer tempering period leading to high energy savings (up to 65%). It was also noted that the drying rates of intermittent pressure LPSSD were higher than those of continuous drying (in the range of 50–58%).

In terms of the quality of the dried chips it was found that the effect of intermittency in intermittent temperature drying in almost all cases, when compared with continuous drying, was not significant. However, intermittent temperature drying led to higher level of ascorbic acid retention, especially at longer tempering (off) periods.

On the other hand, it was noted that the colors of the products in the case of intermittent pressure drying were worse than those in the case of continuous drying. Shrinkage of the samples dried by intermittent pressure drying was also more obvious than in the case of continuous drying at all conditions. In addition, intermittent pressure drying led to greater degradation of ascorbic acid. This drying scheme is therefore not appropriate for heat- and, in particular, oxygen-sensitive products, as oxygen (air) is necessarily introduced to the drying chamber during the off period.

5.5 MATHEMATICAL MODELING OF LPSSD OF FOODS AND BIOMATERIALS

Several models with different degrees of complexity and predictability have been proposed for LPSSD. In this section only selected models applied to LPSSD of foods and biomaterials are reviewed, however. Mathematical models for LPSSD of other products are available in the literature (e.g. Shibata *et al*., 1990; Pang, 1997; Elustondo *et al*., 2002; Defo *et al*., 2004; Suvarnakuta *et al*., 2005b).

Elustondo *et al*. (2001) developed a mathematical model based on a theoretical drying mechanism, which assumes that the water removal is carried out by evaporation in a moving boundary allowing the vapor to flow through the dry layer built as drying proceeds to predict the drying characteristics of foodstuffs undergoing LPSSD. A simplified expression, which has two experimentally determined parameters, was derived and used to predict the drying rate of test samples. Despite its simplicity it was noted that the model could predict the drying kinetics of the tested materials adequately.

Suvarnakuta *et al*. (2007) proposed the use of a simple three-dimensional liquid diffusion based model to predict the evolutions of the moisture content and temperature of a biomaterial (carrot cube) undergoing LPSSD. The model consists of coupled heat conduction and mass diffusion equations along with an empirical equation, which describes shrinkage of the product during drying. An empirical equation that expresses the β-carotene degradation in carrot is also included in the model so as to predict the evolution of β-carotene content in carrot during drying.

The model assumes that the sample is isotropic and homogenous. Initial condensation of steam is also neglected in the model. In addition, mass transfer within the material is controlled only by liquid diffusion; it is thus assumed that no vaporization occurs within the drying material. Finally, it is assumed that shrinkage of the material is significant, and that it is accounted for in all three directions. The volumetric shrinkage depends on the operating temperature and moisture content and is described by an empirically determined correlation.

The conduction equation to describe energy transfer is written as follows:

$$\rho C_p \frac{\partial T}{\partial t} = \frac{\partial}{\partial x}\left(k_x \frac{\partial T}{\partial x}\right) + \frac{\partial}{\partial y}\left(k_y \frac{\partial T}{\partial y}\right) + \frac{\partial}{\partial z}\left(k_z \frac{\partial T}{\partial z}\right) \tag{5.3}$$

where $k_x = k_y = k_z = k$ due to the product isotropy.

The equation to describe the mass transfer during LPSSD is:

$$\frac{\partial X_f}{\partial t} = \frac{\partial}{\partial x}\left(D_{eff} \frac{\partial X_f}{\partial x}\right) + \frac{\partial}{\partial y}\left(D_{eff} \frac{\partial X_f}{\partial y}\right) + \frac{\partial}{\partial z}\left(D_{eff} \frac{\partial X_f}{\partial z}\right) \tag{5.4}$$

At the onset of the LPSSD process the temperature and moisture content of the material are uniform.

$$T = T_i \tag{5.5}$$

$$X = X_{f\,i} \tag{5.6}$$

For the material subjected to convective drying the boundary condition (equation (5.7)) at the surface is used:

$$-k(\nabla T \cdot n) = h(T_{steam} - T_s) - \rho\lambda D_{eff}(\nabla X_f \cdot n) \tag{5.7}$$

where the term on the left-hand side refers to heat conducted from the outer surface to the inside of the cube, the first term on the right-hand side is heat penetrating from low-pressure superheated steam to the solid body by means of convection and the second term on the right-hand side denotes the latent heat of vaporization.

Mass transfer at the surface is modeled by assuming that there is no mass transfer resistance at the surface of the material since water possesses no self-resistance in its own body. This is certainly not a very realistic assumption and a model should be developed in future to better represent the phenomenon (by, for example, recognizing that the driving force for mass transfer from the surface is the difference between the vapor pressure of moisture at the surface temperature and the steam pressure in the bulk phase).

$$X_f = 0 \tag{5.8}$$

where X_f denotes free moisture content ($X_f = X - X_{eq}$) . This condition simply implies that the moisture content at the surface was always at its equilibrium value at the corresponding operating condition.

The detailed estimation of the parameters required in the model is described in Suvarnakuta *et al*. (2007). It is only important to note here that the values of the effective diffusion coefficient (D_{eff}) obtained, assuming that the material suffers no shrinkage, are different from those obtained assuming that the material suffers uniform shrinkage.

The above-mentioned model was validated by the available experimental data. The estimated values of the heat transfer coefficient were set in the range of ±20% (see Table 5.1) to investigate the sensitivity of this parameter on the predictability of the product temperature and moisture content.

Figure 5.17 illustrates the sample evolutions of the moisture ratio and the center temperature of carrot cube undergoing LPSSD. It was found that the trends of moisture ratio prediction are in good agreement with the experimental data. However, at the highest operating pressure (13 kPa) the model was not able to predict the experimental data well (see Figures 5.18 and 5.19). This is due to the fact that a larger amount of steam condensation occurred during the start-up period at a higher operating pressure (since steam at a lower degree of superheat tended to condense more easily) and this led to under-prediction of the moisture ratio since the model, as mentioned earlier, did not take into account the effect of initial condensation. The same reason could also be used to explain a rather larger discrepancy between simulated and experimental results at lower drying steam temperatures as well.

Representative product center temperature profiles over time are also presented in Figures 5.17–5.19. The center temperature increased over time until it reached the boiling point of water at the corresponding operating pressure; after this point, the temperature slowly increased while latent heating prevented a temperature rise. It is seen from these figures that the simulated predictions did not quite agree with the experimental data. This is due to the fact that carrots undergoing LPSSD in fact shrank non-uniformly. Thus, the assumption of

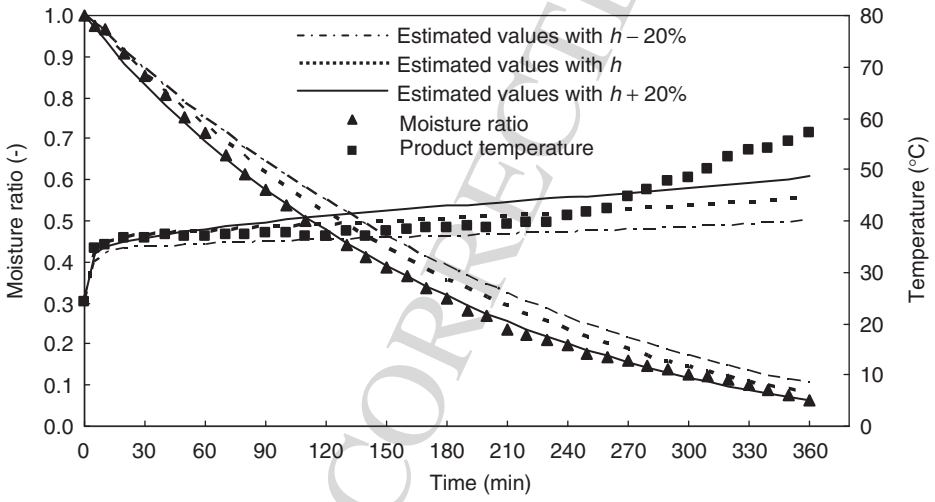

Fig. 5.17 Comparison between predicted (assuming shrinkage) and experimental moisture content and temperature variation with time of carrot cube at 60°C and 7 kPa (X_{eq} = 0.10 kg kg^{-1} (d.b.)). Lines represent predicted data; symbols represent experimental data.

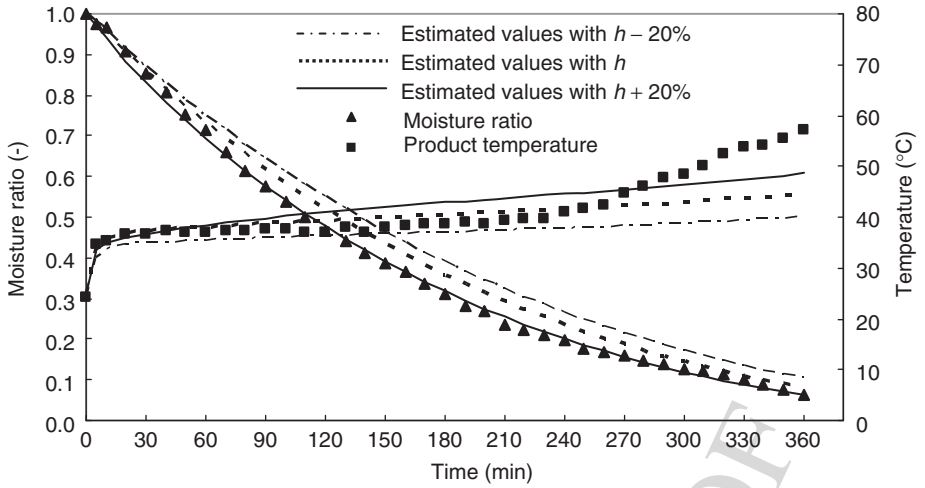

Fig. 5.18 Comparison between predicted (assuming shrinkage) and experimental moisture content and temperature of carrot cube at 70°C and 13 kPa ($X_{eq} = 0.10\ \text{kg kg}^{-1}$ (d.b.)).

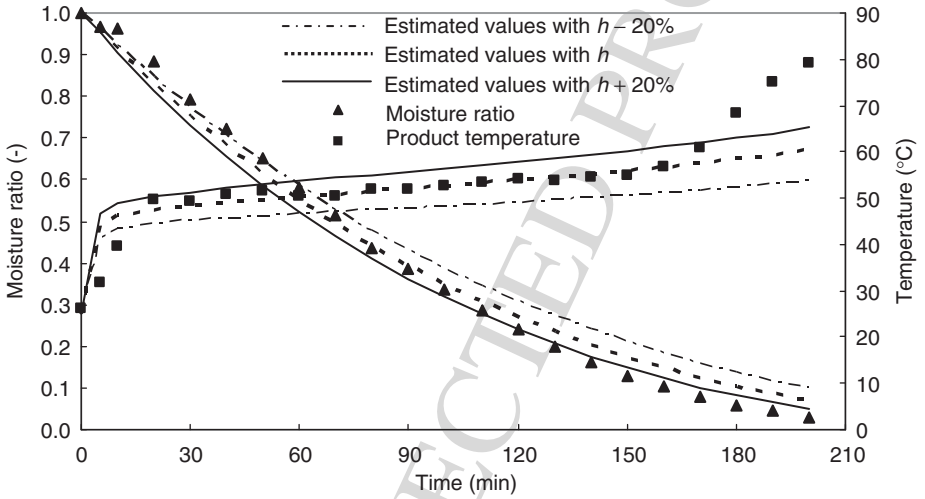

Fig. 5.19 Comparison between predicted (assuming shrinkage) and experimental moisture content and temperature of carrot cube at 80°C and 13 kPa ($X_{eq} = 0.10\ \text{kg kg}^{-1}$ (d.b.)).

uniform shrinkage used in this study was not quite correct. Another factor that contributed to the deviation of the simulated results from the experimental data is the fact that once the boiling point was reached there was vapor generation, which could give rise to an increase in the internal pressure in pores. Thus, it was possible that hydrostatic pressure gradients were generated within the product, which could in turn drive the liquid-form moisture out of the product faster than that permissible by liquid diffusion alone. Furthermore, the change in porosity and physical structure of carrot during drying could, in principle, change the diffusivity from what was predicted by the empirical correlations used.

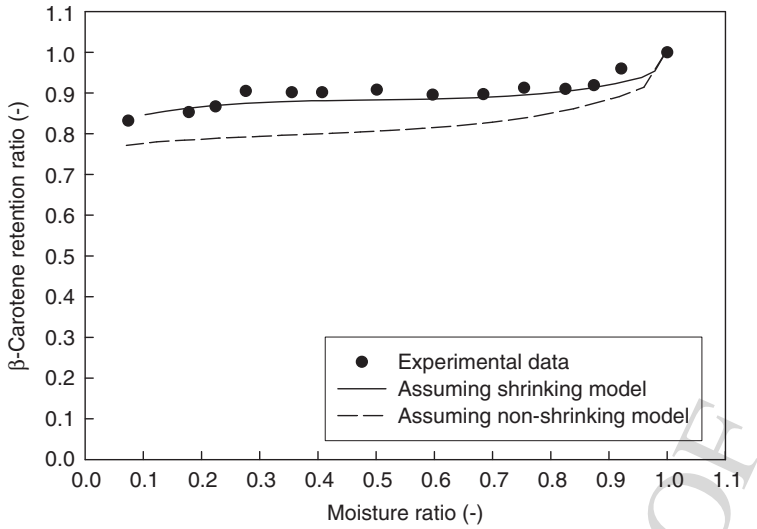

Fig. 5.20 Comparison between predicted and experimental β-carotene degradation of carrot at 60°C.

Figure 5.20 shows a sample predicted β-carotene degradation in carrot during LPSSD using the middle values of heat transfer coefficients. The β-carotene degradation predictions, which follow from the simulated moisture content and temperature based on the assuming shrinking model, show good agreement with the experimental data under all conditions.

The next step for model development should be directed towards the use of more realistic assumptions, boundary conditions and inclusion of phenomena that really occur during LPSSD, for example, vaporization of moisture within the drying material.

5.6 CONCLUDING REMARKS

Owing to several limitations of near-atmospheric pressure superheated steam drying, low-pressure superheated steam drying (LPSSD) has emerged as an alternative for drying heat- and/or oxygen-sensitive food products. Over the past several years, many attempts have been made to apply this technology to a wide array of foods and it has been shown that LPSSD could produce dried products with superior quality, either in terms of physical or chemical (nutritional) quality, compared with products dried by conventional hot air drying or vacuum drying. In addition to applying this technology to drying foods *per se*, LPSSD also has the potential to produce engineered biomaterials for different applications in food engineering, for example, production of antioxidant/antimicrobial edible films for active packaging applications. Preliminary results have indeed shown that LPSSD could yield edible films with higher strength, compared with films obtained from vacuum drying, due to its ability to enhance crystallinity of the film structure.

Future developments in this area should aim towards developing a more realistic mathematical model that enables predictions of moisture content and temperature evolutions within the drying material. Further use of the technology for the production of advanced materials should also be investigated.

5.7 NOTATION

C_p heat capacity, J kg^{-1} K^{-1}
D_{eff} effective diffusivity, m^2 s^{-1}
h heat transfer coefficient, W m^{-2} K^{-1}
k thermal conductivity, W m^{-1} K^{-1}
MR moisture ratio, $\dfrac{X - X_{eq}}{X_i - X_{eq}}$
n unit vector
N evaporation rate, kg s^{-1}
q heat transfer rate, W
t time, s
T temperature, °C
T_i initial temperature, °C
X total moisture content, kg water per kg dry solid (d.b.)
X_{eq} equilibrium moisture content, kg water per kg dry solid (d.b.)
X_f free moisture content, kg water per kg dry solid (d.b.)

Greek letters

λ latent heat of vaporization, J kg^{-1}
ρ density, kg m^{-3}

Subscripts

f free
i initial
s surface of product
steam superheated steam

REFERENCES

Abe, T. and Miyashita, K. (2006) Surface sterilization of dried fishery products in superheated steam and hot air. *Nippon Shokuhin Kagaku Kogaku Kaishi*, **53**, 373–379.

Achanta, S. and Okos, M.R. (2000) Quality changes during drying of food polymers. In: *Drying Technology in Agriculture and Food Science* (ed. A.S. Mujumdar). Science Publishers, Enfield, NH, pp. 133–147.

Barbieri, S., Elustondo, M. and Urbicain, M. (2004) Retention of aroma compounds in basil dried with low pressure superheated steam. *Journal of Food Engineering*, **65**, 109–115.

Bond, J.F., Mujumdar, A.S., van Heiningen, A.R.P. and Douglas, W.J.M. (1994) Drying paper by impinging jets of superheated steam. Part 2: Comparison of steam and air as drying fluids. *Canadian Journal of Chemical Engineering*, **72**, 452–456.

Cenkowski, S., Pronyk, C., Zmidzinska, D. and Muir, W.E. (2007) Decontamination of food products with superheated steam. *Journal of Food Engineering*, **83**, 68–75.

Chen, S.R., Chen, J.Y. and Mujumdar, A.S. (1992) Preliminary study of steam drying of silkworm cocoons. *Drying Technology*, **10**, 251–260.

Chow, L.C. and Chung, J.N. (1983) Evaporation of water into a laminar stream of air and superheated steam. *International Journal of Heat and Mass Transfer*, **26**, 373–380.

Defo, M., Fortin, Y. and Cloutier, A. (2004) Modeling superheated steam vacuum drying of wood. *Drying Technology*, **22**, 2231–2253.

Devahastin, S. and Suvarnakuta, P. (2004) Superheated-steam-drying of food products. In: *Dehydration of Products of Biological Origin* (ed. A.S. Mujumdar). Science Publishers, Enfield, NH, pp. 493–512.

Devahastin, S., Suvarnakuta, P., Soponronnarit, S. and Mujumdar, A.S. (2004) A comparative study of low-pressure superheated steam and vacuum drying of a heat-sensitive material. *Drying Technology*, **22**, 1845–1867.

Douglas, W.J.M. (1994) Drying paper in superheated steam. *Drying Technology*, **12**, 1341–1355.

Elustondo, D., Elustondo, M.P. and Urbicain, M.J. (2001) Mathematical modeling of moisture evaporation from foodstuffs exposed to subatmospheric pressure superheated steam. *Journal of Food Engineering*, **49**, 15–24.

Elustondo, D.M., Mujumdar, A.S. and Urbicain, M.J. (2002) Optimum operating conditions in drying of foodstuffs with superheated steam. *Drying Technology*, **20**, 381–402.

Furukawa, T. and Akao, T. (1983) Deodorization by superheated steam drying. *Drying Technology*, **2**, 407–418.

Haji, M. and Chow, L.C. (1988) Experimental measurement of water evaporation rates into air and superheated steam. *Journal of Heat Transfer*, **110**, 237–242.

Incropera, F.P. and DeWitt, D.P. (2002) *Fundamentals of Heat and Mass Transfer*, 5th edn. Wiley, New York.

Iyota, H., Konishi, Y., Inoue, T., Yoshida, K., Nishimura, N. and Nomura, T. (2005) Popping of Amaranth seeds in hot air and superheated steam. *Drying Technology*, **23**, 1273–1287.

Iyota, H., Nishimura, N., and Nomura, T. (2001) Drying of sliced raw potatoes in superheated steam and hot air. *Drying Technology*, **19**, 1411–1424.

Jamradloedluk, J., Nathakaranakule, A., Soponronnarit, S. and Prachayawarakorn, S. (2007) Influences of drying medium and temperature on drying kinetics and quality attributes of durian chips. *Journal of Food Engineering*, **78**, 198–205.

Kongsoontornkijkul, P., Ekwongsupasarn, P., Chiewchan, N. and Devahastin, S. (2006) Effects of drying methods and tea preparation temperature on the amount of vitamin C in Indian gooseberry tea. *Drying Technology*, **24**, 1509–1513.

Kozanoglu, B., Vazquez, A.C., Chanes, J.W. and Patino, J.L. (2006) Drying of seeds in a superheated steam vacuum fluidized bed. *Journal of Food Engineering*, **75**, 383–387.

Leeratanarak, N., Devahastin, S. and Chiewchan, N. (2006) Drying kinetics and quality of potato chips undergoing different drying techniques. *Journal of Food Engineering*, **77**, 635–643.

Methakhup, S., Chiewchan, N. Devahastin, S. (2005) Effects of drying methods and conditions on drying kinetics and quality of Indian gooseberry flake. *LWT – Food Science and Technology*, **38**, 579–587.

Moreira, R.G. (2001) Impingement drying of foods using hot air and superheated steam. *Journal of Food Engineering*, **49**, 291–295.

Mujumdar, A.S. (2000) Superheated steam drying – Technology of the future. In: *Mujumdar's Practical Guide to Industrial Drying* (ed. S. Devahastin). Exergex Corp., Brossard, Canada, pp. 115–138.

Mujumdar, A.S. (2007) Superheated steam drying. In: *Handbook of Industrial Drying*, 3rd edn. (ed. A.S. Mujumda). CRC Press, Boca Raton, FL, pp. 439–452.

Namsanguan, Y., Tia, W., Devahastin, S. and Soponronnarit, S. (2004) Drying kinetics and quality of shrimp undergoing different two-stage drying processes. *Drying Technology*, **22**, 759–778.

Nathakaranakule, A., Kraiwanichkul, W. and Soponronnarit, S. (2007) Comparative study of different combined superheated-steam drying techniques for chicken meat. *Journal of Food Engineering*, **80**, 1023–1030.

Nimmol, C., Devahastin, S., Swasdisevi, T. and Soponronnarit, S. (2007) Drying of banana slices using combined low-pressure superheated steam and far-infrared radiation. *Journal of Food Engineering*, **81**, 624–633.

Pang, S. (1997) Some considerations in simulation of superheated steam drying of softwood lumber. *Drying Technology*, **15**, 651–670.

Pang, S. and Dakin, M. (1999) Drying rate and temperature profile for superheated steam vacuum drying and moist air drying of softwood lumber. *Drying Technology*, **17**, 1135–1147.

Panyawong, S. and Devahastin, S. (2007) Determination of deformation of a food product undergoing different drying methods and conditions via evolution of a shape factor. *Journal of Food Engineering*, **78**, 151–161.

Pimpaporn, P., Devahastin, S. and Chiewchan, N. (2007) Effects of combined pretreatments on drying kinetics and quality of potato chips undergoing low-pressure superheated steam drying. *Journal of Food Engineering*, **81**, 318–329.

Prachayawarakorn, S., Soponronnarit, S., Wetchacama, S. and Jaisut, D. (2002) Desorption isotherms and drying characteristics of shrimp in superheated steam and hot air. *Drying Technology*, **20**, 669–684.

Prachayawarakorn, S., Prachayawasin, P. and Soponronnarit, S. (2006) Heating process of soybean using hot-air and superheated-steam fluidized-bed dryers. *LWT – Food Science and Technology*, **39**, 770–778.

Pronyk, C., Cenkowski, S. and Abramson, D. (2006) Superheated steam reduction of deoxynivalenol in naturally contaminated wheat kernels. *Food Control*, **17**, 789–796.

Rordprapat, W., Nathakaranakule, A., Tia, W. and Soponronnarit, S. (2005) Comparative study of fluidized bed paddy drying using hot air and superheated steam. *Journal of Food Engineering*, **71**, 28–36.

Sano, A., Senda, Y., Oyama, K., Tanigawara, R., Bando, Y., Nakamura, M., Sugimura, Y. and Shibata, M. (2005) Drying characteristics in superheated steam drying at reduced pressure. *Drying Technology*, **23**, 2437–2447.

Schwartze, J.P. and Brocker, S. (2002) A theoretical explanation for the inversion temperature. *Chemical Engineering Journal*, **86**, 61–67.

Sheikholeslami, R. and Watkinson, A.P. (1992) Rate of evaporation of water into superheated steam and humidified air. *International Journal of Heat and Mass Transfer*, **35**, 1743–1751.

Shibata, H., Mada, J. and Shinohara, H. (1988) Steam drying of sintered glass bead spheres under vacuum. *Industrial & Engineering Chemistry Research*, **27**, 2385–2387.

Shibata, H., Mada, J. and Funatsu, K. (1990) Prediction of drying rate curves on sintered spheres of glass beads in superheated steam under vacuum. *Industrial & Engineering Chemistry Research*, **29**, 614–617.

Shibata, H. (2006) Drying rate curves of porous solids in steam and in air under low-pressure conditions. *Drying Technology*, **24**, 37–43.

Soponronnarit, S., Nathakaranakule, A., Jirajindalert, A. and Taechapairoj, C. (2006) Parboiling brown rice using superheated steam fluidization technique. *Journal of Food Engineering*, **75**, 423–432.

Sotome, I., Suzuki, K., Koseki, S., *et al.* (2006) Blanching of potato with superheated steam containing micro-droplets of hot water. *Nippon Shokuhin Kagaku Kogaku Kaishi*, **53**, 451–458.

Suvarnakuta, S., Devahastin, S. and Mujumdar, A.S. (2005a) Drying kinetics and β-carotene degradation in carrot undergoing different drying processes. *Journal of Food Science*, **70**, S520–S526.

Suvarnakuta, S., Devahastin, S. and Mujumdar, A.S. (2007) A mathematical model for low-pressure superheated steam drying of a biomaterial. *Chemical Engineering and Processing*, **46**, 675–683.

Suvarnakuta, S., Devahastin, S., Soponronnarit, S. and Mujumdar, A.S. (2005b) Drying kinetics and inversion temperature in a low-pressure superheated steam-drying system. *Industrial & Engineering Chemistry Research*, **44**, 1934–1941.

Taechapairoj, C., Prachayawarakorn, S. and Soponronnarit, S. (2004) Characteristics of rice dried in superheated-steam fluidized-bed. *Drying Technology*, **22**, 719–743.

Tatemoto, Y., Yano, S., Mawatari, Y., Noda, K. and Komatsu, N. (2007) Drying characteristics of porous material immersed in a bed of glass beads fluidized by superheated steam under reduced pressure. *Chemical Engineering Science*, **62**, 471–480.

Thomkapanish, O., Suvarnakuta, S. and Devahastin, S. (2007). Study of intermittent low-pressure superheated steam and vacuum drying of a heat-sensitive material. *Drying Technology*, **25**, 205–223.

Wu, C.-H., Davis, D.C. and Chung, J.N. (1989) Simulated dehydration of wedge-shaped specimens in turbulent flow of superheated steam and air. *Drying Technology*, **7**, 761–782.

Wu, C.-H., Davis, D.C., Chung, J.N. and Chow, L.C. (1987) Simulation of wedge-shaped product dehydration using mixture of superheated steam and air in laminar flow. *Numerical Heat Transfer*, **11**, 109–123.

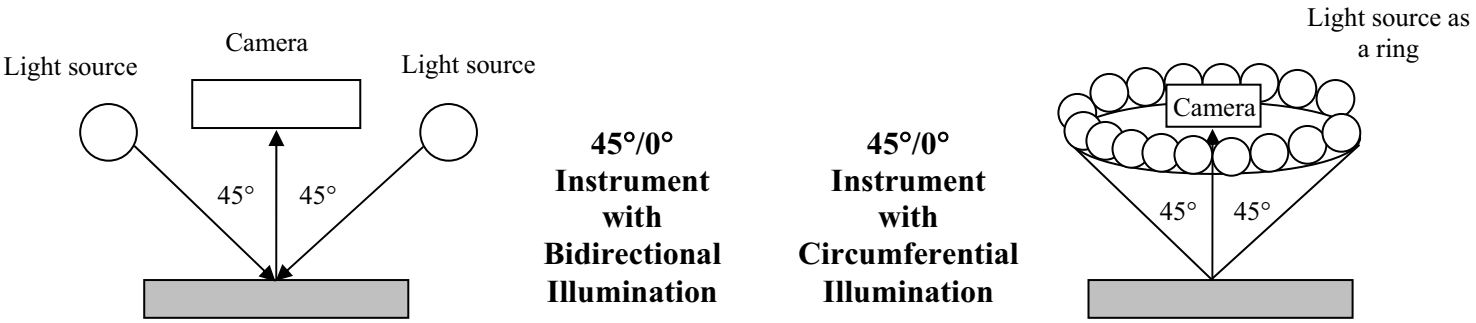

Figure 1. Set-up of a camera and illuminant with 45° reflection

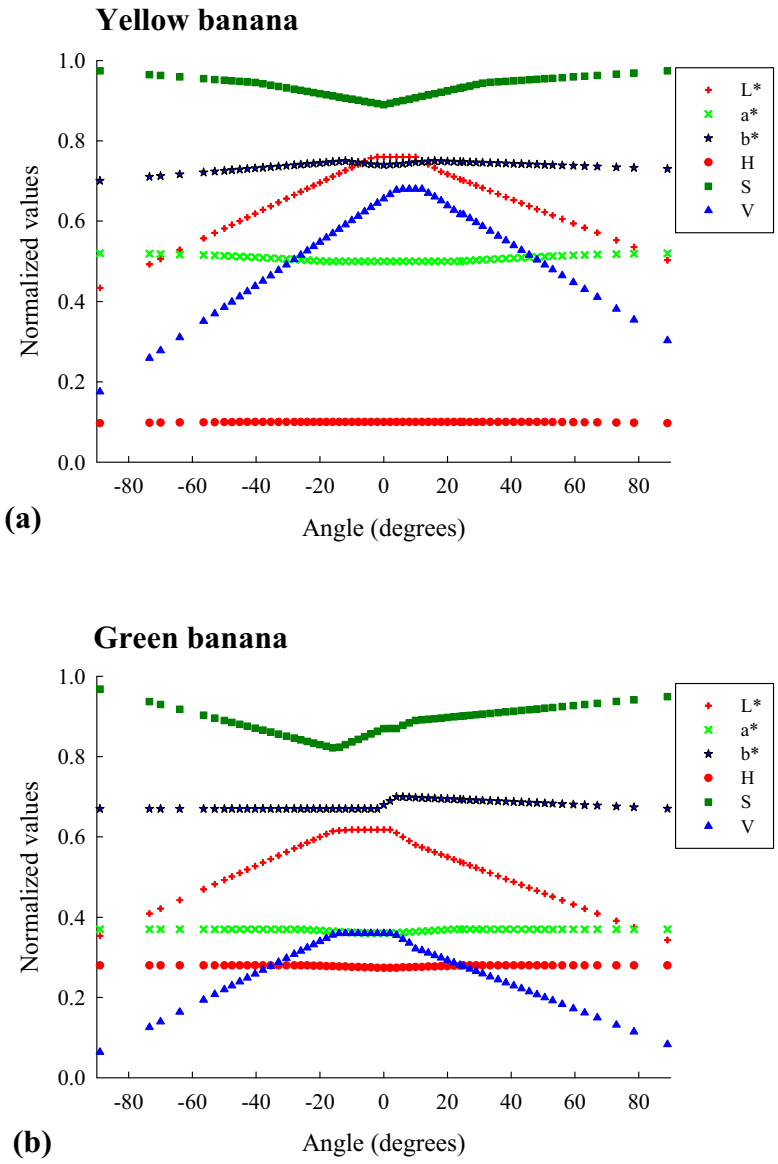

Figure 2. Color profiles expressed in $L^*a^*b^*$ and HSV color scales for: (a) yellow banana; (b) green banana (Mendoza et al., 2006)

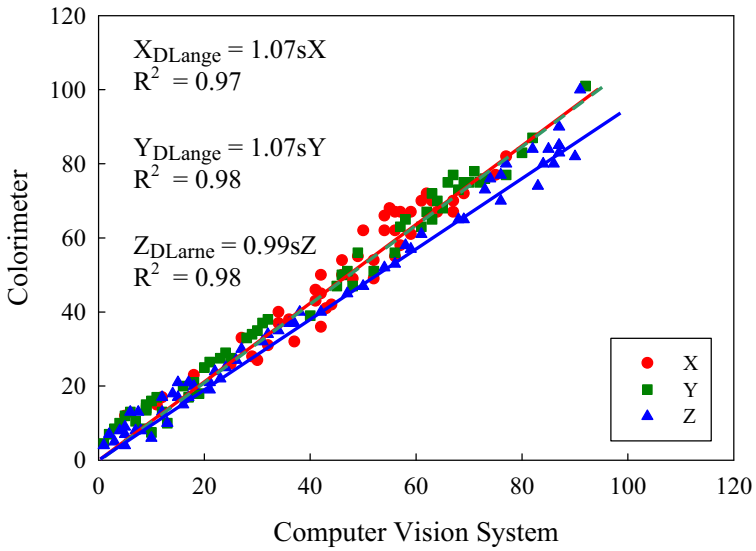

Figure 3. Plots of color scale values acquired by Computer Vision System against values measured by a colorimeter on 125 Pantone® color sheets (Mendoza et al., 2006)

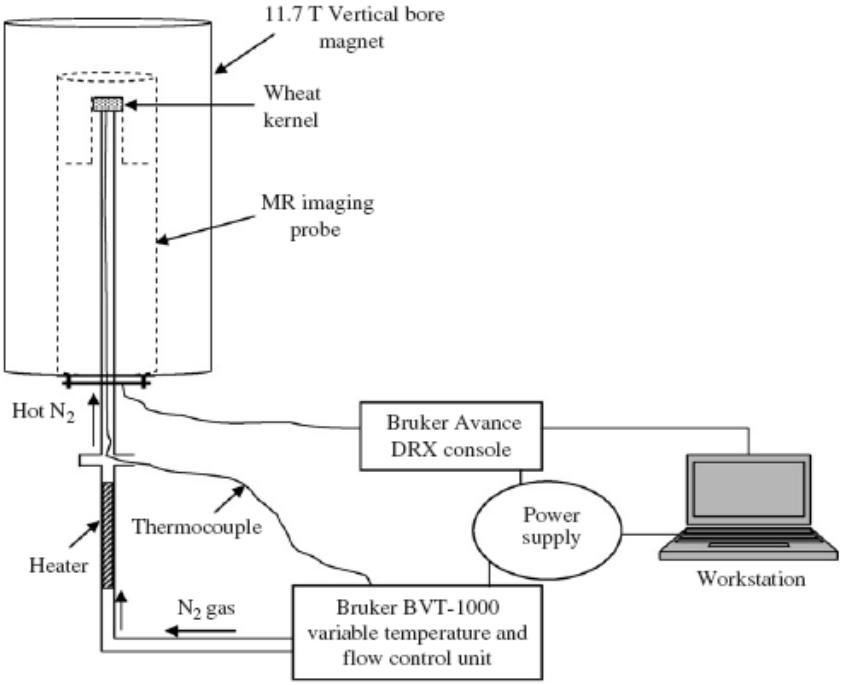

Figure 4. A schematic diagram of MRI experimental set up with the dryer assembly (Ghosh et al., 2007)

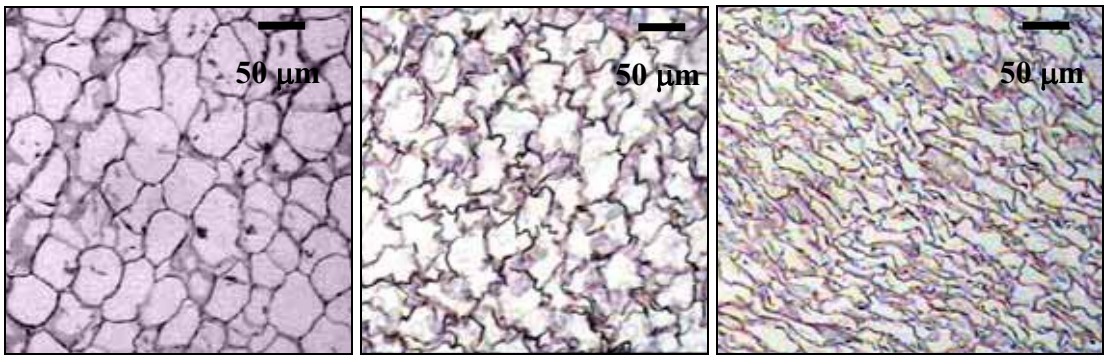

(a) (b) (c)

Figure 5. Microstructure of carrot cube undergoing hot air drying at 60^{o}C, 0.5 m/s after (a) 0 min, (b)150 min and (c) 300 min

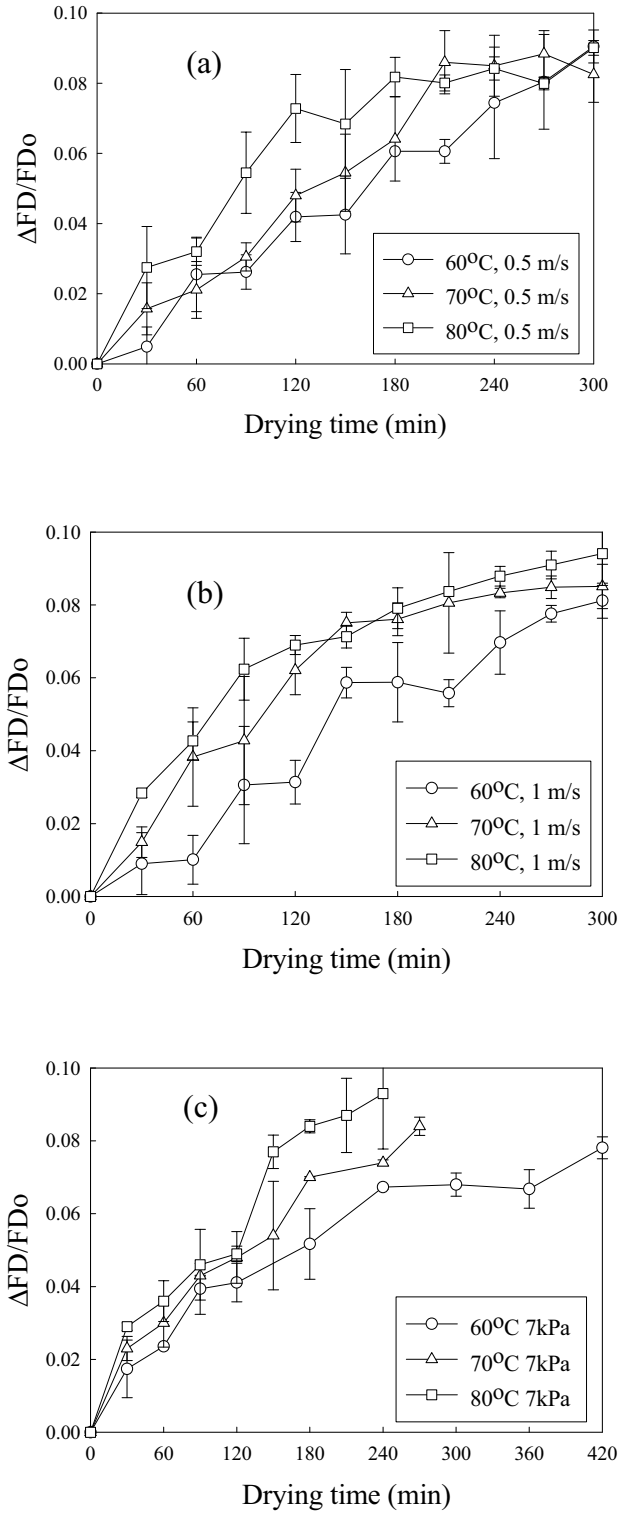

Figure 6. $\Delta FD/FD_o$ of carrot cube undergoing hot air drying (a) velocities of 0.5 m/s and (b) 1 m/s) and (c) LPSSD at 7 kPa

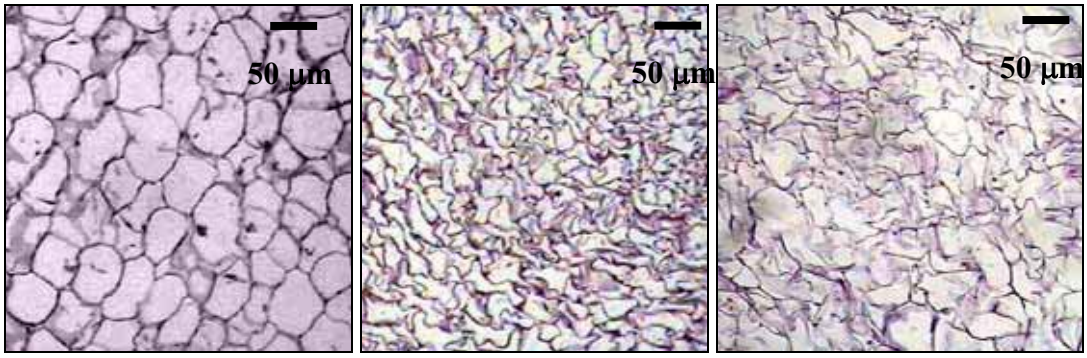

(a) (b) (c)

Figure 7. Microstructure of (a) fresh carrot cube and of carrot cube dried until reaching equilibrium moisture content using (b) hot air drying and (c) LPSSD

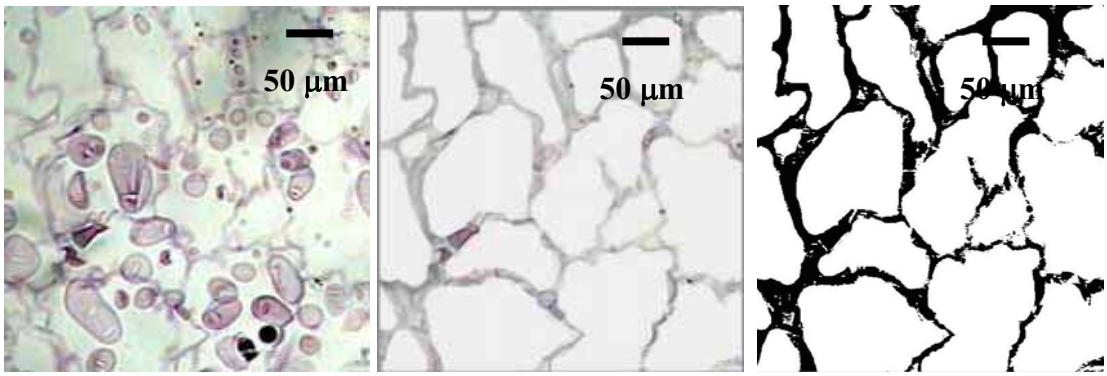

(a) (b) (c)

Figure 8. Image processing of potato cube (a) original image, (b) image after deleting of starch granules and (c) black and white image

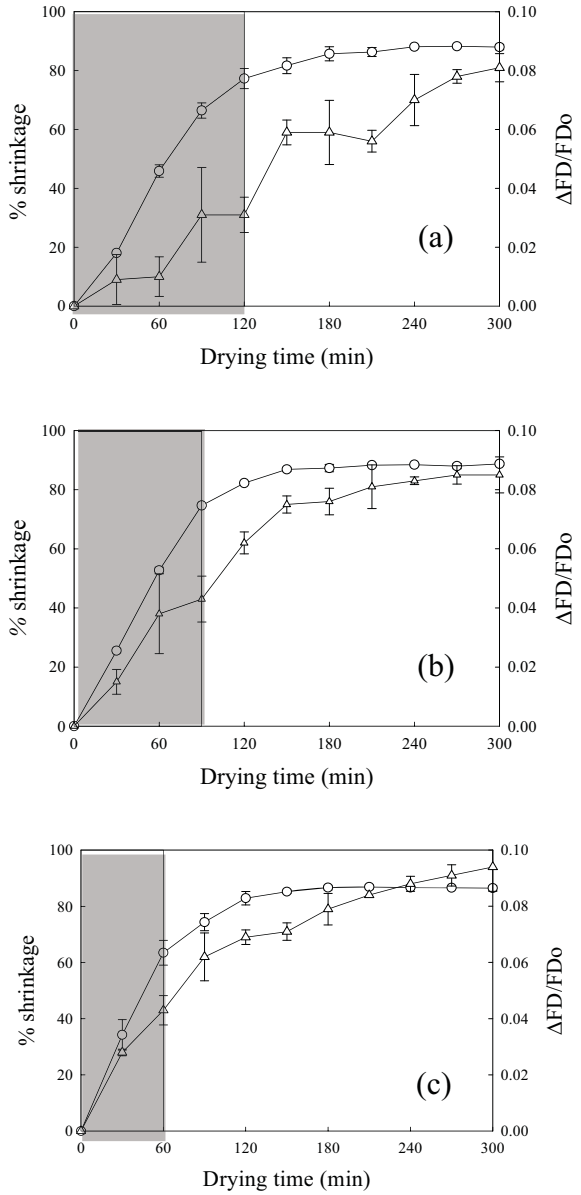

Figure 9. Relationship between % shrinkage (o) and $\Delta FD/FD_o$ (Δ) of carrot cube undergoing hot air drying at velocity of 1 m/s and temperatures of (a) 60^{o}C, (b) 70^{o}C and (c) 80^{o}C

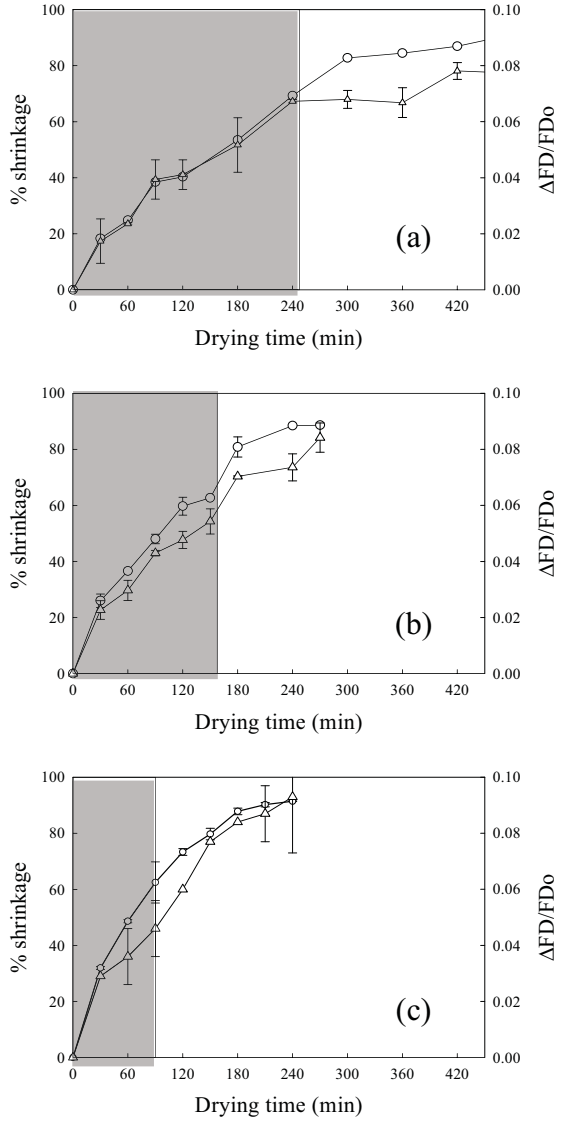

Figure 10. Relationship between % shrinkage (o) and $\Delta FD/FD_o$ (Δ) of carrot cube undergoing LPSSD at temperatures of (a) 60°C, (b) 70°C and (c) 80°C

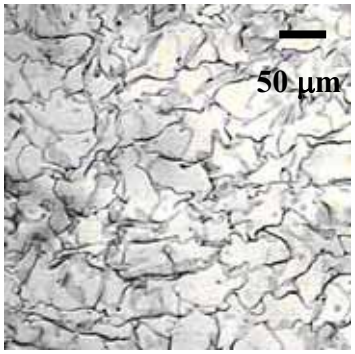

LPSSD, 60°C, 210 min

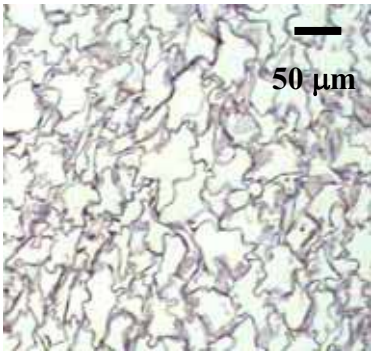

HAD, 60°C, 1 m/s, 150 min

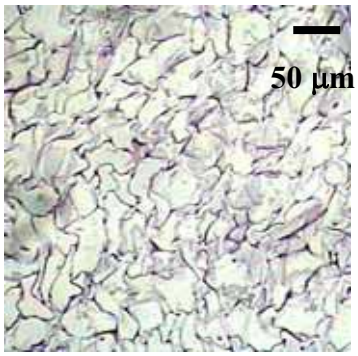

LPSSD, 70°C, 150 min

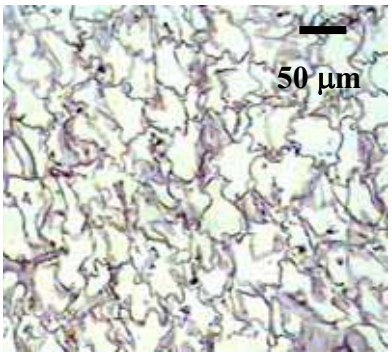

HAD, 70°C, 1m/s, 120 min

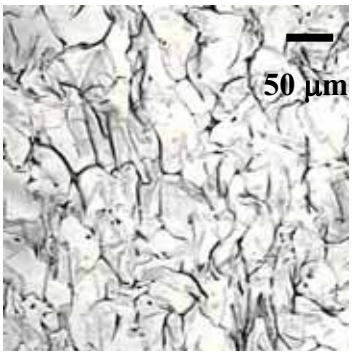

LPSSD, 80°C, 120 min

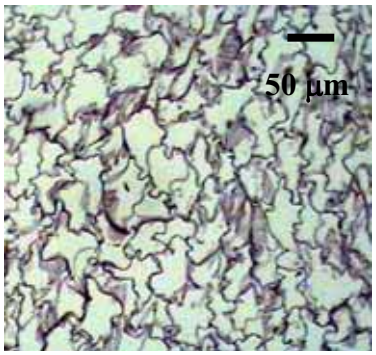

HAD, 80°C, 1m/s, 90 min

Figure 11. Microstructural images of carrot cube at $\Delta FD/FD_o = 0.06$

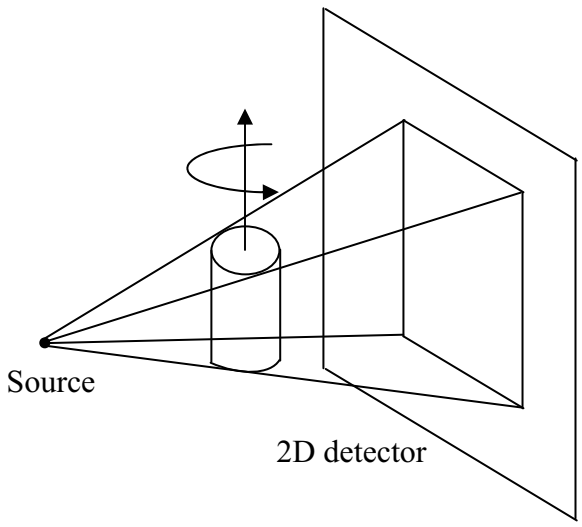

(a)

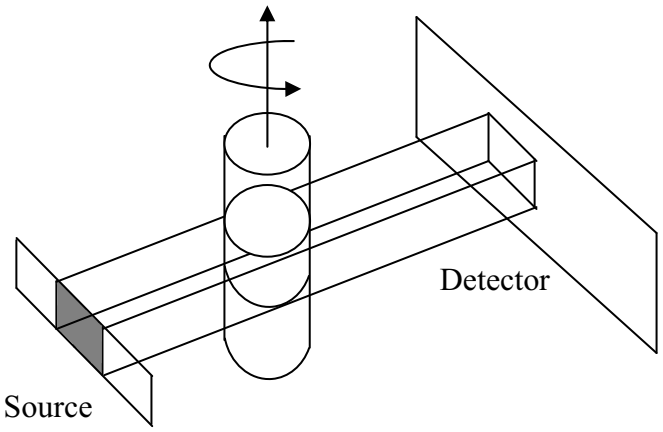

(b)

Figure 12. (a) A schematic view of an X-ray microtomograph with cone-beam geometry; (b) A schematic view of a synchrotron microtomography

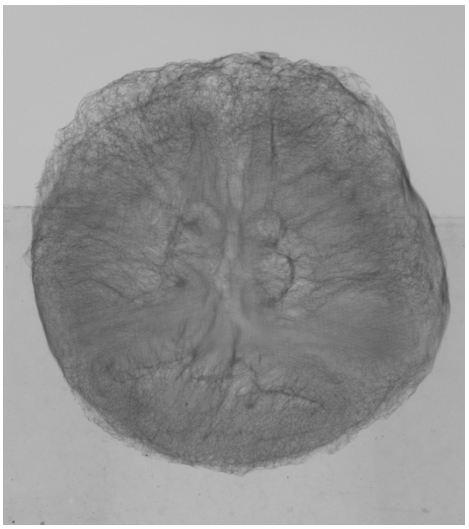

Figure 13. Radiograph of a dried banana slice

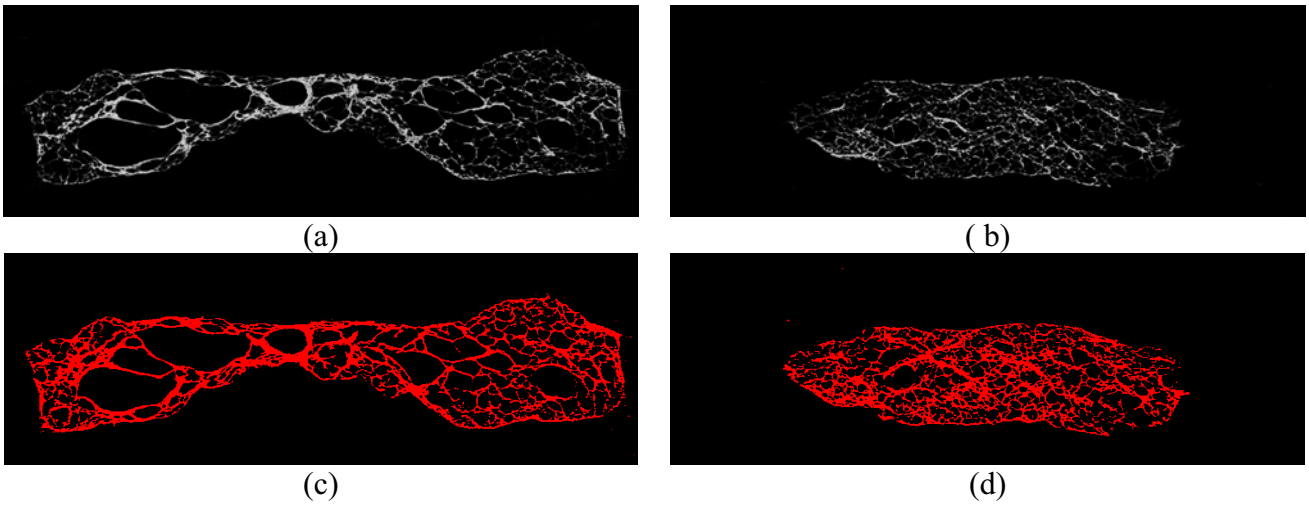

Figure 14. Grey level cross sections (a-b) and the corresponding binary images after thresholding (c-d)

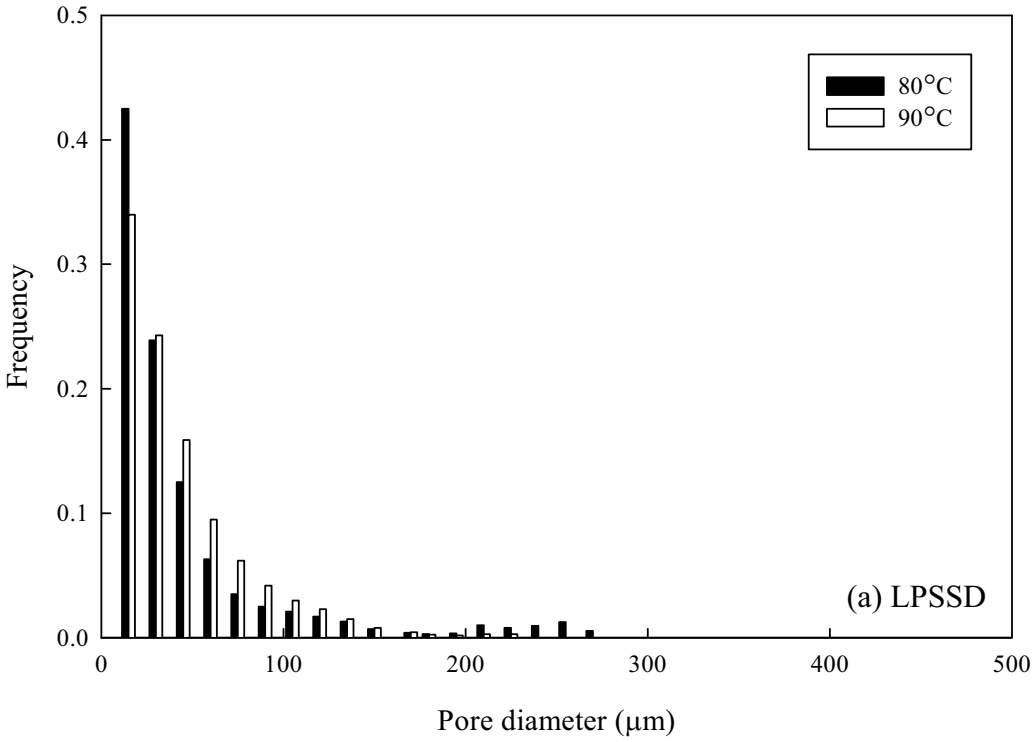

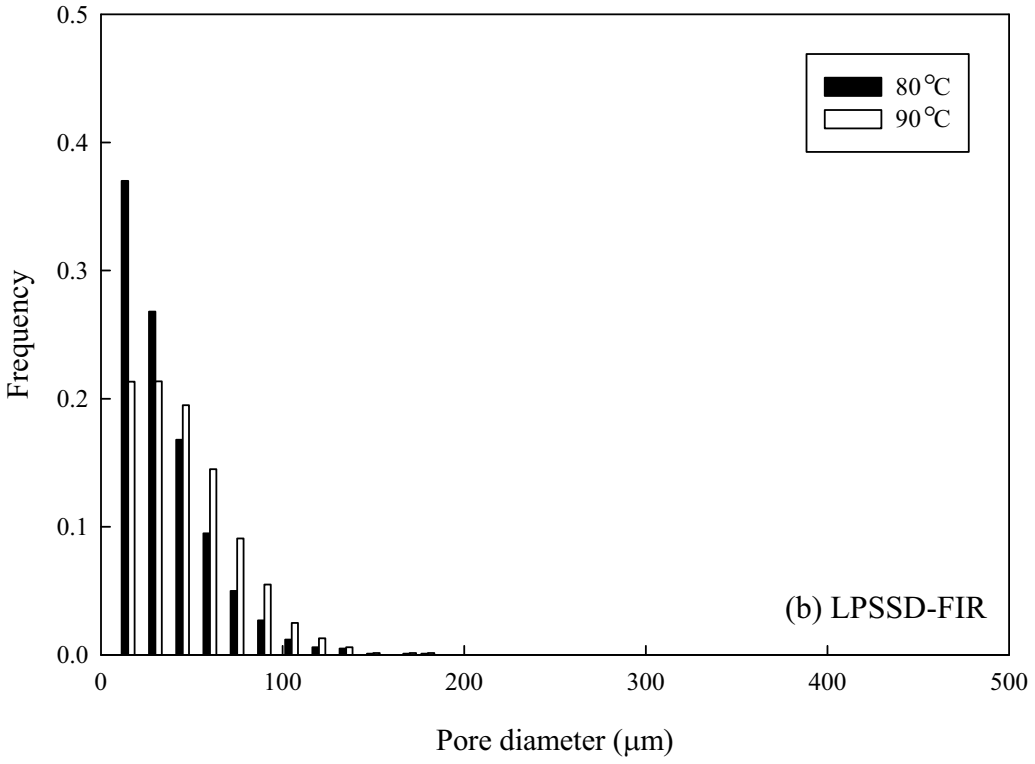

Figure 15. Pore size distributions of the samples dried at 80 and 90°C with (a) LPSSD and (b) LPSSD-FIR